CLOCK-RELATED REGULATION OF MITOCHONDRIAL PHYSIOLOGY IN SKELETAL MUSCLE

Stephen Pastore

A THESIS SUBMITTED TO THE FACULTY OF GRADUATE STUDIES IN PARTIAL

FULFILMENT OF THE REQUIREMENTS FOR THE DEGREE OF

MASTER'S OF SCIENCE

GRADUATE PROGRAM IN KINESIOLOGY AND HEALTH SCIENCE

YORK UNIVERSITY

TORONTO, ONTARIO

DECEMBER 2012

Faculty of Graduate Studies

I recommend that the thesis prepared
under my supervision by

Stephen Pastore

entitled

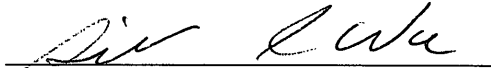## Clock-related Regulation of Mitochondrial Physiology in Skeletal Muscle

be accepted in partial fulfillment of the
requirements for the degree of

Master of Science
December 2012
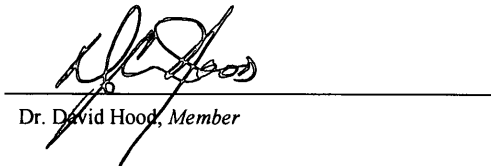
_____

Dr. David Hood, *Supervisor*

Recommendation concurred in by the following Examining Committee

_____   _____

Dr. Gillian Wu, *Chair*   Dr. Patricia Lakin-Thomas, *Outside Member*

_____

Dr. David Hood, *Member*

December 2012

YORK

redefine THE POSSIBLE.

UNIVERSITÉ
UNIVERSITY

Abstract

Biological rhythms regulate numerous functional processes within organisms, including the expression of peroxisome proliferator-activated receptor-γ coactivator 1-α (PGC-1α), a potent regulator of mitochondrial biogenesis. Homozygous *Clock* mutant mice are characterized by arrhythmic and suppressed expression of circadian genes within skeletal muscle, including PGC-1α. The present study sought to investigate mitochondrial physiology within these mutant animals, and to assess their adaptability to a chronic voluntary endurance training protocol. Our results indicate that *Clock* mutant mice exhibit decreased mitochondrial content, and this contributes to exercise intolerance in these mutant animals. Interestingly, endurance training ameliorates the decrement in mitochondrial content, as well as restores exercise capacity to levels evident in the wildtype mice. Thus, a functional CLOCK protein is necessary for optimal mitochondrial physiology, however *Clock* mutant mice retain the ability to adapt to chronic exercise.

Acknowledgments

The completion of this thesis could not have been accomplished without the help of so many individuals, and I would to take this time to thank them.

First, I would like to thank my supervisor, Dr. David Hood, for accepting me into your lab, mentoring me, and for teaching me how to become a scientist. I learned a great deal from you, and I will always appreciate the many things that you have done for me over the past three years.

I would like to thank my girlfriend Heidy, for all of the help, support and encouragement that you have given to me throughout these past five years. You are the driving force behind everything that I do. You are my best friend, and I love you with all of my heart.

I would like to thank my parents, Sam and Frances, and my brother Nicholas and my sister Natalie for all of their help, the lunches that they made me, the rides to and from school, and for so much more. I love you guys very much.

I would like to thank all of my lab-mates, past and present, for all of their help, guidance and support. Olga, my best buddy, it has been a pleasure going through this journey with you. Thank you for your constant support. Sobia, as my KINE 4010 TA you were my first introduction to the world of exercise physiology. Thank you for the laughs, the sushi lunch sessions, as well as for giving me the motivating factor that I needed to complete my graduate studies, the Roberto Alomar bobblehead. Keir, thank you for helping me get acclimated to graduate school, as well as for all of the hours you spent training me. I knew I could always count on you for help whenever I needed it. Liam, thank you for the many (many) laughs. I'll miss watching wrestling videos on YouTube, as well as our baseball conversations (we both owe the Barrie Holiday Inn a pack of fluorescent light bulbs, by the way). Alex, my fellow Canucks fan, thank you for the great insights that you have given me, and for helping me to understand the events at the summer Olympics. Michael, my neighbour in the MHRC, thank you for all of your help, as well as for preserving my sanity as I completed the final stages of my thesis. Ayesha, my pal, thank you for all of the great conversations, movie recommendations, and help that you have given me. Giulia, thank you for welcoming me into the lab and for all of your help, as well as the unexpected breakfast treats.

TABLE OF CONTENTS

LIST OF FIGURES

LIST OF ABBREVIATIONS

ADP	adenine diphosphate
AMP	adenine monophosphate
AMPK	AMP-activated protein kinase
ARNTL	aryl hydrocarbon receptor nuclear translocator-like
ATP	adenosine triphosphate
ATG7	autophagy-related protein 7
bHLH	basic helix-loop-helix
BMAL1	brain and muscle ARNT-like protein 1
CCG	CLOCK-controlled gene
CK1ϵ	casein kinase 1ϵ
CLOCK	circadian locomotor output cycles kaput
COX	cytochrome c oxidase
Cry	cryptochrome
DNA	deoxyribonucleic acid
ETC	electron transport chain
FADH$_2$	flavin adenine dinucleotide
GSK-3β	glycogen synthase kinase-3β
HAT	histone acetyltransferase
HDAC	histone deacetylase
IMF	intermyofibrillar
LC3	microtubule-associated proteins 1A-1B light chain 3A
MAP	mean arterial pressure
mRNA	messenger ribonucleic acid
mtDNA	mitochondrial DNA
MyoD	myogenic determination factor 1
NAD$^+$	nicotinamide adenine dinucleotide
NAMPT	nicotinamide phosphoribosyltransferase
NRF	nuclear respiratory factor
NUGEMP	nuclear gene-encoded mitochondrial protein
O$_2^-$	superoxide anion
p300	E1A binding protein p300
p53	tumor protein 53
PAS	per-ARNT-sim
Per	period
PGC-1α	peroxisome proliferator-activated receptor-γ coactivator-1α
RHT	retinohypothalamic tract
PINK1	phosphatase and tensin homolog-induced putative kinase 1
RORα	retinoid-related orphan receptor α
ROS	reactive oxygen species
SCN	suprachiasmatic nucleus
SDH	succinate dehydrogenase
Sim	single-minded homolog

SirT1	sirtuin 1
SS	subsarcolemmal
Tfam	mitochondrial transcription factor-A
TA	tibialis anterior

REVIEW OF LITERATURE

1.0 CIRCADIAN RHYTHM

1.1. Overview

Circadian rhythm refers to the periodic fluctuation of various biochemical, physiological and behavioural parameters within organisms. The term circadian comes from the Latin *circa*, "around," and *diem*, "day," meaning "about a day." Nearly all organisms, ranging from single-cell bacteria to complex mammals, exhibit internal rhythmicity of a wide array of physiological processes over a 24-hour period (60; 68; 122). Body temperature (35; 90), muscle strength (99), hormone secretion (12; 55), oxygen uptake (110), gene expression (60; 68; 122), metabolic rate (107), blood pressure (28; 67) and heart rate (90) are examples of physiological and biochemical variables that have been found to exhibit *diurnal*, or "daily," oscillations.

Circadian rhythms are typically discussed in terms of the period and phase of a particular oscillator. The period of a rhythm refers to the length of one complete circadian cycle, while the phase refers to the timing of a particular point within the rhythm in relation to another oscillator (60). For example, the peak of cyclic mRNA expression for a particular gene may be expressed in relation to the peak of melatonin secretion by the pineal gland.

The molecular mechanism that generates circadian rhythms involves a highly-conserved regulatory network of transcriptional-translational feedback loops which have been observed in a multitude of mammalian tissues and cell types. These complex molecular pathways are synchronized to the 24-hour light-dark cycle of the earth (60;

122), and likely evolved due to the significant survival advantage provided by the ability to anticipate daily environmental changes (60; 80; 122).

1.2. Central and Peripheral Clocks

Endogenous molecular clocks have been found to exist in several tissues, including liver (6; 40), heart (66; 87), brain (40), adipose tissue (123) and skeletal muscle (68). There is a central, or "master," circadian clock located within the suprachiasmatic nucleus (SCN) of the hypothalamus that is responsible for the synchronization of clocks in peripheral tissues (65; 93). The importance of the SCN in the maintenance of systemic behavioural rhythmicity has been made quite apparent in studies that involve the surgical ablation of this region of the hypothalamus. Diurnal locomotor activity and food consumption have been found to be arrhythmic in animals with SCN lesions (21; 61; 102). In addition, transplantation of cells from the SCN of intact animals has restored the circadian rhythmicity of locomotor activity in previously-arrythmic animals with SCN lesions (21; 61). The mechanism of the synchronization of peripheral clocks by the SCN has not been fully established, however it is believed to rely on the coordinated release of various neural and humoral factors (65; 93) (Fig. 1).

1.3. Zeitgebers and Entrainment

The ability to synchronize the endogenous circadian clock with environmental time cues provides organisms with a unique selective advantage. An animal is considered entrained when its endogenous rhythm is congruent with a fixed environmental cue, such

as light (10; 60). An entrained animal will exhibit an endogenous circadian period length that is equal to that of the environmental cue, which is approximately 24 hours. Circadian research in mammals has been predominantly conducted on rodents. Rodents are nocturnal, and therefore exhibit increased metabolic activity, locomotor activity and food consumption during the active dark phase (107; 110).

Environmental stimuli that are utilized for entrainment are referred to as zeitgebers, which is derived from the Latin *zeit*, "time," and *geber*, "giver." Zeitgebers are essential to ensure that the mammalian molecular clock remains synchronized with the 24-hour light-dark cycle of the earth. The primary circadian zeitgeber is sunlight, while secondary zeitgebers include temperature and nutrient availability (93; 122). Synchronization of the central circadian clock in the SCN with the light-dark cycle of the earth occurs through the retinohypothalamic tract (RHT), which directly connects the photosensitive retinal ganglion cells of the mammalian eye to the SCN (49; 50; 60). Circadian rhythmicity has been shown to persist even in the absence of external signals. The period that is exhibited under these conditions is referred to as the endogenous circadian period (32; 110; 112). The endogenous period is not exactly 24 hours, however, and exhibits slight variations depending on the species (23; 38; 110). This disparity emphasizes the importance of zeitgebers, such as light, in maintaining the synchronicity of the mammalian clock with the surrounding environment.

The relationship between central and peripheral circadian clocks has been an important subject of recent research. Contrary to the initial paradigm, it appears that the molecular clock in peripheral tissues can be phase-dissociated from the central molecular

clock in the SCN by restrictive feeding (19; 103) and by scheduled bouts of physical activity (47; 117; 119; 121). Studies have ascertained that the presentation of food during the light cycle, which is out-of-phase relative to the innate onset of food consumption that occurs during the dark cycle, can alter the phase of cyclic gene expression by 10 – 12 hours in peripheral tissues, but not in the SCN (19; 103). In addition to food as a non-photic zeitgeber, scheduled bouts of voluntary or involuntary physical activity can also synchronize biological rhythms in animals. It has been observed that scheduled exercise bouts result in reduced time required for re-entrainment to a new light-dark cycle (119; 121). Furthermore, scheduled exercise bouts during the inactive light phase cause accelerated phase-shifts of gene expression in skeletal muscle (117) (Fig. 1).

1.4. Evolutionary Adaptive Value

Biological rhythms evolved due to their adaptive value, as they allow for the anticipation and subsequent evasion of environmental hazards, therefore conferring a significant selective advantage (60; 122). Specifically, a study by Paranjpe and Sharma (2005) employed surgical ablation of the SCN as a model of disrupting the circadian clock in squirrels. Following release into the wilderness, animals with SCN lesions exhibited a mortality rate that was two-fold greater in comparison with the control group. The increased rate of mortality in the absence of a properly-functioning circadian clock emphasizes the importance of biological timekeeping in the survival of organisms.
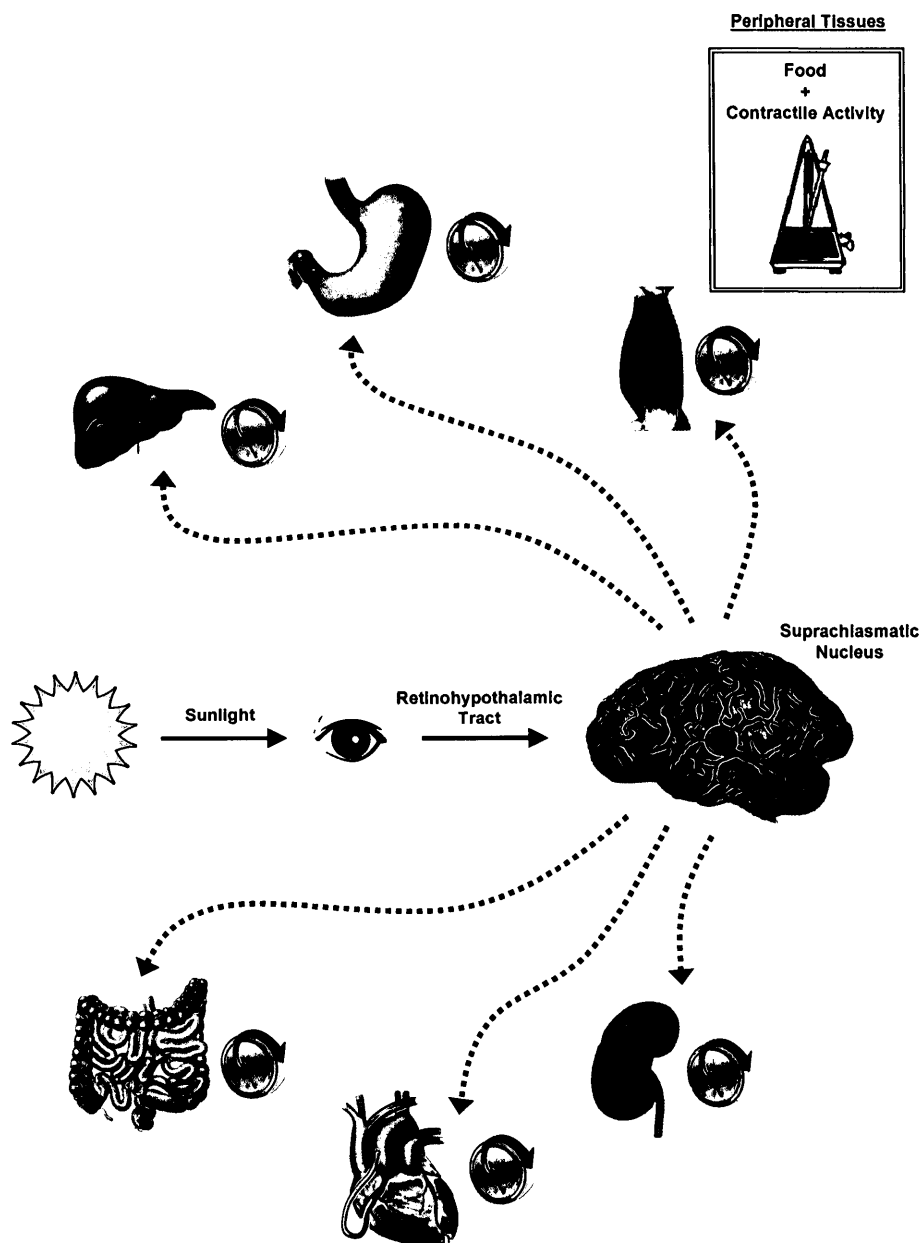
Figure 1. *Central and peripheral circadian clocks.* Biological timekeeping mechanisms persist in all bodily tissues. The central circadian clock is located in the SCN within the hypothalamus. Light, the primary zeitgeber that is used to synchronize the central molecular clock, is absorbed by the eye and conveyed by the RHT to the hypothalamus, where it is interpreted by the SCN. This information is then disseminated to circadian clocks within peripheral tissues. Within peripheral tissues, nutrient availability and contractile activity are additional zeitgebers that synchronize the molecular clock, and have been shown to be more significant than light in terms of altering circadian parameters.

1.6. The Core Molecular Clock

The core molecular mechanism that governs the periodic oscillation of these processes involves a highly-conserved regulatory network of transcriptional-translational feedback loops. Within this network there are two sub-pathways, the positive and negative feedback components, which collectively govern rhythmic gene expression. The positive component of the molecular clock is primarily comprised of two proteins, circadian locomotor output cycles kaput (CLOCK) and brain and muscle aryl hydrocarbon receptor nuclear translocator (ARNT)-like protein 1 (BMAL1), which belong to the basic helix-loop-helix (bHLH) Per-ARNT-Sim (PAS) family of transcription factors (60; 122). The functionality of these types of transcription factors is dependent upon their bHLH-PAS domain-mediated dimerization (51; 81). CLOCK and BMAL1, therefore, form a heterodimer and subsequently translocate into the nucleus. The rate-limiting step in this heterodimerization is the cytoplasmic abundance of BMAL1 (89). The CLOCK:BMAL1 heterodimer binds to E-box sequences (CACGTG) within the promoter regions of CLOCK-controlled genes (CCGs) and enhances their transcription (60; 122) (Fig. 2).

An important subset of CCGs is those that encode for the negative component of the molecular clock, which is comprised of Period (Per1, Per2) and Cryptochrome (Cry1, Cry2, Cry3). The binding of CLOCK and BMAL1 to E-box regulatory sequences enhances the transcription of Per and Cry. CLOCK:BMAL1-mediated expression of Per and Cry eventually results in the accumulation of these protein products within the cytoplasm. Per and Cry proteins form a multimeric protein aggregate with casein kinase

1ε (CK1ε) and subsequently translocate into the nucleus. The rate-limiting step in the formation of this complex is the cytoplasmic availability of Per1 (113). This multimeric protein repressor complex comprises the negative component of the molecular clock. The repressor complex binds to and inhibits the CLOCK:BMAL1 transcription-activation complex (60; 122). Per appears to facilitate nuclear entry of the repressor complex (59), while Cry attenuates the histone acetyltransferase capability of the CLOCK:BMAL1 heterodimer (26). Due to the inhibition Per and Cry impose upon their own transcription, the amalgamation of both the positive and negative components of the molecular clock (CLOCK:BMAL1–Cry:Per) is collectively referred to as the central autoregulatory feedback loop (60; 122) (Fig. 2).

1.5.1. Histone Modifications and Chromatin Remodelling

Acetylation and deacetylation of histones are important enzymatic reactions that regulate diurnal gene expression. Acetylation of histones alters chromatin to expose promoter regions to the transcriptional machinery, and is therefore associated with activation of gene expression. Conversely, histone deacetylation leads to chromatin condensation and is correlated with gene repression (26; 57). Chromatin-remodelling events are essential in the temporal regulation of gene expression (33; 39; 76).

1.5.1.1. CLOCK

It has been shown by Etchegaray *et al.* (2003) that the histone acetyltransferase (HAT) E1A binding protein p300 (p300) diurnally colocalizes with CLOCK in the nucleus, suggestive of the notion that p300 is likely an additional constituent of the transcription-activation complex. It has also been observed that p300 is a target for Cry-

mediated inhibition (26), further implicating p300 in the rhythmic expression of CCGs. Similarly, in addition to its role as a transcription factor, CLOCK also possesses intrinsic histone acetyltransferase activity (22; 37). CLOCK rhythmically acetylates BMAL1 at a specific residue that allows Cry of the repressor complex to bind to and inhibit the transcription-activation complex (39) (Fig. 2).

1.5.1.2. SirT1

The histone deacetylase (HDAC) sirtuin 1 (SirT1) has been associated with rhythmic gene silencing. SirtT1 requires oxidized nicotinamide adenine dinucleotide (NAD^+) as an obligatory cosubstrate in order to function properly (17; 69). Cellular levels of NAD^+, as well as the rate-limiting enzyme that is involved in its synthesis, nicotinamide phosphoribosyltransferase (NAMPT), have both been shown to exhibit diurnal expression (69; 77; 78). Despite its role as a histone deacetylase, SirtT1 does not possess intrinsic DNA-binding capabilities. Recent research has discovered that histone deacetylation by SirT1 is facilitated through its binding with the CLOCK:BMAL1 heterodimer within the promoter region of CCGs (77). Further contributing to the temporal regulation of gene expression, SirT1 also deacetylates Per2 within the repressor complex, leading to its degradation (11). Lastly, rhythmic SirT1 deacetylase activity has been reported to be significantly out of phase in relation to oscillating histone acetylation (77). The antiphasic oscillatory relationship of HAT and HDAC activity implies that chromatin-remodelling is an essential mechanism in the circadian regulation of gene expression (Fig. 2).

1.5.2. Phosphorylation of Clock Proteins

Rhythmic phosphorylation of molecular clock components is integral in maintaining the appropriate length of the circadian period. Phosphorylation modulates the period of biological rhythms by controlling the initiation, duration and termination of both the positive and negative components of the molecular clock (36; 45; 59; 89; 100; 113). Two important serine-threonine protein kinases are involved in regulating the temporal activity of components of the molecular clock: 1) glycogen synthase kinase-3β (GSK-3β) and 2) CK1ε.

1.5.2.1. GSK-3β

GSK-3β requires phosphorylation by an upstream kinase in order to be functionally active. GSK-3β activity has been found to exhibit circadian rhythmicity in both the SCN as well as certain peripheral tissues, with GSK-3β reaching its peak level of activity during the early stages of the light cycle (60). Dependant upon the time of day, GSK-3β will phosphorylate either positive (89; 100) or negative (36; 45) components of the molecular clock, exerting a wide array of effects on its downstream targets.

Early in the light phase, GSK-3β phosphorylates members of the positive component of the molecular clock. GSK-3β interacts with BMAL1, targeting it for ubiquitination and subsequent degradation (89). Furthermore, it has been observed by Spengler et al. (2009) that BMAL1 phosphorylates CLOCK, allowing it to be further activated by GSK-3β and subsequently degraded. GSK-3β has also been observed to phosphorylate and stabilize Rev-erbα, a transcriptional co-repressor, enabling it to inhibit BMAL1 transcription (120). GSK-3β stabilizes CLOCK and BMAL1 abundance at a

time when there is elevated BMAL1 protein content in the cytoplasm (60; 68), therefore imposing a necessary time-delay between the accumulation of cytoplasmic BMAL1 and the activity of the CLOCK:BMAL1 transcription-activation complex (Fig. 2).

Early in the dark phase, GSK-3β phosphorylates members of the negative component of the molecular clock. It has been observed by Iitaka et al. (2005) that GSK-3β interacts with Per2 within the repressor complex, enhancing its ability to enter the nucleus and inhibit the transcription of CCGs. Conversely, GSK-3β phosphorylates Cry2 within the repressor complex and targets it for subsequent degradation (36). In addition to temporally regulating the transcription-activation complex, GSK-3β can also delay or advance the molecular clock by altering the time of onset of transcriptional repression, thereby modulating the length of the circadian period (Fig. 2).

1.5.2.2. CK1ε

CK1ε abundance at the protein level has not been found to exhibit circadian oscillations (59). CK1ε primarily interacts with components of the repressor complex (5; 98), and dependant upon the time of day, CK1ε will exert a variety of effects on its downstream targets within the repressor complex (59; 113).

Late in the light phase, CK1ε phosphorylates Per1, inducing a conformational change that encumbers its nuclear localization signal. This hindrance prevents nuclear translocation of the repressor complex, and thereby indirectly allows for CLOCK:BMAL1-mediated transcription of CCGs (113). CK1ε also interacts with Per3, signalling it for degradation (5; 98). Late in the dark phase, CK1ε hyper-phosphorylates proteins within the repressor complex, targeting the entire complex for degradation and

indirectly allowing the transcription-activation complex to begin to induce the expression of CCGs (59), thus assisting in the initiation of a new circadian cycle. CK1ε modulates the initiation, duration and termination of the repressor complex, thereby wielding an important level of temporal influence on the circadian period (Fig. 2).

1.6. The Molecular Clock in Skeletal Muscle

Endogenous biological rhythms have been found to persist in a multitude of peripheral tissues, including skeletal muscle. Gene expression profiling in skeletal muscle by McCarthy et al. (2007) concluded that 215 genes exhibited a circadian pattern of expression. These genes encompass a broad range of functions within skeletal muscle, including transcription, intracellular signalling and metabolism. Myogenic determination factor 1 (MyoD), a protein that is important for skeletal muscle cell development, was one of the genes that was reported to exhibit a diurnal expression pattern (68).

The inherent relationship between the SCN and molecular clocks in peripheral tissues has not been fully determined, although it has been postulated to involve the modulated release of neural and humoral factors (65; 93). Metabolic sensors are responsive to extracellular physiological stimuli, such as contractile activity (94; 106), nutrient availability (35) and energy homeostasis (16; 17; 69). Metabolic sensors impose post-translational modifications on the molecular clock components, thereby modulating the length and phase of the circadian period. Three important circadian metabolic sensors that interact with the molecular clock are: 1) adenine monophosphate (AMP)-activated protein kinase (AMPK), 2) peroxisome proliferator-activated receptor-γ coactivator-1α

(PGC-1α) and 3) SirT1. These metabolic sensors exhibit inherent circadian rhythmicity in their activity levels, suggesting a mutually-dependent relationship between circadian rhythm and cellular metabolism (60).

1.6.1. MyoD

MyoD is a skeletal muscle-specific bHLH-PAS transcription factor that is activated during the early stages of muscle tissue formation, a process that is known as myogenesis. MyoD influences undifferentiated mesodermal cells to commit to the muscle lineage. MyoD coordinates muscle cell differentiation by regulating the expression of various structural, functional and metabolic skeletal muscle-specific genes during myogenesis (13; 14).

It has been recently postulated by both Andrews et al. (2010) and McCarthy et al. (2007) that MyoD is a CCG. MyoD has been observed to exhibit circadian fluctuations at the mRNA level (68). This diurnal expression pattern of MyoD mRNA is abolished in CLOCK$^{\Delta 19}$ and BMAL1$^{-/-}$ circadian mutant mice (8). Furthermore, skeletal muscle from both CLOCK$^{\Delta 19}$ and BMAL1$^{-/-}$ mice exhibit severely impaired force production and myofilament organization (8), implying that the circadian clock influences skeletal muscle phenotype by regulating MyoD expression.

1.6.2. AMPK

AMPK is a well-established mediator of metabolic pathways. In skeletal muscle, AMPK is activated by stimuli that increase the intracellular AMP:ATP ratio, such as contractile activity (94; 106) and glucose restriction (16; 29). In response to physiological stimuli, AMPK regulates pathways in the metabolism of carbohydrates, proteins and

lipids (116). AMPK exists as a heterotrimeric protein that is composed of α-, β-, and γ-subunits. Activation of AMPK occurs through phosphorylation at the threonine-172 residue within the catalytic α-subunit (101; 110).

In addition to its roles in intracellular metabolism, AMPK is an important secondary component in the proper functioning of the molecular clock. AMPK has been observed to exhibit diurnal activation in the hypothalamus (110) and in the liver (58), although this temporal pattern has not yet been evaluated in skeletal muscle. AMPK interacts with the molecular clock through phosphorylation of Cry1, which targets it for degradation (58). The de-stabilization of Cry1 attenuates the time interval that the repressor complex is active, thereby indirectly contributing to lengthening of the circadian period. Therefore, under conditions of contractile activity or nutrient deprivation, potential activation of AMPK may lengthen the circadian period by increasing the duration of CLOCK:BMAL1-mediated transcription (Fig. 2).

1.6.3. PGC-1α

PGC-1α is an important transcriptional co-activator that is involved in many cellular processes. PGC-1α has principally been recognized for its involvement in the regulation of mitochondrial content and function (4; 109). In addition to this role, PGC-1α is also involved in skeletal muscle fiber-type specialization (62) and glucose metabolism (70). PGC-1α promotes gene expression by binding with transcription factors and subsequently assisting in recruitment of HAT proteins to the promoter region (85).

Recent literature has implicated PGC-1α as a significant contributor in the coordinated regulation of the biological clock. PGC-1α has been reported to exhibit

diurnal oscillations at the mRNA level in skeletal muscle (72). Furthermore, PGC-1α binds with retinoid-related orphan receptor α (RORα) when it is bound to its respective ROR response element within the BMAL1 promoter. This binding facilitates the recruitment of the HAT p300, thereby inducing BMAL1 transcription (48; 64). This interaction is consistent with the finding that peak PGC-1α mRNA expression coincides with peak BMAL1 transcription (64). Therefore, by modulating the duration of BMAL1 transcription, PGC-1α assists in the regulation of the circadian period (Fig. 2).

1.6.4. SirT1

As has been previously discussed in section 1.5.1.2., the oscillatory HDAC activity of SirT1 is essential in counteracting the transcriptional activity of the CLOCK:BMAL1 heterodimer, thereby maintaining the integrity of the timekeeping mechanism (77). SirT1 also mediates the duration of activity of the repressor complex by rhythmically deacetylating Per2 (11). SirT1 activity is inherently dependent upon the intracellular NAD^+:NADH ratio, which is reflective of the energy homeostasis and the cellular redox status (17; 69). Therefore, by functioning as a metabolic sensor, SirT1 HDAC activity manipulates the length of the circadian period based upon cellular energy demands.
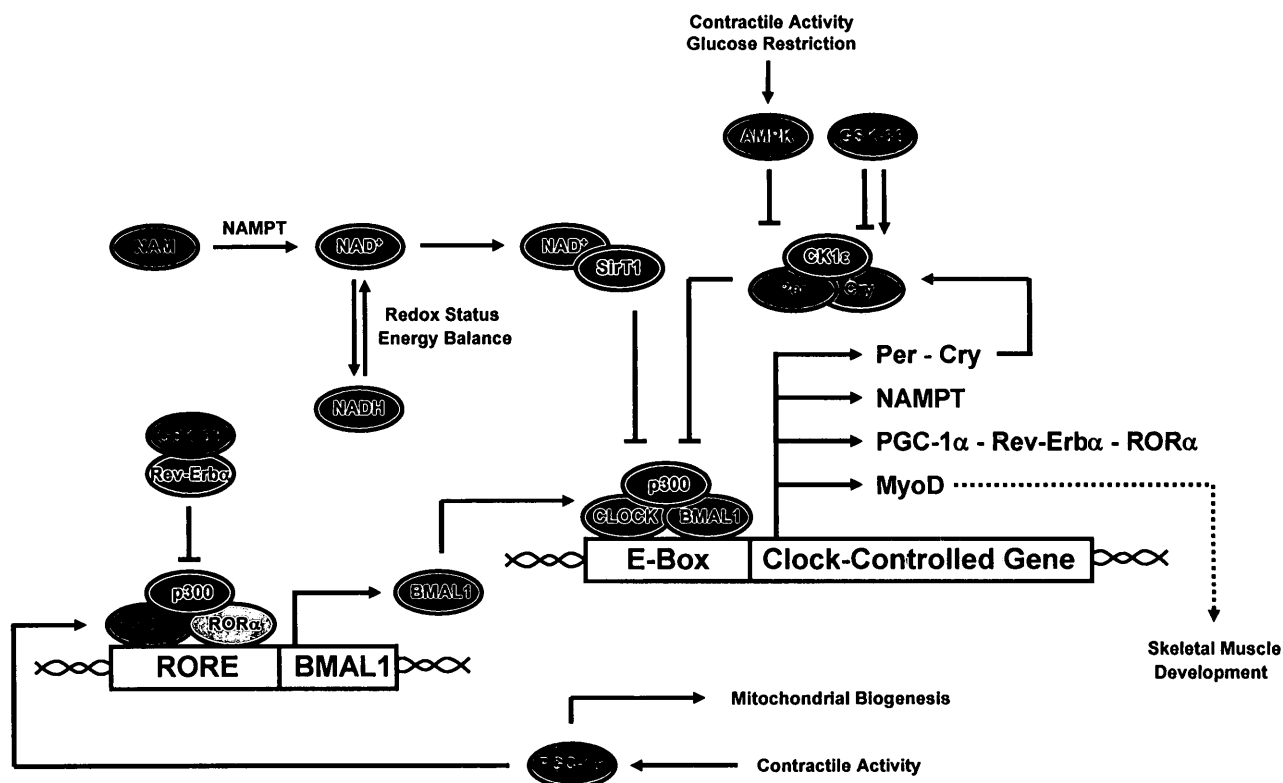
Figure 2. *The core molecular clock in skeletal muscle.* CLOCK:BMAL1 heterodimers comprise the transcription-activation complex (positive component) of the molecular clock. This heterodimer binds to E-Box DNA sequences within the promoter regions of CCGs. Through the recruitment of numerous HATs, such as p300, the CLOCK:BMAL1 heterodimer rhythmically induces the transcription of CCGs. A repressor complex (negative component) that consists primarily of two CCG products, period and cryptochrome, aggregate in the cytoplasm and translocate into the nucleus. This repressor protein aggregate rhythmically inhibits the transcription-activation complex. In peripheral tissues, intracellular metabolic sensors (AMPK, PGC-1α and SirT1) interact with the molecular clock via post-translational modifications as a means of altering the circadian period and phase to correspond with extracellular stimuli. AMPK periodically phosphorylates and destabilizes Cry1, thereby regulating the active duration of the transcriptional repressor complex. PGC-1α, which exhibits diurnal expression, binds to response elements in the BMAL1 promoter, thereby inducing its transcription. The HDAC SirT1 rhythmically counteracts the transcriptional activity of the CLOCK:BMAL1 heterodimer.

2.0 THE *CLOCK* GENE

2.1. Overview

The *Clock* gene was initially characterized in mammals by Vitaterna et al. in 1994. This study utilized N-ethyl-N-nitrosourea, a potent murine mutagen (88), to induce mutations to spermatogonial cells of male mice. Mutations in genes that affect circadian rhythms were identified by increased circadian period length, which was indirectly measured through aberrations in the pattern of daily locomotor activity under conditions of constant darkness (114). Analyses of subsequent generations of mutant progeny revealed that this mutation is heritable, and in addition to an elongated endogenous circadian period, circadian rhythmicity is eventually completely absent under conditions of constant darkness (114).

The *Clock* gene has been extensively studied over the past 18 years. The *Clock* gene encodes for the protein CLOCK, which as previously discussed in section 1.1.5., heterodimerizes with BMAL1 to form the transcription-activation complex that is a component of the central autoregulatory feedback loop (60; 122). CLOCK also has been observed to facilitate circadian gene expression by recruiting the HAT p300 to the transcription-activation complex within the promoter regions of CCGs (26). It was additionally purported by Hirayama et al. (2007) that CLOCK-mediated acetylation of BMAL1 was an essential event to maintain the integrity of the biological timekeeping mechanism.

2.2. Structure

The murine *Clock* gene is approximately 100,000 base pairs in length (9; 53), and has been mapped to chromosome 5 (53; 114). The murine CLOCK protein consists of 855 amino acids that are organized into 24 exons, and it has a predicted molecular mass of 96.4 kDa (53). CLOCK contains two distinct functional regions within its secondary structure: 1) a bHLH-domain and 2) a PAS-domain. The bHLH-domain consists of two amphipathic α-helices connected by a loop, as well as a downstream sequence of basic amino acid residues (51). The α-helices are required for dimerization (20), while the sequence of basic amino acids facilitates the interaction with the E-Box DNA sequence within the promoter region (75). The PAS-domain is composed of a five-strand anti-parallel β-sheet followed by numerous downstream α-helices (73; 81). The association of respective PAS-domains has been implicated in stabilizing protein dimerization (24).

2.3. Expression

The temporal and tissue-specific patterns of *Clock* expression have been well-characterized. Northern blot analysis of *Clock* expression in several types of murine tissue by King et al. (1997) revealed that *Clock* mRNA expression is not limited to the SCN. Significant *Clock* mRNA expression was evident in the retina, as well as in the testis, ovaries, liver, kidney and heart tissues (53). The *Clock* gene has been observed to be constitutively-expressed in the SCN throughout the light-dark cycle (96; 97). In contrast to the SCN, Lee et al. (2001) reported that *Clock* mRNA appears to exhibit modest rhythmicity within the liver *in vivo*. The isolation of cytoplasmic and nuclear

intracellular fractions has revealed minor diurnal fluctuations in nuclear CLOCK protein abundance in the SCN (56) and in the liver (59).

The temporal intracellular expression and localization patterns of CLOCK and its binding partner, BMAL1, reveal a unique level of transcriptional control within the molecular clock mechanism. It has been well-documented that BMAL1 gene expression exhibits robust oscillations within both the SCN (1; 41) and peripheral tissues (7; 68). The dimerization of CLOCK and BMAL1 occurs through the interaction of their respective bHLH-PAS domains (20; 24), and is essential for nuclear translocation of the transcription-activation complex (56). Therefore, the fact that CLOCK displays relatively constant temporal cytoplasmic protein expression lends credibility to the finding that rhythmic cytoplasmic BMAL1 protein accumulation modulates the formation of the transcription-activation complex (89). The temporal expression pattern of the *Clock* gene confers an intricate level of transcriptional control to the biological clock.

2.4. *Clock* Mutant Mice

As has been previously discussed in section 2.1., a mutation within the *Clock* gene was first distinguished by Vitaterna et al. (1994). This study involved inducing genetic mutations within spermatogonial cells of male mice, and subsequently identifying mutant progeny according to elongated endogenous circadian periods (114). King et al. (1997) ascertained that the genetic basis of this mutation was characterized by a single point mutation, an A → T transversion, within the 5' splice donor site of intron 19. Subsequent analyses reveal that this mutation results in a splice variant that does not contain exon 19,

a segment that consists of 51 amino acids, within the functional polypeptide (53). The

abnormal CLOCK$^{\Delta 19}$ mutant polypeptide retains the ability to both heterodimerize with

BMAL1, as well as to bind to E-Box DNA sequences, however the CLOCK$^{\Delta 19}$:BMAL1

transcription-activation capability is severely impaired (30) (Fig. 3).
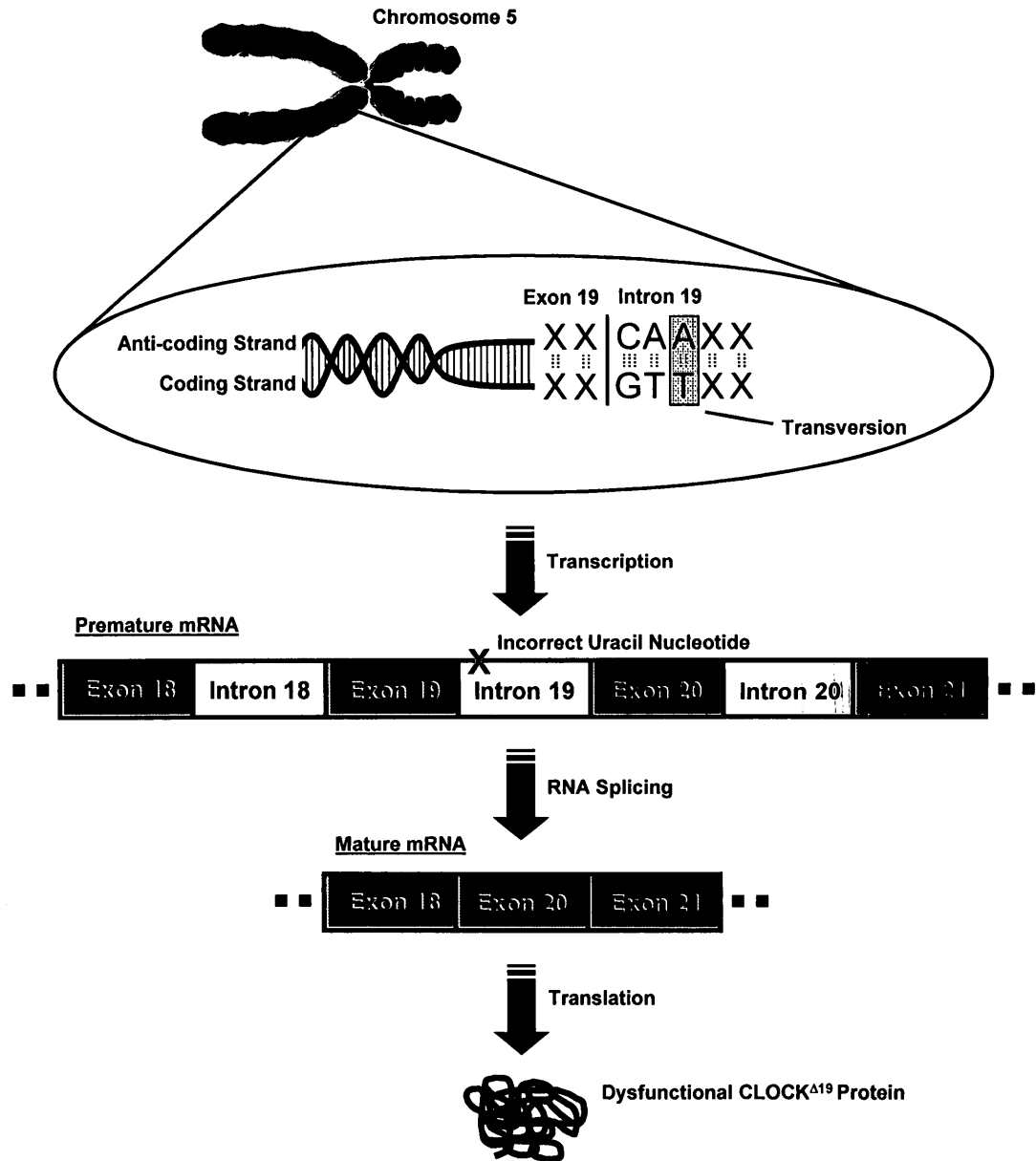
Figure 3. *The Clock mutation.* The *Clock* mutation is characterized by a single point mutation, an A → T transversion, at the third base position of the 5' splice donor site within intron 19 of the coding (sense) DNA strand. The corresponding mRNA transcript erroneously contains a uracil ribonucleotide in place of an adenine ribonucleotide. This alteration potentially inhibits the biochemical interaction between the mRNA and the spliceosome. The result is that exon 19 is absent from the mature mRNA transcript, resulting in a dysfunctional CLOCK$^{\Delta 19}$ protein that does not contain the 51-amino acid segment encoded by exon 19.

2.4.1. Gene Expression

The circadian transcriptome was first characterized in skeletal muscle by McCarthy et al. (2007). This study collected gastrocnemius hindlimb muscles under conditions of constant darkness from wild-type and homozygous *Clock* mutant mice at 4-hour intervals, and subsequently utilized gene expression profiling to measure the activity of multiple genes. A cosine wave-fitting algorithm was then applied in order to determine which mRNA transcripts exhibited a circadian pattern of expression (68). In accordance with these rigorous criteria, it was observed that 215 genes exhibited a circadian pattern of expression in skeletal muscle, including numerous components of the molecular clock, such as BMAL1, Per2 and Cry2. Interestingly, the expression pattern of the *Clock* gene was not statistically-determined to exhibit circadian rhythmicity as defined by the parameters employed in this study (68). The 215 circadian genes were observed to encompass a wide array of physiological processes, most notably transcription (18%), cellular signalling (15%) and protein metabolism (12%). The times of peak gene expression were very broad, however they were similarly-distributed between the subjective day (48%) and the subjective night (52%) (68). In accordance with the statistical parameters of this study, it was concluded that PGC-1α mRNA did not exhibit a circadian pattern of expression, although more recent work by Miyazaki et al. (2011) purported that PGC-1α does, in fact, exhibit diurnal expression in skeletal muscle.

McCarthy et al. (2007) also measured the alteration in skeletal muscle gene expression as a consequence of the aforementioned *Clock* mutation. To compute these alterations, the expression of a particular gene was averaged between all of the respective

time points in order to condense the diurnal expression pattern into a single arithmetic mean. Interestingly, the arithmetic mean of diurnal PGC-1α gene expression was found to exhibit over 50% reduction in the *Clock* mutant mice in comparison with the wild-type mice (8; 68). In addition to PGC-1α, numerous structural, functional and metabolic genes were suppressed in skeletal muscle as a consequence of the *Clock* mutation (68).

2.4.2. Phenotypic Characteristics

As has been previously discussed in sections 2.1. and 2.4., the *Clock* mutation is a autosomal germline mutation (30; 53; 114), and therefore all somatic cells within the fully-developed organism will express the abnormal CLOCK$^{\Delta 19}$ protein. Extensive research has been conducted on homozygous *Clock* mutant mice, and consequently, many neurological and behavioural phenotypic aberrations have been described in these animals. The preliminary study by Vitaterna et al. (1994) reported that homozygous *Clock* mutant mice display a 24-hour circadian period when light is provided as a zeitgeber. Over this 24-hour period, these animals slept approximately 18% less than the wild-type animals (79). In the absence of photic time cues, the circadian period of homozygous *Clock* mutant mice initially lengthened to approximately 27.3 hours before exhibiting complete arrythmicity after 10 days of exposure to constant darkness (114). Lastly, homozygous *Clock* mutant mice exhibit increased food intake, basal metabolic rate and levels of locomotor activity during the light phase, as well as accelerated body mass accumulation beginning at four weeks of age (107).

Homozygous *Clock* mutant mice exhibit disrupted circadian gene expression and altered phenotypic characteristics within peripheral tissues. It was observed by Oishi et

al. (2000) that, in homozygous *Clock* mutant mice, the amplitude of BMAL1 mRNA expression was diminished in liver, heart and kidney. Disruption in the diurnal variation of mean arterial pressure (MAP) has also been observed in these animals (18). In addition, Kennaway et al. (2006) reported disrupted diurnal mRNA expression of BMAL1, Per2 and Rev-erbα in skeletal muscle of homozygous *Clock* mutant mice. Furthermore, both Nampt gene expression and intracellular NAD^+ content have been observed to be attenuated in liver and white adipose tissue in these animals (86). Homozygous *Clock* mutant mice have also been associated with diminished glucose tolerance (52), as well as obesity and metabolic syndrome (107). It has also been reported by Andrews et al. (2011) that MyoD, PGC-1α and PGC-1β mRNA expression were impaired in the skeletal muscle of homozygous *Clock* mutant mice. In conjunction, these animals exhibit impaired myofilament organization, attenuated muscle contractility and reduced mitochondrial volume (8).

3.0 MITOCHONDRIA

3.1. Overview

Mitochondria are dynamic, membrane-bound organelles that exist within eukaryotic cells. These organelles were first identified by Altmann in 1890 (25), and are essential for the production of the energy-providing compound adenosine triphosphate (ATP), thereby ensuring the proper functioning, survival and adaptation of eukaryotic organisms. Mitochondria possess a unique and intricate molecular structure that consists of distinct outer- and inner-mitochondrial membranes, which are composed of phospholipid bilayers. The inner mitochondrial membrane defines the boundaries of the mitochondrial matrix, which contains mitochondrial DNA (mtDNA). The convoluted inner mitochondrial membrane contains numerous integral complexes, collectively referred to as the electron transport chain (ETC), which facilitate a series of redox reactions (43). Mitchell (1961) initially postulated that these reactions generate an electrochemical proton gradient, which is required for the production of ATP through chemiosmosis (25; 71). A consequence of mitochondrial oxidative phosphorylation is the coupled production of reactive oxygen species (ROS) (46; 104).

The process of mitochondrial biogenesis is heavily reliant on initial transcriptional co-activation by PGC-1α, which has been observed to catalyze the induction of numerous genes that are involved in the biosynthesis of these organelles (108; 118). There are two distinct intramuscular populations of mitochondria that have been observed within skeletal muscle fibers: 1) a subsarcolemmal (SS) subfraction that is located superficially inside the sarcolemmal membrane, and 2) an intermyofibrillar (IMF) subfraction that is

interspersed amongst the myofibrils (54). These discrete mitochondrial subfractions have been observed to exhibit distinct metabolic properties with respect to mitochondrial respiration, membrane potential and ROS production (2; 3).

3.2. Mitochondrial Biogenesis

Mitochondrial biogenesis is a complex process that involves the coordinated expression and assembly of multiple nuclear- and mitochondrially-encoded gene products (27; 44). This process is initiated by the PGC-1α-mediated coactivation of nuclear respiratory factors (NRF)-1 and -2, followed by the subsequent binding of these transcription factors to the promoter regions of nuclear genes encoding mitochondrial proteins (NUGEMPs), inducing their transcription (31; 108). NUGEMPs encode for structural and functional components of the mitochondrial ETC (83), as well as mtDNA-specific transcription factors, such as mitochondrial transcription factor-A (Tfam) (92). Mitochondrial proteins are imported into mitochondria, and subsequently assembled into multi-subunit enzyme complexes (42; 44) (Fig. 4   ).

3.3. Mitochondrial Respiration

As has been previously alluded to in section 3.1., mitochondria are primarily required for the production of ATP. The mitochondrial ETC contains five embedded complexes: 1) NADH dehydrogenase, 2) succinate dehydrogenase (SDH), 3) cytochrome b-c_l complex, 4) cytochrome c oxidase (COX) and 5) ATP synthase. Electron transport chain complexes accept electrons from the reduced coenzymes NADH and flavin adenine

dinucleotide (FADH$_2$), and subsequently transfer these electrons to a downstream electron acceptor within the ETC. Electron navigation through the ETC is coupled with proton movement from the mitochondrial matrix into the inter-membrane space, producing an electrochemical proton gradient. Passive proton diffusion into the mitochondrial matrix through ATP synthase provides chemical energy that is utilized to synthesize ATP from adenosine diphosphate (ADP) and inorganic phosphate (P$_i$).

As has been previously stated in section 3.1., there are two spatially- and metabolically-distinct mitochondrial subfractions within skeletal muscle fibers. It has been observed by Adhihetty et al. (2005) that both *active* ADP-induced (state III) and *passive* glutamate-induced (state IV) rates of mitochondrial respiration are significantly elevated in the IMF mitochondria subfractions, in comparison with SS mitochondria.

3.3.1. ROS

As has been previously mentioned in section 3.1., the production of ROS is a consequence of mitochondrial oxidative phosphorylation. As electrons are transferred along the ETC, two constituents of this chain, NADH dehydrogenase and cytochrome b-c_1 complex, erroneously donate electrons to oxygen, resulting in the production of superoxide anions (O$_2^-$) (74). ROS are deleterious molecules that can damage intracellular DNA. Despite this ROS-mediated oxidative stress, recent evidence has implicated ROS as a signalling mechanism in the induction of mitochondrial biogenesis. ROS have been associated with elevations in the mRNA expression of PGC-1α (46), as well as two additional mitochondrial biogenesis precursors, Tfam and NRF-2 (105). The concept of the ROS-mediated induction of mitochondrial biogenesis is strengthened by

the finding that contractile activity stimulated ROS production *in vitro* in skeletal muscle myotubes (82). Additionally, it has been reported that respiration-induced ROS production in the SS mitochondrial subfractions is considerably higher, in comparison with IMF mitochondria (2; 3).

3.4. Adaptation to Chronic Training

It has been very well-established that chronic endurance training increases skeletal muscle mitochondrial content, as inferred by cytochrome *c* oxidase enzymatic activity (91; 111). Furthermore, chronic endurance training has been correlated with augmentations in both mitochondrial content as well as endurance capacity (115). Recent research has supported the concept that exercise-induced mitochondrial biogenesis may be mediated by PGC-1α. Endurance-trained subjects exhibited elevated PGC-1α mRNA content following a single acute bout of exercise, in comparison with untrained subjects (84). In addition, chronic bouts of endurance exercise have resulted in amplified levels of PGC-1α protein abundance at rest (95). Therefore, it appears that there is a direct causal association between chronic endurance training, PGC-1α expression and skeletal muscle mitochondrial content. In regards to the relationship between chronic endurance training and mitochondrial function, it has been reported that chronic endurance training does not alter the substrate-induced respiratory capacity of murine skeletal muscle-isolated mitochondrial subfractions *in vivo* (2; 4; 91). This result, however, is in contrast to work that has been performed by Wu et al. (1999), which asserted that *in vitro* over-expression of PGC-1α in cultured murine myoblasts results in an increased rate of basal oxygen

consumption. Mitochondrial adaptations to chronic endurance training *in vivo* appear to be limited to increases in mitochondrial content and enzymatic activity, and do not necessarily induce improvements in properly-functioning mitochondria.

3.5. PGC-1α

As has been previously discussed in sections 3.1. and 3.2., transcriptional co-activation by PGC-1α is essential for the initiation and propagation of mitochondrial biogenesis. It has also been established in section 3.3. that the exercise-mediated induction of PGC-1α elevates mitochondrial content in skeletal muscle. Numerous studies have utilized *in vivo* models of PGC-1α over-expression and ablation to further investigate the importance of this gene in the regulation of mitochondrial biogenesis and function.

Recent research has observed that *in vivo* muscle-specific over-expression of PGC-1α has been associated with elevated levels of NUGEMP expression (15; 62). Lin et al. (2002) observed increased mRNA content of two subunits that comprise the COX complex within the ETC, COX II (mitochondrially-encoded) and COX IV (nuclear-encoded), as well as elevated cytochrome *c* protein abundance. Furthermore, muscle-specific over-expression of PGC-1α allows for phenotypic adaptations that are consistent with elevated mitochondrial content. This was evident as Calvo et al. (2008) reported improved performance ability in these animals during a forced-endurance exercise test.

The integral function of PGC-1α has become readily apparent as a result of numerous *in vivo* studies that have utilized PGC-1α$^{-/-}$ animals. These animals exhibit

attenuated mRNA content of both nuclear- and mitochondrially-encoded gene products (63), as well as reduced mitochondrial content (4). Adhihetty et al. (2009) further observed impairments in the respiratory capacity of mitochondria that were isolated from PGC-1$\alpha^{-/-}$ animals. Due to these phenotypic mitochondrial aberrations, PGC-1$\alpha^{-/-}$ animals also exhibited an expected impairment in performance ability during a forced-endurance test (34).
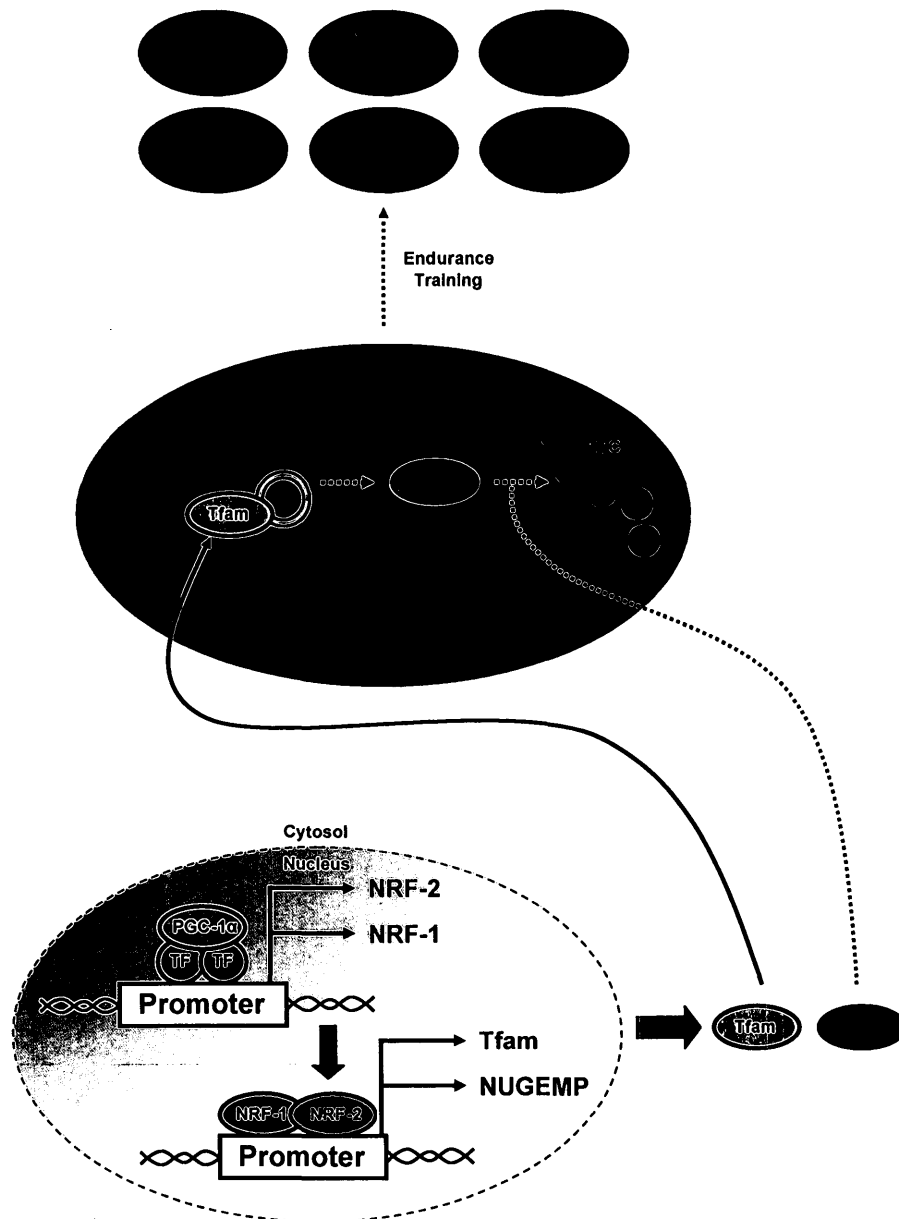
Figure 4. *Mitochondrial biogenesis.* The transcriptional coactivator PGC-1α binds to transcription factors within the promoter regions of NRF-1 and -2, thereby inducing the expression of these nuclear respiratory factors. NRF-1 and -2 subsequently induce the expression of Tfam, as well as NUGEMPs, such as COX IV. Tfam is imported into the mitochondrion, and it subsequently induces transcription of components of the mitochondrial genome, such as COX I. NUGEMPS, as well as mitochondrially-encoded gene products, are assembled into multi-subunit enzyme complexes. Endurance training induces the expression of PGC-1α, thereby resulting in increased mitochondrial biogenesis.

4.0 THESIS OBJECTIVES

Therefore, based on this review of literature, the primary objectives of my thesis utilizing *Clock* mutant mice are to:

1. Assess the repercussions of the *Clock* mutation on exercise tolerance, metabolism and skeletal muscle mitochondrial physiology.

2. Evaluate the efficacy of chronic voluntary endurance training on eliciting physiological and metabolic adaptations within *Clock* mutant mice.

4.1 Hypotheses

We hypothesized that:

1. *Clock* mutant mice would exhibit accelerated body mass and lipid accumulation, diminished protein expression, attenuated mitochondrial content and function, impaired glucose tolerance and reduced exercise capacity.

2. Endurance training would elicit metabolic adaptations within the *Clock* mutant mice that would improve mitochondrial function and content, glucose tolerance and exercise capacity, and attenuate the accelerated accumulation of body mass.

Reference List

1. **Abe H, Honma S, Namihira M, Tanahashi Y, Ikeda M and Honma K.** Circadian rhythm and light responsiveness of BMAL1 expression, a partner of mammalian clock gene Clock, in the suprachiasmatic nucleus of rats. *Neurosci Lett* 258: 93-96, 1998.

2. **Adhihetty PJ, Ljubicic V and Hood DA.** Effect of chronic contractile activity on SS and IMF mitochondrial apoptotic susceptibility in skeletal muscle. *Am J Physiol Endocrinol Metab* 292: E748-E755, 2007.

3. **Adhihetty PJ, Ljubicic V, Menzies KJ and Hood DA.** Differential susceptibility of subsarcolemmal and intermyofibrillar mitochondria to apoptotic stimuli. *Am J Physiol Cell Physiol* 289: C994-C1001, 2005.

4. **Adhihetty PJ, Uguccioni G, Leick L, Hidalgo J, Pilegaard H and Hood DA.** The role of PGC-1alpha on mitochondrial function and apoptotic susceptibility in muscle. *Am J Physiol Cell Physiol* 297: C217-C225, 2009.

5. **Akashi M, Tsuchiya Y, Yoshino T and Nishida E.** Control of intracellular dynamics of mammalian period proteins by casein kinase I epsilon (CKIepsilon) and CKIdelta in cultured cells. *Mol Cell Biol* 22: 1693-1703, 2002.

6. **Akhtar RA, Reddy AB, Maywood ES, Clayton JD, King VM, Smith AG, Gant TW, Hastings MH and Kyriacou CP.** Circadian cycling of the mouse liver transcriptome, as revealed by cDNA microarray, is driven by the suprachiasmatic nucleus. *Curr Biol* 12: 540-550, 2002.

7. **Ando H, Ushijima K, Yanagihara H, Hayashi Y, Takamura T, Kaneko S and Fujimura A**. Clock gene expression in the liver and adipose tissues of non-obese type 2 diabetic Goto-Kakizaki rats. *Clin Exp Hypertens* 31: 201-207, 2009.

8. **Andrews JL, Zhang X, McCarthy JJ, McDearmon EL, Hornberger TA, Russell B, Campbell KS, Arbogast S, Reid MB, Walker JR, Hogenesch JB, Takahashi JS and Esser KA**. CLOCK and BMAL1 regulate MyoD and are necessary for maintenance of skeletal muscle phenotype and function. *Proc Natl Acad Sci U S A* 107: 19090-19095, 2010.

9. **Antoch MP, Song EJ, Chang AM, Vitaterna MH, Zhao Y, Wilsbacher LD, Sangoram AM, King DP, Pinto LH and Takahashi JS**. Functional identification of the mouse circadian Clock gene by transgenic BAC rescue. *Cell* 89: 655-667, 1997.

10. **Aschoff J, Hoffmann K, Pohl H and Wever R**. Re-entrainment of circadian rhythms after phase-shifts of the Zeitgeber. *Chronobiologia* 2: 23-78, 1975.

11. **Asher G, Gatfield D, Stratmann M, Reinke H, Dibner C, Kreppel F, Mostoslavsky R, Alt FW and Schibler U**. SIRT1 regulates circadian clock gene expression through PER2 deacetylation. *Cell* 134: 317-328, 2008.

12. **Benloucif S, Guico MJ, Reid KJ, Wolfe LF, L'hermite-Baleriaux M and Zee PC**. Stability of melatonin and temperature as circadian phase markers and their relation to sleep times in humans. *J Biol Rhythms* 20: 178-188, 2005.

13. **Bergstrom DA, Penn BH, Strand A, Perry RL, Rudnicki MA and Tapscott SJ.** Promoter-specific regulation of MyoD binding and signal transduction cooperate to pattern gene expression. *Mol Cell* 9: 587-600, 2002.

14. **Berkes CA and Tapscott SJ.** MyoD and the transcriptional control of myogenesis. *Semin Cell Dev Biol* 16: 585-595, 2005.

15. **Calvo JA, Daniels TG, Wang X, Paul A, Lin J, Spiegelman BM, Stevenson SC and Rangwala SM.** Muscle-specific expression of PPARgamma coactivator-1alpha improves exercise performance and increases peak oxygen uptake. *J Appl Physiol* 104: 1304-1312, 2008.

16. **Canto C and Auwerx J.** Glucose restriction: longevity SIRTainly, but without building muscle? *Dev Cell* 14: 642-644, 2008.

17. **Chabi B, Adhihetty PJ, O'Leary MF, Menzies KJ and Hood DA.** Relationship between Sirt1 expression and mitochondrial proteins during conditions of chronic muscle use and disuse. *J Appl Physiol* 107: 1730-1735, 2009.

18. **Curtis AM, Cheng Y, Kapoor S, Reilly D, Price TS and FitzGerald GA.** Circadian variation of blood pressure and the vascular response to asynchronous stress. *Proc Natl Acad Sci U S A* 104: 3450-3455, 2007.

19. **Damiola F, Le MN, Preitner N, Kornmann B, Fleury-Olela F and Schibler U.** Restricted feeding uncouples circadian oscillators in peripheral tissues from the central pacemaker in the suprachiasmatic nucleus. *Genes Dev* 14: 2950-2961, 2000.

20. **Davis RL, Cheng PF, Lassar AB and Weintraub H**. The MyoD DNA binding domain contains a recognition code for muscle-specific gene activation. *Cell* 60: 733-746, 1990.

21. **DeCoursey PJ and Buggy J**. Circadian rhythmicity after neural transplant to hamster third ventricle: specificity of suprachiasmatic nuclei. *Brain Res* 500: 263-275, 1989.

22. **Doi M, Hirayama J and Sassone-Corsi P**. Circadian regulator CLOCK is a histone acetyltransferase. *Cell* 125: 497-508, 2006.

23. **Duffy JF and Czeisler CA**. Effect of light on human circadian physiology. *Sleep Med Clin* 4: 165-177, 2009.

24. **Erbel PJ, Card PB, Karakuzu O, Bruick RK and Gardner KH**. Structural basis for PAS domain heterodimerization in the basic helix--loop--helix-PAS transcription factor hypoxia-inducible factor. *Proc Natl Acad Sci U S A* 100: 15504-15509, 2003.

25. **Ernster L and Schatz G**. Mitochondria: a historical review. *J Cell Biol* 91: 227s-255s, 1981.

26. **Etchegaray JP, Lee C, Wade PA and Reppert SM**. Rhythmic histone acetylation underlies transcription in the mammalian circadian clock. *Nature* 421: 177-182, 2003.

27. **Falkenberg M, Gaspari M, Rantanen A, Trifunovic A, Larsson NG and Gustafsson CM**. Mitochondrial transcription factors B1 and B2 activate transcription of human mtDNA. *Nat Genet* 31: 289-294, 2002.

28. **Feldstein C, Akopian M, Olivieri AO and Garrido D**. Association between Nondipper Behavior and Serum Calcium in Hypertensive Patients with Mild-to-Moderate Chronic Renal Dysfunction. *Clin Exp Hypertens* 2012.

29. **Fulco M, Cen Y, Zhao P, Hoffman EP, McBurney MW, Sauve AA and Sartorelli V**. Glucose restriction inhibits skeletal myoblast differentiation by activating SIRT1 through AMPK-mediated regulation of Nampt. *Dev Cell* 14: 661-673, 2008.

30. **Gekakis N, Staknis D, Nguyen HB, Davis FC, Wilsbacher LD, King DP, Takahashi JS and Weitz CJ**. Role of the CLOCK protein in the mammalian circadian mechanism. *Science* 280: 1564-1569, 1998.

31. **Gleyzer N, Vercauteren K and Scarpulla RC**. Control of mitochondrial transcription specificity factors (TFB1M and TFB2M) by nuclear respiratory factors (NRF-1 and NRF-2) and PGC-1 family coactivators. *Mol Cell Biol* 25: 1354-1366, 2005.

32. **Godinho SI, Maywood ES, Shaw L, Tucci V, Barnard AR, Busino L, Pagano M, Kendall R, Quwailid MM, Romero MR, O'neill J, Chesham JE, Brooker D, Lalanne Z, Hastings MH and Nolan PM**. The after-hours mutant reveals a role for Fbxl3 in determining mammalian circadian period. *Science* 316: 897-900, 2007.

33. **Grimaldi B, Nakahata Y, Sahar S, Kaluzova M, Gauthier D, Pham K, Patel N, Hirayama J and Sassone-Corsi P**. Chromatin remodeling and circadian control: master regulator CLOCK is an enzyme. *Cold Spring Harb Symp Quant Biol* 72: 105-112, 2007.

34. **Handschin C, Chin S, Li P, Liu F, Maratos-Flier E, Lebrasseur NK, Yan Z and Spiegelman BM.** Skeletal muscle fiber-type switching, exercise intolerance, and myopathy in PGC-1alpha muscle-specific knock-out animals. *J Biol Chem* 282: 30014-30021, 2007.

35. **Hannibal J, Hsiung HM and Fahrenkrug J**. Temporal phasing of locomotor activity, heart rate rhythmicity, and core body temperature is disrupted in VIP receptor 2-deficient mice. *Am J Physiol Regul Integr Comp Physiol* 300: R519-R530, 2011.

36. **Harada Y, Sakai M, Kurabayashi N, Hirota T and Fukada Y**. Ser-557-phosphorylated mCRY2 is degraded upon synergistic phosphorylation by glycogen synthase kinase-3 beta. *J Biol Chem* 280: 31714-31721, 2005.

37. **Hardin PE and Yu W**. Circadian transcription: passing the HAT to CLOCK. *Cell* 125: 424-426, 2006.

38. **Hasan S, Santhi N, Lazar AS, Slak A, Lo J, von SM, Archer SN, Johnston JD and Dijk DJ**. Assessment of circadian rhythms in humans: comparison of real-time fibroblast reporter imaging with plasma melatonin. *FASEB J* 2012.

39. **Hirayama J, Sahar S, Grimaldi B, Tamaru T, Takamatsu K, Nakahata Y and Sassone-Corsi P**. CLOCK-mediated acetylation of BMAL1 controls circadian function. *Nature* 450: 1086-1090, 2007.

40. **Hogenesch JB, Panda S, Kay S and Takahashi JS**. Circadian transcriptional output in the SCN and liver of the mouse. *Novartis Found Symp* 253: 171-180, 2003.

41. **Honma S, Ikeda M, Abe H, Tanahashi Y, Namihira M, Honma K and Nomura M**. Circadian oscillation of BMAL1, a partner of a mammalian clock gene Clock, in rat suprachiasmatic nucleus. *Biochem Biophys Res Commun* 250: 83-87, 1998.

42. **Hood DA**. Mechanisms of exercise-induced mitochondrial biogenesis in skeletal muscle. *Appl Physiol Nutr Metab* 34: 465-472, 2009.

43. **Hood DA**. Invited Review: contractile activity-induced mitochondrial biogenesis in skeletal muscle. *J Appl Physiol* 90: 1137-1157, 2001.

44. **Hood DA, Irrcher I, Ljubicic V and Joseph AM**. Coordination of metabolic plasticity in skeletal muscle. *J Exp Biol* 209: 2265-2275, 2006.

45. **Iitaka C, Miyazaki K, Akaike T and Ishida N**. A role for glycogen synthase kinase-3beta in the mammalian circadian clock. *J Biol Chem* 280: 29397-29402, 2005.

46. **Irrcher I, Ljubicic V and Hood DA**. Interactions between ROS and AMP kinase activity in the regulation of PGC-1alpha transcription in skeletal muscle cells. *Am J Physiol Cell Physiol* 296: C116-C123, 2009.

47. **Janik D and Mrosovsky N**. Gene expression in the geniculate induced by a nonphotic circadian phase shifting stimulus. *Neuroreport* 3: 575-578, 1992.

48. **Jetten AM, Kurebayashi S and Ueda E**. The ROR nuclear orphan receptor subfamily: critical regulators of multiple biological processes. *Prog Nucleic Acid Res Mol Biol* 69: 205-247, 2001.

49. **Johnson RF, Moore RY and Morin LP**. Loss of entrainment and anatomical plasticity after lesions of the hamster retinohypothalamic tract. *Brain Res* 460: 297-313, 1988.

50. **Johnson RF, Morin LP and Moore RY**. Retinohypothalamic projections in the hamster and rat demonstrated using cholera toxin. *Brain Res* 462: 301-312, 1988.

51. **Kadesch T**. Consequences of heteromeric interactions among helix-loop-helix proteins. *Cell Growth Differ* 4: 49-55, 1993.

52. **Kennaway DJ, Owens JA, Voultsios A and Wight N**. Adipokines and adipocyte function in Clock mutant mice that retain melatonin rhythmicity. *Obesity (Silver Spring)* 20: 295-305, 2012.

53. **King DP, Zhao Y, Sangoram AM, Wilsbacher LD, Tanaka M, Antoch MP, Steeves TD, Vitaterna MH, Kornhauser JM, Lowrey PL, Turek FW and**

Takahashi JS. Positional cloning of the mouse circadian clock gene. *Cell* 89: 641-653, 1997.

54. **Kirkwood SP, Munn EA and Brooks GA**. Mitochondrial reticulum in limb skeletal muscle. *Am J Physiol* 251: C395-C402, 1986.

55. **Klerman EB, Gershengorn HB, Duffy JF and Kronauer RE**. Comparisons of the variability of three markers of the human circadian pacemaker. *J Biol Rhythms* 17: 181-193, 2002.

56. **Kondratov RV, Chernov MV, Kondratova AA, Gorbacheva VY, Gudkov AV and Antoch MP**. BMAL1-dependent circadian oscillation of nuclear CLOCK: posttranslational events induced by dimerization of transcriptional activators of the mammalian clock system. *Genes Dev* 17: 1921-1932, 2003.

57. **Kurdistani SK, Tavazoie S and Grunstein M**. Mapping global histone acetylation patterns to gene expression. *Cell* 117: 721-733, 2004.

58. **Lamia KA, Sachdeva UM, DiTacchio L, Williams EC, Alvarez JG, Egan DF, Vasquez DS, Juguilon H, Panda S, Shaw RJ, Thompson CB and Evans RM**. AMPK regulates the circadian clock by cryptochrome phosphorylation and degradation. *Science* 326: 437-440, 2009.

59. **Lee C, Etchegaray JP, Cagampang FR, Loudon AS and Reppert SM**. Posttranslational mechanisms regulate the mammalian circadian clock. *Cell* 107: 855-867, 2001.

60. **Lefta M, Wolff G and Esser KA**. Circadian rhythms, the molecular clock, and skeletal muscle. *Curr Top Dev Biol* 96: 231-271, 2011.

61. **Lehman MN, Silver R, Gladstone WR, Kahn RM, Gibson M and Bittman EL**. Circadian rhythmicity restored by neural transplant. Immunocytochemical characterization of the graft and its integration with the host brain. *J Neurosci* 7: 1626-1638, 1987.

62. **Lin J, Wu H, Tarr PT, Zhang CY, Wu Z, Boss O, Michael LF, Puigserver P, Isotani E, Olson EN, Lowell BB, Bassel-Duby R and Spiegelman BM**. Transcriptional co-activator PGC-1 alpha drives the formation of slow-twitch muscle fibres. *Nature* 418: 797-801, 2002.

63. **Lin J, Wu PH, Tarr PT, Lindenberg KS, St-Pierre J, Zhang CY, Mootha VK, Jager S, Vianna CR, Reznick RM, Cui L, Manieri M, Donovan MX, Wu Z, Cooper MP, Fan MC, Rohas LM, Zavacki AM, Cinti S, Shulman GI, Lowell BB, Krainc D and Spiegelman BM**. Defects in adaptive energy metabolism with CNS-linked hyperactivity in PGC-1alpha null mice. *Cell* 119: 121-135, 2004.

64. **Liu C, Li S, Liu T, Borjigin J and Lin JD**. Transcriptional coactivator PGC-1alpha integrates the mammalian clock and energy metabolism. *Nature* 447: 477-481, 2007.

65. **Lowrey PL and Takahashi JS**. Mammalian circadian biology: elucidating genome-wide levels of temporal organization. *Annu Rev Genomics Hum Genet* 5: 407-441, 2004.

66. **Martino T, Arab S, Straume M, Belsham DD, Tata N, Cai F, Liu P, Trivieri M, Ralph M and Sole MJ**. Day/night rhythms in gene expression of the normal murine heart. *J Mol Med (Berl)* 82: 256-264, 2004.

67. **Martino TA, Tata N, Simpson JA, Vanderlaan R, Dawood F, Kabir MG, Khaper N, Cifelli C, Podobed P, Liu PP, Husain M, Heximer S, Backx PH and Sole MJ**. The primary benefits of angiotensin-converting enzyme inhibition on cardiac remodeling occur during sleep time in murine pressure overload hypertrophy. *J Am Coll Cardiol* 57: 2020-2028, 2011.

68. **McCarthy JJ, Andrews JL, McDearmon EL, Campbell KS, Barber BK, Miller BH, Walker JR, Hogenesch JB, Takahashi JS and Esser KA**. Identification of the circadian transcriptome in adult mouse skeletal muscle. *Physiol Genomics* 31: 86-95, 2007.

69. **Menzies KJ and Hood DA**. The role of SirT1 in muscle mitochondrial turnover. *Mitochondrion* 12: 5-13, 2012.

70. **Michael LF, Wu Z, Cheatham RB, Puigserver P, Adelmant G, Lehman JJ, Kelly DP and Spiegelman BM**. Restoration of insulin-sensitive glucose transporter (GLUT4) gene expression in muscle cells by the transcriptional coactivator PGC-1. *Proc Natl Acad Sci U S A* 98: 3820-3825, 2001.

71. **Mitchell P**. Coupling of phosphorylation to electron and hydrogen transfer by a chemi-osmotic type of mechanism. *Nature* 191: 144-148, 1961.

72. **Miyazaki M, Schroder E, Edelmann SE, Hughes ME, Kornacker K, Balke CW and Esser KA**. Age-associated disruption of molecular clock expression in skeletal muscle of the spontaneously hypertensive rat. *PLoS One* 6: e27168, 2011.

73. **Moglich A, Ayers RA and Moffat K**. Structure and signaling mechanism of Per-ARNT-Sim domains. *Structure* 17: 1282-1294, 2009.

74. **Murphy MP**. How mitochondria produce reactive oxygen species. *Biochem J* 417: 1-13, 2009.

75. **Murre C, Bain G, van Dijk MA, Engel I, Furnari BA, Massari ME, Matthews JR, Quong MW, Rivera RR and Stuiver MH**. Structure and function of helix-loop-helix proteins. *Biochim Biophys Acta* 1218: 129-135, 1994.

76. **Nakahata Y, Grimaldi B, Sahar S, Hirayama J and Sassone-Corsi P**. Signaling to the circadian clock: plasticity by chromatin remodeling. *Curr Opin Cell Biol* 19: 230-237, 2007.

77. **Nakahata Y, Kaluzova M, Grimaldi B, Sahar S, Hirayama J, Chen D, Guarente LP and Sassone-Corsi P**. The NAD+-dependent deacetylase SIRT1 modulates CLOCK-mediated chromatin remodeling and circadian control. *Cell* 134: 329-340, 2008.

78. **Nakahata Y, Sahar S, Astarita G, Kaluzova M and Sassone-Corsi P**. Circadian control of the NAD+ salvage pathway by CLOCK-SIRT1. *Science* 324: 654-657, 2009.

79. **Naylor E, Bergmann BM, Krauski K, Zee PC, Takahashi JS, Vitaterna MH and Turek FW**. The circadian clock mutation alters sleep homeostasis in the mouse. *J Neurosci* 20: 8138-8143, 2000.

80. **Paranjpe DA and Sharma VK**. Evolution of temporal order in living organisms. *J Circadian Rhythms* 3: 7, 2005.

81. **Partch CL and Gardner KH**. Coactivator recruitment: a new role for PAS domains in transcriptional regulation by the bHLH-PAS family. *J Cell Physiol* 223: 553-557, 2010.

82. **Pattwell DM, McArdle A, Morgan JE, Patridge TA and Jackson MJ**. Release of reactive oxygen and nitrogen species from contracting skeletal muscle cells. *Free Radic Biol Med* 37: 1064-1072, 2004.

83. **Pierron D, Wildman DE, Huttemann M, Markondapatnaikuni GC, Aras S and Grossman LI**. Cytochrome c oxidase: evolution of control via nuclear subunit addition. *Biochim Biophys Acta* 1817: 590-597, 2012.

84. **Pilegaard H, Saltin B and Neufer PD**. Exercise induces transient transcriptional activation of the PGC-1alpha gene in human skeletal muscle. *J Physiol* 546: 851-858, 2003.

85. **Puigserver P, Adelmant G, Wu Z, Fan M, Xu J, O'Malley B and Spiegelman BM**. Activation of PPARgamma coactivator-1 through transcription factor docking. *Science* 286: 1368-1371, 1999.

86. **Ramsey KM, Yoshino J, Brace CS, Abrassart D, Kobayashi Y, Marcheva B, Hong HK, Chong JL, Buhr ED, Lee C, Takahashi JS, Imai S and Bass J.** Circadian clock feedback cycle through NAMPT-mediated NAD+ biosynthesis. *Science* 324: 651-654, 2009.

87. **Rudic RD, McNamara P, Reilly D, Grosser T, Curtis AM, Price TS, Panda S, Hogenesch JB and FitzGerald GA.** Bioinformatic analysis of circadian gene oscillation in mouse aorta. *Circulation* 112: 2716-2724, 2005.

88. **Russell WL, Kelly EM, Hunsicker PR, Bangham JW, Maddux SC and Phipps EL.** Specific-locus test shows ethylnitrosourea to be the most potent mutagen in the mouse. *Proc Natl Acad Sci U S A* 76: 5818-5819, 1979.

89. **Sahar S, Zocchi L, Kinoshita C, Borrelli E and Sassone-Corsi P.** Regulation of BMAL1 protein stability and circadian function by GSK3beta-mediated phosphorylation. *PLoS One* 5: e8561, 2010.

90. **Saini C, Morf J, Stratmann M, Gos P and Schibler U.** Simulated body temperature rhythms reveal the phase-shifting behavior and plasticity of mammalian circadian oscillators. *Genes Dev* 26: 567-580, 2012.

91. **Saleem A, Adhihetty PJ and Hood DA.** Role of p53 in mitochondrial biogenesis and apoptosis in skeletal muscle. *Physiol Genomics* 37: 58-66, 2009.

92. **Scarpulla RC.** Nuclear control of respiratory gene expression in mammalian cells. *J Cell Biochem* 97: 673-683, 2006.

93. **Schibler U, Ripperger J and Brown SA.** Peripheral circadian oscillators in mammals: time and food. *J Biol Rhythms* 18: 250-260, 2003.

94. **Scott JW, Hawley SA, Green KA, Anis M, Stewart G, Scullion GA, Norman DG and Hardie DG.** CBS domains form energy-sensing modules whose binding of adenosine ligands is disrupted by disease mutations. *J Clin Invest* 113: 274-284, 2004.

95. **Serpiello FR, McKenna MJ, Bishop DJ, Aughey RJ, Caldow MK, Cameron-Smith D and Stepto NK.** Repeated sprints alter signaling related to mitochondrial biogenesis in humans. *Med Sci Sports Exerc* 44: 827-834, 2012.

96. **Shearman LP, Sriram S, Weaver DR, Maywood ES, Chaves I, Zheng B, Kume K, Lee CC, van der Horst GT, Hastings MH and Reppert SM.** Interacting molecular loops in the mammalian circadian clock. *Science* 288: 1013-1019, 2000.

97. **Shearman LP, Zylka MJ, Reppert SM and Weaver DR.** Expression of basic helix-loop-helix/PAS genes in the mouse suprachiasmatic nucleus. *Neuroscience* 89: 387-397, 1999.

98. **Shirogane T, Jin J, Ang XL and Harper JW.** SCFbeta-TRCP controls clock-dependent transcription via casein kinase 1-dependent degradation of the mammalian period-1 (Per1) protein. *J Biol Chem* 280: 26863-26872, 2005.

99. **Souissi H, Chaouachi A, Chamari K, Dogui M, Amri M and Souissi N.** Time-of-day effects on short-term exercise performances in 10- to 11-year-old boys. *Pediatr Exerc Sci* 22: 613-623, 2010.

100. **Spengler ML, Kuropatwinski KK, Schumer M and Antoch MP**. A serine cluster mediates BMAL1-dependent CLOCK phosphorylation and degradation. *Cell Cycle* 8: 4138-4146, 2009.

101. **Stapleton D, Mitchelhill KI, Gao G, Widmer J, Michell BJ, Teh T, House CM, Fernandez CS, Cox T, Witters LA and Kemp BE**. Mammalian AMP-activated protein kinase subfamily. *J Biol Chem* 271: 611-614, 1996.

102. **Stephan FK and Zucker I**. Circadian rhythms in drinking behavior and locomotor activity of rats are eliminated by hypothalamic lesions. *Proc Natl Acad Sci U S A* 69: 1583-1586, 1972.

103. **Stokkan KA, Yamazaki S, Tei H, Sakaki Y and Menaker M**. Entrainment of the circadian clock in the liver by feeding. *Science* 291: 490-493, 2001.

104. **Suliman HB, Carraway MS and Piantadosi CA**. Postlipopolysaccharide oxidative damage of mitochondrial DNA. *Am J Respir Crit Care Med* 167: 570-579, 2003.

105. **Suliman HB, Carraway MS, Welty-Wolf KE, Whorton AR and Piantadosi CA**. Lipopolysaccharide stimulates mitochondrial biogenesis via activation of nuclear respiratory factor-1. *J Biol Chem* 278: 41510-41518, 2003.

106. **Suter M, Riek U, Tuerk R, Schlattner U, Wallimann T and Neumann D**. Dissecting the role of 5'-AMP for allosteric stimulation, activation, and deactivation of AMP-activated protein kinase. *J Biol Chem* 281: 32207-32216, 2006.

107. **Turek FW, Joshu C, Kohsaka A, Lin E, Ivanova G, McDearmon E, Laposky A, Losee-Olson S, Easton A, Jensen DR, Eckel RH, Takahashi JS and Bass J.** Obesity and metabolic syndrome in circadian Clock mutant mice. *Science* 308: 1043-1045, 2005.

108. **Uguccioni G, D'souza D and Hood DA.** Regulation of PPARgamma coactivator-1alpha function and expression in muscle: effect of exercise. *PPAR Res* 2010: 2010.

109. **Uguccioni G and Hood DA.** The importance of PGC-1alpha in contractile activity-induced mitochondrial adaptations. *Am J Physiol Endocrinol Metab* 300: E361-E371, 2011.

110. **Um JH, Pendergast JS, Springer DA, Foretz M, Viollet B, Brown A, Kim MK, Yamazaki S and Chung JH.** AMPK regulates circadian rhythms in a tissue- and isoform-specific manner. *PLoS One* 6: e18450, 2011.

111. **Vainshtein A, Kazak L and Hood DA.** Effects of endurance training on apoptotic susceptibility in striated muscle. *J Appl Physiol* 110: 1638-1645, 2011.

112. **van der Horst GT, Muijtjens M, Kobayashi K, Takano R, Kanno S, Takao M, de WJ, Verkerk A, Eker AP, van LD, Buijs R, Bootsma D, Hoeijmakers JH and Yasui A.** Mammalian Cry1 and Cry2 are essential for maintenance of circadian rhythms. *Nature* 398: 627-630, 1999.

113. **Vielhaber E, Eide E, Rivers A, Gao ZH and Virshup DM.** Nuclear entry of the circadian regulator mPER1 is controlled by mammalian casein kinase I epsilon. *Mol Cell Biol* 20: 4888-4899, 2000.

114. **Vitaterna MH, King DP, Chang AM, Kornhauser JM, Lowrey PL, McDonald JD, Dove WF, Pinto LH, Turek FW and Takahashi JS.** Mutagenesis and mapping of a mouse gene, Clock, essential for circadian behavior. *Science* 264: 719-725, 1994.

115. **Wibom R, Hultman E, Johansson M, Matherei K, Constantin-Teodosiu D and Schantz PG.** Adaptation of mitochondrial ATP production in human skeletal muscle to endurance training and detraining. *J Appl Physiol* 73: 2004-2010, 1992.

116. **Witczak CA, Sharoff CG and Goodyear LJ.** AMP-activated protein kinase in skeletal muscle: from structure and localization to its role as a master regulator of cellular metabolism. *Cell Mol Life Sci* 65: 3737-3755, 2008.

117. **Wolff G and Esser KA.** Scheduled exercise phase shifts the circadian clock in skeletal muscle. *Med Sci Sports Exerc* 2012.

118. **Wu Z, Huang X, Feng Y, Handschin C, Feng Y, Gullicksen PS, Bare O, Labow M, Spiegelman B and Stevenson SC.** Transducer of regulated CREB-binding proteins (TORCs) induce PGC-1alpha transcription and mitochondrial biogenesis in muscle cells. *Proc Natl Acad Sci U S A* 103: 14379-14384, 2006.

119. **Yamanaka Y, Honma S and Honma K.** Scheduled exposures to a novel environment with a running-wheel differentially accelerate re-entrainment of mice peripheral clocks to new light-dark cycles. *Genes Cells* 13: 497-507, 2008.

120. **Yin L, Wang J, Klein PS and Lazar MA.** Nuclear receptor Rev-erbalpha is a critical lithium-sensitive component of the circadian clock. *Science* 311: 1002-1005, 2006.

121. **Zambon AC, McDearmon EL, Salomonis N, Vranizan KM, Johansen KL, Adey D, Takahashi JS, Schambelan M and Conklin BR**. Time- and exercise-dependent gene regulation in human skeletal muscle. *Genome Biol* 4: R61, 2003.

122. **Zhang X, Dube TJ and Esser KA**. Working around the clock: circadian rhythms and skeletal muscle. *J Appl Physiol* 107: 1647-1654, 2009.

123. **Zvonic S, Ptitsyn AA, Conrad SA, Scott LK, Floyd ZE, Kilroy G, Wu X, Goh BC, Mynatt RL and Gimble JM**. Characterization of peripheral circadian clocks in adipose tissues. *Diabetes* 55: 962-970, 2006.

MANUSCRIPT

The writing of this manuscript, the data collection and statistical analyses, the experiments and preparation of the animals used in this study were all performed by Stephen Pastore. David Hood was the research director of this study.

Raw data and statistical analyses for results within this manuscript are presented in **Appendix A**. Experimental protocols utilized in this study are presented in **Appendix D**.

December, 2012

Endurance training ameliorates the metabolic and performance characteristics of circadian *Clock* mutant mice

Stephen Pastore [1,2] and David A. Hood [1,2]

[1]Muscle Health Research Center, and [2]School of Kinesiology and Health Science, York

University, Toronto, Ontario M3J 1P3, Canada

To whom correspondence should be addressed:
David A. Hood,
Muscle Health Research Center, Farquharson Life Science Bldg.,
York University, 4700 Keele St.,
Toronto, Ontario,
M3J 1P3, Canada
Tel: (416) 736-2100 ext. 66640
Fax: (416) 736-5698
E-mail: dhood@yorku.ca

Abstract

Circadian locomotor output cycles kaput (CLOCK) is a nuclear transcription factor which is a component of the central autoregulatory feedback loop that governs the generation of biological rhythms. Homozygous *Clock* mutant mice contain a truncated CLOCK$^{\Delta 19}$ protein within somatic cells, subsequently causing an impaired ability to rhythmically express circadian genes. The present study sought to investigate whether the *Clock* mutation affects mitochondrial physiology within skeletal muscle, as well as the responsiveness of these mutant animals to adapt to a chronic voluntary endurance training protocol. Within muscle, *Clock* mutant mice displayed 44% and 45% reductions in peroxisome proliferator-activated receptor-γ coactivator 1-α (PGC-1α) and mitochondrial transcription factor-A (Tfam) protein content, respectively, and an accompanying 16% decrease in mitochondrial content, as determined by cytochrome c oxidase enzyme activity. These decrements contributed to a 50% decrease in exercise tolerance in *Clock* mutant mice. Interestingly, the *Clock* mutation did not appear to alter subsarcolemmal (SS) or intermyofibrillar (IMF) mitochondrial respiration within muscle, or systemic glucose tolerance. Daily locomotor activity levels were similar between wildtype and *Clock* mutant mice throughout the training protocol. Endurance training ameliorated the decrease in PGC-1α protein expression and mitochondrial content in the *Clock* mutant mice, eliciting a 2.9-fold improvement in exercise tolerance. Thus, our data suggest that a functional CLOCK protein is essential to ensure the maintenance of mitochondrial content within muscle, although the absence of a functional CLOCK protein does not impair the ability of animals to adapt to chronic exercise.

Introduction

Circadian rhythms govern a wide variety of biochemical, physiological and behavioural processes within organisms. Body temperature (19; 43), hormone secretion (7; 31), blood pressure (15; 36) and gene expression (3; 39) are among the physiological and biochemical variables that exhibit rhythmic fluctuation. The mechanism that regulates the rhythmicity of these processes involves complex temporal interaction of the positive and negative feedback components of the molecular clock. The positive component of the molecular clock is comprised of two proteins, circadian locomotor output cycles kaput (CLOCK) and brain and muscle ARNT-like protein 1 (BMAL1). These proteins heterodimerize and bind to E-box sequences within promoters to induce the expression of CLOCK-controlled genes (CCGs) (32; 57). A notable subset of CCGs encode for two constituents of the negative component of the molecular clock, Period (Per) and Cryptochrome (Cry). Per and Cry form a multimeric protein aggregate that rhythmically inhibits the transcriptional activity of the CLOCK:BMAL1 heterodimer (32; 57).

Homozygous *Clock* mutant mice possess a truncated CLOCK$^{\Delta 19}$ protein within somatic cells (30), and are characterized by an impaired ability to rhythmically activate transcription (16). Consequently, *Clock* mutant mice were reported to exhibit disrupted skeletal muscle myofilament organization, as well as attenuations in muscle contractility, mitochondrial volume and peroxisome proliferator-activated receptor-γ coactivator 1-α (PGC-1α) mRNA expression (3). In addition, these animals have been associated with altered glucose metabolism (29), as well as obesity and metabolic syndrome (49).

The central circadian clock is located within the suprachiasmatic nucleus (SCN) of the hypothalamus (35; 45). This circadian pacemaker is responsive to light, and is essential for the synchronization of molecular clocks in peripheral tissues. Molecular clocks have also been observed within numerous peripheral tissue types, including skeletal muscle (37). These peripheral clocks can be phase-dissociated from the central clock by various types of external stimuli, such contractile activity (54; 56), restrictive feeding (10; 48) and alterations in energy homeostasis (5; 40). Biological rhythms have been well-documented in skeletal muscle. McCarthy et al. (37) were the first to conduct gene expression profiling in skeletal muscle, and it was concluded that over 200 genes exhibited a rhythmic pattern of expression. These genes were observed to encompass a broad range of physiological processes, including transcription, cellular signaling and protein metabolism (37).

Mitochondria are dynamic organelles that are a very important component of properly-functioning skeletal muscle. The convoluted inner mitochondrial membrane contains the mitochondrial electron transport chain (ETC), which is comprised of five integral complexes: 1) NADH dehydrogenase, 2) succinate dehydrogenase (SDH), 3) cytochrome $b\text{-}c_1$ complex, 4) cytochrome c oxidase (COX) and 5) ATP synthase (23). The ETC facilitates a series of redox reactions that generates an electrochemical proton gradient, which is required for the production of adenosine triphosphate (ATP) (13; 38). Interestingly, it has been reported that components of the mitochondrial ETC are encoded by both the nuclear and mitochondrial genomes (14; 24). The process of mitochondrial biogenesis, however, requires initial nuclear stimulation by PGC-1α, followed by

subsequent induction of the mitochondrial genome by mitochondrial transcription factor-A (Tfam). It has been well-documented that chronic endurance training results in elevations in PGC-1α (42; 46) and Tfam (17) gene expression. Consequently, chronic endurance training has been reported to induce a PGC-1α-mediated increase in skeletal muscle mitochondrial content (44; 51), concomitant with increases in endurance capacity (52).

The purpose of the present study was to assess the physiological and biochemical ramifications of the murine *Clock* mutation. In particular, we sought to measure indices that may be affected as a result of the significant reduction in PGC-1α mRNA levels that have been observed in these animals (3; 37). It had previously been reported that PGC-1α ablation resulted in attenuated mitochondrial content and impaired mitochondrial function (1), and therefore we hypothesized that homozygous *Clock* mutant mice would exhibit these same deficient mitochondrial characteristics. Consequently, we speculated that these potential physiological impairments would translate into diminished endurance performance. Lastly, we evaluated the effects of an eight-week chronic voluntary endurance training protocol on the restoration of PGC-1α content, as well as the impact of exercise on the improvement of the same aforementioned physiological indices. Our results help to clarify the relationship between circadian rhythm and skeletal muscle function, as well as provide insight as to the role of the *Clock* gene in the adaptations of skeletal muscle to chronic exercise.

Materials and Methods

Animal breeding. Heterozygous *Clock* mutant mice (maintained on a C57BL-6J genetic background) were obtained from the Jackson Laboratory (Bar Harbor, Maine, USA). Animals were bred in accordance with the guidelines of the York University Animal Care Committee. Progeny were genotyped similarly to Herzog et al. (20). Briefly, ear clippings were utilized for crude DNA extraction. DNA extracts were incubated with Jumpstart RED-Taq DNA Polymerase (Sigma; St. Louis, Missouri, USA), as well as forward and reverse primers for the wildtype or mutant nucleotide sequences, and amplified using polymerase chain reaction (PCR). The reaction products were separated on a 1.5% agarose gel, and visualized with the use of ethidium bromide (20).

Voluntary wheel-running exercise model. Twelve-week old male wildtype and *Clock* mutant mice were assigned to control or trained experiment groups. All mice were maintained on a 12-hour light:dark cycle and were allowed access to food and water *ad libitum*. Trained mice were housed individually and were permitted access to a freely-rotating running wheel. The number of revolutions were recorded daily for each animal and converted into distance (kilometres; (44). This training model was utilized for eight weeks. During the ninth week, all animals were subjected to an intraperitoneal glucose tolerance test and an exercise capacity test, followed by the animals being sacrificed.

Muscle extraction. Animals were anesthetized in accordance with the guidelines of the York University Animal Care Committee. Animals were injected in the intraperitoneal cavity with a ketamine-xylazine mixture at 0.2 mL·100 g^{-1} of body mass. Hindlimb skeletal muscles [gastrocnemius, tibialis anterior (TA), quadriceps] were quickly excised

and placed in ice-cold mitochondrial isolation buffer. Freshly-harvested skeletal muscles were utilized for mitochondrial isolations, or were frozen in liquid nitrogen. Frozen skeletal muscle tissues were pulverized into powder with a liquid nitrogen-cooled steel mortar, and stored in liquid nitrogen for subsequent tissue analyses.

Protein extraction and quantification. Frozen skeletal muscle tissue powder was re-suspended with a 10-fold dilution in muscle extraction buffer that contained protease inhibitors. Homogenates were rotated end-over-end for 1 hour at 4°C. Homogenates were then sonicated (3 x 3 seconds; 30% power) and centrifuged at 14,000 g for 10 minutes at 4°C. The supernatant fraction was removed, quantified using the Bradford assay (58), and stored at -80°C to be used for subsequent protein analyses.

Intraperitoneal glucose tolerance test. In accordance with the optimal parameters that had been reported by Andrikopolous et al. (4), animals were fasted for six hours (beginning at 8:00 AM), but were still allowed access to water *ad libitum*. A 0.2 $g \cdot mL^{-1}$ solution of D-glucose was prepared, and animals were injected with a 2 $g \cdot kg^{-1}$ dosage of the glucose solution in the intraperitoneal cavity. Blood measurements were obtained from tail veins. Blood glucose was measured prior to injection, as well as 15-, 30-, 60- and 120-minutes post-injection (4). Blood glucose measurements were assayed using a Bayer Contour blood glucose meter (Toronto, Ontario, Canada).

Cytochrome c oxidase (COX) enzyme activity. Enzyme extracts were prepared from powdered muscle tissue, and COX enzyme activity was evaluated similarly to Cogswell et al. (9). Briefly, enzyme extracts were sonicated (3 x 3 seconds; 30% power) and COX enzyme activity was determined spectrophotometrically as the maximal rate of oxidation

of fully-reduced cytochrome c (Sigma; St. Louis, Missouri, USA), measured by the change in absorbance at 550 nm using a Synergy HT microplate reader at 30°C (9).

Exercise capacity test. Animals were acclimatized to the treadmill (10° incline) over a period of three days during the eighth week of the exercise protocol. The first day of acclimatization involved the animals being placed on the stationary treadmill belt for five minutes. The second and third days of acclimatization involved briefly running on the treadmill at speeds of 5 m·min^{-1} and 10 m·min^{-1}, respectively. The exercise capacity test protocol was adapted from Calvo et al. (8). Briefly, the speed of the treadmill was progressively increased by increments of 4 m·min^{-1} until animals reached exhaustion. Exhaustion was defined as the animals inability to run on the rear of the treadmill for more than five consecutive seconds (8).

Mitochondrial isolation. Freshly-harvested skeletal muscles were minced, homogenized and subjected to differential centrifugation to isolate the subsarcolemmal (SS) and intermyofibrillar (IMF) mitochondrial subfractions, as described previously (9; 34). Mitochondrial subfractions were then suspended in re-suspension medium (100 mM KCl, 10 mM MOPS, 0.2% BSA, pH 7.4), quantified and immediately utilized for analysis of mitochondrial respiration.

Mitochondrial respiration. Freshly-isolated SS and IMF mitochondrial subfractions were incubated with VO_2 buffer (250 mM sucrose, 50 mM KCl, 25 mM Tris-HCl, 10 mM K_2HPO_4, pH 7.4) at 30°C in a water-jacketed respiratory chamber with continuous stirring. Respiration rates (n atoms O_2 · min^{-1} · mg^{-1}) were evaluated in the presence of 10 mM glutamate (state IV; passive respiration) and 0.44 mM ADP (state III; active

respiration) utilizing a Mitocell S200 Micro-Respirometry System (Strathkelvin Instruments; Motherwell, UK) (1; 9; 34). Inner mitochondrial membrane integrity was assayed through the addition of NADH, which did not alter the rate of oxygen consumption in the respiratory chamber.

Immunoblotting. Skeletal muscle protein extracts were separated utilizing 10-12% sodium dodecyl sulfate polyacrylamide gel electrophoresis and transferred to a nitrocellulose membrane. The membranes were incubated with primary antibodies targeting α-tubulin (Calbiochem; 1:10,000), PGC-1α (Millipore; 1:500), CLOCK (Santa-Cruz Biotechnology; 1:1000), BMAL1 (Abcam; 1:500), COX I (Abcam; 1:1000), Tfam [Gordon et al. (17); 1:2500] and COX IV (Invitrogen; 1:250) overnight at 4°C. Blots were subsequently incubated with the appropriate species-specific secondary antibody for one hour at 25°C. Blots were developed with Western Blot Luminol Reagent (Santa-Cruz Biotechnology; Santa Cruz, California, USA) and films were scanned and analyzed using SigmaScan Pro software (version 5.0). The quantification of all blots was corrected for loading using α-tubulin protein expression.

Statistical analyses. Data are expressed as mean ± standard error (SE). Two-way analyses of variance (ANOVA) were performed when the control and trained condition were being compared between wildtype and *Clock* mutant animals, followed by the Bonferroni post-hoc test when appropriate. Statistical differences were considered significant if $p < 0.05$.

Results

Physical and locomotor characteristics. To assess alterations in body mass progression, animals were weighed on a weekly basis. *Clock* mutant control and trained mice exhibited elevated body mass throughout the duration of the study, culminating in increases of approximately 11 - 12% in comparison to their wildtype counterparts (Fig. 1A). Furthermore, chronic voluntary endurance training produced significant attenuations in body mass in both the wildtype and *Clock* mutant mice. These differences were initially evident after one week of training, and persisted throughout the duration of the study, ultimately resulting in reductions in body mass of approximately 10 – 11% for both the wildtype and *Clock* mutant trained mice (Fig. 1A). At the conclusion of the sixth week, food pellet consumption was evaluated for three complete daily cycles at 7:00 AM (ZT 0; lights on) and 7:00 PM (ZT 12; lights off). As expected, food consumption was markedly increased during the dark phase in comparison to the light phase for all four experimental groups. Interestingly, daily food intake was distinctly elevated in the *Clock* mutant control mice by 67% relative to the wildtype control mice. Endurance training resulted in further increases in daily food consumption of 76% and 37% in the wildtype and *Clock* mutant mice, respectively (Fig. 1B; $p < 0.05$). Concomitantly, *Clock* mutant control mice exhibited 4.3-fold greater food consumption during the light phase in comparison to the wildtype control mice. Endurance training further produced 2.6- and 1.4-fold increases in food consumption during the light phase in the wildtype and *Clock* mutant mice, respectively (Fig. 1C; $p < 0.05$).

Clock mutant mice displayed a 1.8-fold reduction in mean daily locomotor activity relative to the wildtype mice during the final week of training (Fig. 2A; $p < 0.05$). In addition, locomotor activity was assessed at ZT 0 and ZT 12 for three complete daily cycles during the sixth week of training. Interestingly, Clock mutant mice were observed to perform 13.5% of their daily locomotor activity during the light phase in comparison to only 0.3% in wildtype mice (Fig. 2B; $p < 0.05$). After the final week of training, animals were sacrificed and the gastrocnemius muscle complex, visceral fat depots and heart were harvested, weighed and frozen in liquid nitrogen. The visceral fat-to-body mass ratio was increased in the Clock mutant control mice by 66% relative to the wildtype control mice. Endurance training was an effective intervention and was observed to decrease this ratio by 19% and 32% in the wildtype and Clock mutant mice, respectively (Fig. 3A; $p < 0.05$). No significant differences were detected in gastrocnemius- or heart-to-body mass ratios among these same experimental groups (Fig. 3B and 3C).

Mitochondrial and physiological adaptations. To determine the tolerance of these animals to maximal-intensity exercise, a treadmill test was administered. Clock mutant control mice were only able to run on the treadmill for 51% of the time exhibited by the wildtype control mice. Endurance training was able to ameliorate this, leading to a marked 2.9-fold improvement in exercise tolerance. Training had a modest 1.4-fold effect on exercise tolerance in the wildtype mice (Fig. 4A; $p < 0.05$). Whole-muscle COX enzyme activity, a well-established indicator of muscle mitochondrial content, was reduced in the Clock mutant control mice by 16% in comparison to the wildtype control

mice (Fig. 4B; $p < 0.05$). Endurance training produced an augmentation in COX enzyme activity of 12% in wildtype mice. Interestingly, endurance training reversed the decrement in COX activity that was evident in the *Clock* mutant mice, increasing the level by 19% (Fig. 4B; $p < 0.05$). As expected, a significant correlation was evident between whole-muscle COX enzyme activity and the time necessary to reach exhaustion (Fig. 4C; $p < 0.05$).

Intraperitoneal glucose tolerance. To assess the ability of these animals to metabolize glucose, an intraperitoneal glucose tolerance test was utilized. No significant difference was observed in blood-glucose levels between the wildtype and *Clock* mutant mice. Endurance training resulted in 35% and 29% reductions in blood-glucose levels 60-minutes post-injection in the wildtype and *Clock* mutant mice, respectively (Fig. 5A; $p < 0.05$). No significant differences were observed in glucose tolerance between wildtype and *Clock* mutant mice. However, as expected, endurance training produced 20% and 21% improvements in glucose tolerance, respectively (Fig. 5B; $p < 0.05$).

SS and IMF mitochondrial respiration. To evaluate mitochondrial, state III and state IV respiration rates were measured in both the SS and IMF mitochondrial subfractions. There were no differences observed in state III or state IV respiration rates between wildtype and *Clock* mutant control mice, nor was an effect of training observed, in either the SS or the IMF mitochondrial subfractions (Fig. 6A and 6B).

Mitochondrial and circadian protein expression. To determine the extent to which protein expression in muscle tissue differed due to mutation of the *Clock* gene or endurance training, western blotting was utilized. *Clock* mutant control mice exhibited a

marked 44% reduction in PGC-1α protein content relative to the wildtype control mice. Endurance training had a curative effect in the *Clock* mutant trained mice, restoring PGC-1α protein content to the levels observed in the wildtype mice (Fig. 7A; $p < 0.05$). Similarly, expression of the nuclear-encoded products Tfam and COX IV mitochondrial subunit were attenuated in the *Clock* mutant control mice by 45% and 41%, respectively (Fig. 7B and 7C; $p < 0.05$). Endurance training did not alter COX IV protein expression in the present study, however it did elicit 22% and 49% increases in Tfam protein expression in the wildtype and *Clock* mutant mice, respectively (Fig. 7B and 7C). In contrast to COX IV, there was no effect of genotype on the protein expression of the mitochondrially-encoded COX I mitochondrial subunit. However, endurance training produced marked elevations in COX I protein expression of 41% and 50% in the wildtype and *Clock* mutant mice, respectively (Fig. 7D; $p < 0.05$). The levels of CLOCK and BMAL1 protein expression were not significantly altered with either mutation of the *Clock* gene or endurance training (Fig. 7E)

Discussion

It has been established that skeletal muscle exhibits considerable metabolic plasticity in response to chronic exercise (21), and that the transcriptional coactivator PGC-1α is a partial regulator of the exercise-induced mitochondrial adaptations that occur within skeletal muscle (2; 6; 8; 22; 50). Recent research has shown that PGC-1α displays a rhythmic gene expression pattern (39), and that it may serve to assist in synchronization of the molecular clock in peripheral tissues (26; 33). Indeed, PGC-1α is a component of an immense subset of genes that exhibit circadian rhythmicity, and which are centrally regulated by CLOCK (32; 57). The accumulation of evidence suggests a crucial role of biological rhythms in the regulation and coordination of physiological performance, as it has been observed that there are diurnal variations in both peak neuromuscular function (18; 55) and maximal oxygen uptake (53). Furthermore, molecular circadian rhythmicity is required to maintain functional skeletal muscle phenotype (3). Despite these advancements, the multifaceted relationship between circadian rhythms and skeletal muscle physiology remains to be fully identified.

An important animal model for the study of circadian rhythms has been the development of the homozygous *Clock* mutant mouse. The truncated CLOCK$^{\Delta 19}$ protein in these animals does not contain exon 19, a polypeptide segment that consists of 51 amino acids (30). Consequently, these animals are characterized by numerous deleterious phenotypic traits, including accelerated body mass and lipid accumulation (49), altered gene expression (28; 41) and dysfunctional skeletal muscle structure and contractility (3). We observed that *Clock* mutant mice displayed increases in both body mass and daily

food consumption in comparison to their wildtype counterparts. These increases are likely due to alterations in the expression of energy-regulating peptides within the hypothalamus of *Clock* mutant mice (49). Hypothalamic injury has previously been correlated with an increase in food consumption, and consequently body mass. In addition, it has been revealed that *Clock* mutant mice have decreased daily energy expenditure, further contributing to a positive energy balance and accelerated accumulation of body mass (49).

Clock mutant control mice exhibited a modest reduction in skeletal muscle COX enzyme activity, a well-established indicator of mitochondrial content, in comparison to the wildtype control mice. This decline is likely a consequence of the decrease in PGC-1α protein content that we observed in the *Clock* mutant control mice, as PGC-1α has previously been correlated with skeletal muscle COX enzyme activity both *in vitro* (50) and *in vivo* (1). The reduction of muscle mitochondrial content was corroborated by the decrease in protein expression of the nuclear-encoded COX IV subunit that was evident in the *Clock* mutant mice. This decrease in mitochondrial content that was displayed in the *Clock* mutant control mice was accompanied by a marked decrease in exercise tolerance in these animals. However, the relatively small decrement in muscle mitochondrial content that was observed in the *Clock* mutant control mice did not parallel the more pronounced 50% reduction in exercise tolerance, nor could this decrease in performance be attributable to mitochondrial dysfunction. In contrast to the mitochondrial dysfunction evident in BMAL1 (3), PGC-1α (1) and p53 (44) knockout mice, no alteration in state III or state IV mitochondrial respiration was evident in the

Clock mutant mice. Since research has revealed that mitochondrial content and function are closely related to endurance performance (25), this suggests that other skeletal muscle deficiencies evident in *Clock* mutant mice, including myofilament disorganization and diminished contractility (3), likely contributed to the impaired exercise tolerance that was evident in these animals.

Chronic voluntary endurance training is a potent exercise model that induces physiological and biochemical adaptations within rodent skeletal muscle (44; 51). Our results indicate that *Clock* mutant mice are complicit and responsive towards a voluntary exercise protocol. Consistent with the data reported by Turek et al. (2005), the *Clock* mutant mice were more active during the light phase in comparison to the wildtype mice, although total daily locomotor activity between these genotypes was similar. Voluntary exercise appeared to ameliorate the accumulation of body mass in the *Clock* mutant mice, resulting in a similar body mass progression as the wildtype control animals. As expected, the *Clock* mutant control mice displayed an increased visceral fat-to-body mass ratio in comparison to their wildtype counterparts, and endurance training was effective in reversing this obese phenotype by increasing daily caloric expenditure. Despite this robust effect of training, the exercise model did not induce either skeletal muscle or cardiac hypertrophy. The decline in voluntary exercise that was observed in the *Clock* mutant mice at the end of the study protocol can potentially be attributable to their increased body mass and adiposity, as this would have resulted in a greater level of work required while exercising on the running wheel.

We sought to ascertain the efficacy of this voluntary endurance training model to elicit metabolic improvements in the skeletal muscle of *Clock* mutant mice. Our results indicate that training restored the expression of skeletal muscle PGC-1α protein content to the levels observed in the wildtype mice, and produced a corresponding increase in muscle mitochondrial content, as evident from the increases in both COX enzyme activity, as well as Tfam and COX I subunit protein expression in both the wildtype and *Clock* mutant mice. Training also markedly improved exercise tolerance in the *Clock* mutant mice, despite the more modest training-induced increase in skeletal muscle mitochondrial content. In addition to increases in mitochondrially-mediated lipid catabolism (11), endurance training in mice elicits improvements in both maximal oxygen consumption (12) and cardiac function (27), and these adaptations likely also contributed to the training-induced improvement in exercise tolerance in the *Clock* mutant mice.

A multitude of metabolic deficiencies have been observed in *Clock* mutant mice, including hyperglycemia (49) and a high-fat diet-induced propensity towards impaired glucose tolerance (29). Thus, we hypothesized that *Clock* mutant control mice would exhibit a corresponding attenuation in glucose tolerance in comparison to the wildtype control mice. Our results suggest that there are no discernible differences in glucose tolerance between the wildtype and *Clock* mutant mice fed a normal diet, as both experimental groups displayed an equal area under the curve of the blood-glucose graph. However, it is relevant to note that endurance training was effective in improving glucose

tolerance in both the wildtype and *Clock* mutant mice, and this is consistent with data that has been previously reported (47).

In summary, our data suggest that the CLOCK protein is vital to maintaining adequate physiological levels of mitochondria within skeletal muscle. Despite the numerous impairments previously observed in the *Clock* mutant mice, the dysfunctional CLOCK protein does not appear to diminish the ability of these animals to adapt to chronic exercise. Furthermore, endurance training is an effective intervention which reverses the metabolic defect observed in the absence of a functional CLOCK protein.

Acknowledgments

Reference List

1. **Adhihetty PJ, Uguccioni G, Leick L, Hidalgo J, Pilegaard H and Hood DA.**
    The role of PGC-1alpha on mitochondrial function and apoptotic susceptibility in
    muscle. *Am J Physiol Cell Physiol* 297: C217-C225, 2009.

2. **Akimoto T, Pohnert SC, Li P, Zhang M, Gumbs C, Rosenberg PB, Williams
    RS and Yan Z.** Exercise stimulates Pgc-1alpha transcription in skeletal muscle
    through activation of the p38 MAPK pathway. *J Biol Chem* 280: 19587-19593,
    2005.

3. **Andrews JL, Zhang X, McCarthy JJ, McDearmon EL, Hornberger TA,
    Russell B, Campbell KS, Arbogast S, Reid MB, Walker JR, Hogenesch JB,
    Takahashi JS and Esser KA.** CLOCK and BMAL1 regulate MyoD and are
    necessary for maintenance of skeletal muscle phenotype and function. *Proc Natl
    Acad Sci U S A* 107: 19090-19095, 2010.

4. **Andrikopoulos S, Blair AR, Deluca N, Fam BC and Proietto J.** Evaluating the
    glucose tolerance test in mice. *Am J Physiol Endocrinol Metab* 295: E1323-
    E1332, 2008.

5. **Asher G, Gatfield D, Stratmann M, Reinke H, Dibner C, Kreppel F,
    Mostoslavsky R, Alt FW and Schibler U.** SIRT1 regulates circadian clock gene
    expression through PER2 deacetylation. *Cell* 134: 317-328, 2008.

6. **Baar K, Wende AR, Jones TE, Marison M, Nolte LA, Chen M, Kelly DP and
    Holloszy JO.** Adaptations of skeletal muscle to exercise: rapid increase in the
    transcriptional coactivator PGC-1. *FASEB J* 16: 1879-1886, 2002.

7. **Benloucif S, Guico MJ, Reid KJ, Wolfe LF, L'hermite-Baleriaux M and Zee PC**. Stability of melatonin and temperature as circadian phase markers and their relation to sleep times in humans. *J Biol Rhythms* 20: 178-188, 2005.

8. **Calvo JA, Daniels TG, Wang X, Paul A, Lin J, Spiegelman BM, Stevenson SC and Rangwala SM**. Muscle-specific expression of PPARgamma coactivator-1alpha improves exercise performance and increases peak oxygen uptake. *J Appl Physiol* 104: 1304-1312, 2008.

9. **Cogswell AM, Stevens RJ and Hood DA**. Properties of skeletal muscle mitochondria isolated from subsarcolemmal and intermyofibrillar regions. *Am J Physiol* 264: C383-C389, 1993.

10. **Damiola F, Le MN, Preitner N, Kornmann B, Fleury-Olela F and Schibler U**. Restricted feeding uncouples circadian oscillators in peripheral tissues from the central pacemaker in the suprachiasmatic nucleus. *Genes Dev* 14: 2950-2961, 2000.

11. **Eaton S, Bartlett K and Pourfarzam M**. Mammalian mitochondrial beta-oxidation. *Biochem J* 320 (Pt 2): 345-357, 1996.

12. **Ericsson M, Andersson KB, Amundsen BH, Torp SH, Sjaastad I, Christensen G, Sejersted OM and Ellingsen O**. High-intensity exercise training in mice with cardiomyocyte-specific disruption of Serca2. *J Appl Physiol* 108: 1311-1320, 2010.

13. **Ernster L and Schatz G**. Mitochondria: a historical review. *J Cell Biol* 91: 227s-255s, 1981.

14. **Falkenberg M, Gaspari M, Rantanen A, Trifunovic A, Larsson NG and Gustafsson CM**. Mitochondrial transcription factors B1 and B2 activate transcription of human mtDNA. *Nat Genet* 31: 289-294, 2002.

15. **Feldstein C, Akopian M, Olivieri AO and Garrido D**. Association between nondipper behavior and serum calcium in hypertensive patients with mild-to-moderate chronic renal dysfunction. *Clin Exp Hypertens* 2012.

16. **Gekakis N, Staknis D, Nguyen HB, Davis FC, Wilsbacher LD, King DP, Takahashi JS and Weitz CJ**. Role of the CLOCK protein in the mammalian circadian mechanism. *Science* 280: 1564-1569, 1998.

17. **Gordon JW, Rungi AA, Inagaki H and Hood DA**. Effects of contractile activity on mitochondrial transcription factor A expression in skeletal muscle. *J Appl Physiol* 90: 389-396, 2001.

18. **Guette M, Gondin J and Martin A**. Time-of-day effect on the torque and neuromuscular properties of dominant and non-dominant quadriceps femoris. *Chronobiol Int* 22: 541-558, 2005.

19. **Hannibal J, Hsiung HM and Fahrenkrug J**. Temporal phasing of locomotor activity, heart rate rhythmicity, and core body temperature is disrupted in VIP receptor 2-deficient mice. *Am J Physiol Regul Integr Comp Physiol* 300: R519-R530, 2011.

20. **Herzog ED, Takahashi JS and Block GD**. Clock controls circadian period in isolated suprachiasmatic nucleus neurons. *Nat Neurosci* 1: 708-713, 1998.

21. **Holloszy JO**. Biochemical adaptations in muscle. Effects of exercise on mitochondrial oxygen uptake and respiratory enzyme activity in skeletal muscle. *J Biol Chem* 242: 2278-2282, 1967.

22. **Hood DA**. Mechanisms of exercise-induced mitochondrial biogenesis in skeletal muscle. *Appl Physiol Nutr Metab* 34: 465-472, 2009.

23. **Hood DA**. Invited Review: contractile activity-induced mitochondrial biogenesis in skeletal muscle. *J Appl Physiol* 90: 1137-1157, 2001.

24. **Hood DA, Irrcher I, Ljubicic V and Joseph AM**. Coordination of metabolic plasticity in skeletal muscle. *J Exp Biol* 209: 2265-2275, 2006.

25. **Irrcher I, Adhihetty PJ, Joseph AM, Ljubicic V and Hood DA**. Regulation of mitochondrial biogenesis in muscle by endurance exercise. *Sports Med* 33: 783-793, 2003.

26. **Jetten AM, Kurebayashi S and Ueda E**. The ROR nuclear orphan receptor subfamily: critical regulators of multiple biological processes. *Prog Nucleic Acid Res Mol Biol* 69: 205-247, 2001.

27. **Kemi OJ, Loennechen JP, Wisloff U and Ellingsen O**. Intensity-controlled treadmill running in mice: cardiac and skeletal muscle hypertrophy. *J Appl Physiol* 93: 1301-1309, 2002.

28. **Kennaway DJ, Owens JA, Voultsios A and Varcoe TJ**. Functional central rhythmicity and light entrainment, but not liver and muscle rhythmicity, are Clock independent. *Am J Physiol Regul Integr Comp Physiol* 291: R1172-R1180, 2006.

29. **Kennaway DJ, Owens JA, Voultsios A and Wight N**. Adipokines and adipocyte function in Clock mutant mice that retain melatonin rhythmicity. *Obesity (Silver Spring)* 20: 295-305, 2012.

30. **King DP, Zhao Y, Sangoram AM, Wilsbacher LD, Tanaka M, Antoch MP, Steeves TD, Vitaterna MH, Kornhauser JM, Lowrey PL, Turek FW and Takahashi JS**. Positional cloning of the mouse circadian clock gene. *Cell* 89: 641-653, 1997.

31. **Klerman EB, Gershengorn HB, Duffy JF and Kronauer RE**. Comparisons of the variability of three markers of the human circadian pacemaker. *J Biol Rhythms* 17: 181-193, 2002.

32. **Lefta M, Wolff G and Esser KA**. Circadian rhythms, the molecular clock, and skeletal muscle. *Curr Top Dev Biol* 96: 231-271, 2011.

33. **Liu C, Li S, Liu T, Borjigin J and Lin JD**. Transcriptional coactivator PGC-1alpha integrates the mammalian clock and energy metabolism. *Nature* 447: 477-481, 2007.

34. **Ljubicic V, Adhihetty PJ and Hood DA**. Role of UCP3 in state 4 respiration during contractile activity-induced mitochondrial biogenesis. *J Appl Physiol* 97: 976-983, 2004.

35. **Lowrey PL and Takahashi JS**. Mammalian circadian biology: elucidating genome-wide levels of temporal organization. *Annu Rev Genomics Hum Genet* 5: 407-441, 2004.

36. **Martino TA, Tata N, Simpson JA, Vanderlaan R, Dawood F, Kabir MG, Khaper N, Cifelli C, Podobed P, Liu PP, Husain M, Heximer S, Backx PH and Sole MJ**. The primary benefits of angiotensin-converting enzyme inhibition on cardiac remodeling occur during sleep time in murine pressure overload hypertrophy. *J Am Coll Cardiol* 57: 2020-2028, 2011.

37. **McCarthy JJ, Andrews JL, McDearmon EL, Campbell KS, Barber BK, Miller BH, Walker JR, Hogenesch JB, Takahashi JS and Esser KA**. Identification of the circadian transcriptome in adult mouse skeletal muscle. *Physiol Genomics* 31: 86-95, 2007.

38. **Mitchell P**. Coupling of phosphorylation to electron and hydrogen transfer by a chemi-osmotic type of mechanism. *Nature* 191: 144-148, 1961.

39. **Miyazaki M, Schroder E, Edelmann SE, Hughes ME, Kornacker K, Balke CW and Esser KA**. Age-associated disruption of molecular clock expression in skeletal muscle of the spontaneously hypertensive rat. *PLoS One* 6: e27168, 2011.

40. **Nakahata Y, Kaluzova M, Grimaldi B, Sahar S, Hirayama J, Chen D, Guarente LP and Sassone-Corsi P**. The NAD+-dependent deacetylase SIRT1 modulates CLOCK-mediated chromatin remodeling and circadian control. *Cell* 134: 329-340, 2008.

41. **Oishi K, Fukui H and Ishida N**. Rhythmic expression of BMAL1 mRNA is altered in Clock mutant mice: differential regulation in the suprachiasmatic nucleus and peripheral tissues. *Biochem Biophys Res Commun* 268: 164-171, 2000.

42. **Pilegaard H, Saltin B and Neufer PD**. Exercise induces transient transcriptional activation of the PGC-1alpha gene in human skeletal muscle. *J Physiol* 546: 851-858, 2003.

43. **Saini C, Morf J, Stratmann M, Gos P and Schibler U**. Simulated body temperature rhythms reveal the phase-shifting behavior and plasticity of mammalian circadian oscillators. *Genes Dev* 26: 567-580, 2012.

44. **Saleem A, Adhihetty PJ and Hood DA**. Role of p53 in mitochondrial biogenesis and apoptosis in skeletal muscle. *Physiol Genomics* 37: 58-66, 2009.

45. **Schibler U, Ripperger J and Brown SA**. Peripheral circadian oscillators in mammals: time and food. *J Biol Rhythms* 18: 250-260, 2003.

46. **Serpiello FR, McKenna MJ, Bishop DJ, Aughey RJ, Caldow MK, Cameron-Smith D and Stepto NK**. Repeated sprints alter signaling related to mitochondrial biogenesis in humans. *Med Sci Sports Exerc* 44: 827-834, 2012.

47. **Song XM, Fiedler M, Galuska D, Ryder JW, Fernstrom M, Chibalin AV, Wallberg-Henriksson H and Zierath JR**. 5-Aminoimidazole-4-carboxamide ribonucleoside treatment improves glucose homeostasis in insulin-resistant diabetic (ob/ob) mice. *Diabetologia* 45: 56-65, 2002.

48. **Stokkan KA, Yamazaki S, Tei H, Sakaki Y and Menaker M**. Entrainment of the circadian clock in the liver by feeding. *Science* 291: 490-493, 2001.

49. **Turek FW, Joshu C, Kohsaka A, Lin E, Ivanova G, McDearmon E, Laposky A, Losee-Olson S, Easton A, Jensen DR, Eckel RH, Takahashi JS and Bass J**.

Obesity and metabolic syndrome in circadian Clock mutant mice. *Science* 308: 1043-1045, 2005.

50. **Uguccioni G and Hood DA.** The importance of PGC-1alpha in contractile activity-induced mitochondrial adaptations. *Am J Physiol Endocrinol Metab* 300: E361-E371, 2011.

51. **Vainshtein A, Kazak L and Hood DA.** Effects of endurance training on apoptotic susceptibility in striated muscle. *J Appl Physiol* 110: 1638-1645, 2011.

52. **Wibom R, Hultman E, Johansson M, Matherei K, Constantin-Teodosiu D and Schantz PG.** Adaptation of mitochondrial ATP production in human skeletal muscle to endurance training and detraining. *J Appl Physiol* 73: 2004-2010, 1992.

53. **Winget CM, DeRoshia CW and Holley DC.** Circadian rhythms and athletic performance. *Med Sci Sports Exerc* 17: 498-516, 1985.

54. **Wolff G and Esser KA.** Scheduled exercise phase shifts the circadian clock in skeletal muscle. *Med Sci Sports Exerc* 2012.

55. **Wyse JP, Mercer TH and Gleeson NP.** Time-of-day dependence of isokinetic leg strength and associated interday variability. *Br J Sports Med* 28: 167-170, 1994.

56. **Yamanaka Y, Honma S and Honma K.** Scheduled exposures to a novel environment with a running-wheel differentially accelerate re-entrainment of mice peripheral clocks to new light-dark cycles. *Genes Cells* 13: 497-507, 2008.

57. **Zhang X, Dube TJ and Esser KA**. Working around the clock: circadian rhythms and skeletal muscle. *J Appl Physiol* 107: 1647-1654, 2009.

58. **Zor T and Selinger Z**. Linearization of the Bradford protein assay increases its sensitivity: theoretical and experimental studies. *Anal Biochem* 236: 302-308, 1996.

Figure Legends

Figure 1. *Body mass progression and food intake.* Mice (wildtype, WT; mutant, CL19; trained, T; untrained, UT) were weighed on a weekly basis for the duration of the study. Food intake was evaluated at lights on and lights off during the sixth week of the study for three consecutive days. **A)** Body mass measurements (n = 6 – 9); **B)** Average daily food intake; **C)** Average food intake during the light and dark circadian phases. Values are displayed as mean ± SE; (n = 3 – 6). †p < 0.05, wildtype trained and *Clock* mutant control relative to wildtype control.

Figure 2. *Running performance and rhythmic locomotor activity.* Voluntary locomotor activity was recorded on a daily basis for eight weeks. **A)** Average daily running performance during each week of running; **B)** Average locomotor activity during the light and dark phases. Values are displayed as mean ± SE; (n = 6 – 8). *p < 0.05, *Clock* mutant relative to wildtype.

Figure 3. *Relative skeletal muscle, cardiac and adipose tissue mass characteristics.* **A)** Visceral fat depots, **B)** the gastrocnemius muscle complex and **C)** the heart were harvested, weighed and normalized to body mass. Values are displayed as mean ± SE; (n = 6 – 8). †p < 0.05, *Clock* mutant relative to wildtype; *p < 0.05, trained relative to control.

Figure 4. *Exercise tolerance and skeletal muscle mitochondrial content.* Mice were subjected to a treadmill test to determine exercise tolerance, and the time necessary to reach exhaustion was correlated with skeletal muscle COX enzyme activity. **A)** Exercise tolerance (n = 5 – 8); **B)** Gastrocnemius COX enzyme activity (n = 5 – 10); **C)** The correlation (r = 0.63; p < 0.05) between exercise tolerance and skeletal muscle COX enzyme activity based on individual animal values and represented as the means of each group. Values are displayed as mean ± SE. †p < 0.05, *Clock* mutant relative to wildtype; *p < 0.05, trained relative to control.

Figure 5. *Intraperitoneal glucose tolerance.* Glucose tolerance was assessed utilizing the intraperitoneal glucose tolerance test. **A)** Changes in blood glucose; **B)** Area under the curve of the blood glucose graph. Values are displayed as mean ± SE; (n = 6 – 8). *p < 0.05, effect of training in both the wildtype and *Clock* mutant mice.

Figure 6. *Mitochondrial respiration in SS and IMF subfractions.* Mitochondrial respiration was measured in isolated **A)** SS and **B)** IMF subfractions to evaluate mitochondrial function. Values are displayed as mean ± SE (n = 4 – 8).

Figure 7. *Metabolic, mitochondrial and circadian rhythm protein expression in muscle.* Representative western blot images and quantifications of **A)** PGC-1α, **B)** Tfam, **C)** COX IV, **D)** COX I and **E)** CLOCK and BMAL1. Values are displayed as mean ± SE (n = 6). †p < 0.05, *Clock* mutant relative to wildtype; *p < 0.05, trained relative to control.

Figures

Fig. 1

A.

B.

C.

Fig. 2

A.

B.

Fig. 3

A.

B.

C.

Fig. 4

A.

B.

C.

Fig. 5

A.

Blood Glucose (mM) vs Post-Injection Time (minutes)

Legend: WT-UT, CL19-UT, WT-T, CL19-T

B.

A.U.C. (A.U.) for Control and Trained groups in Wildtype and Mutant
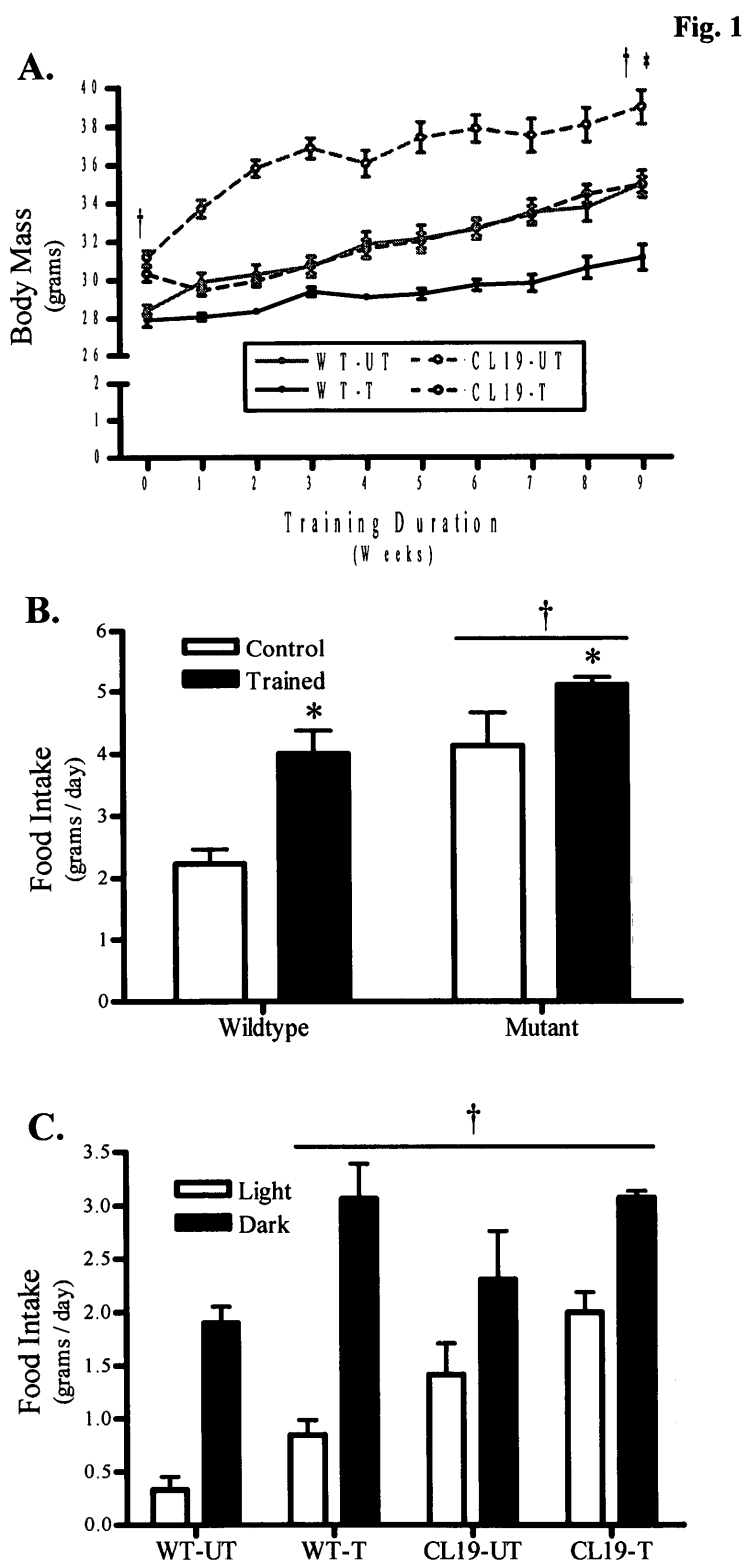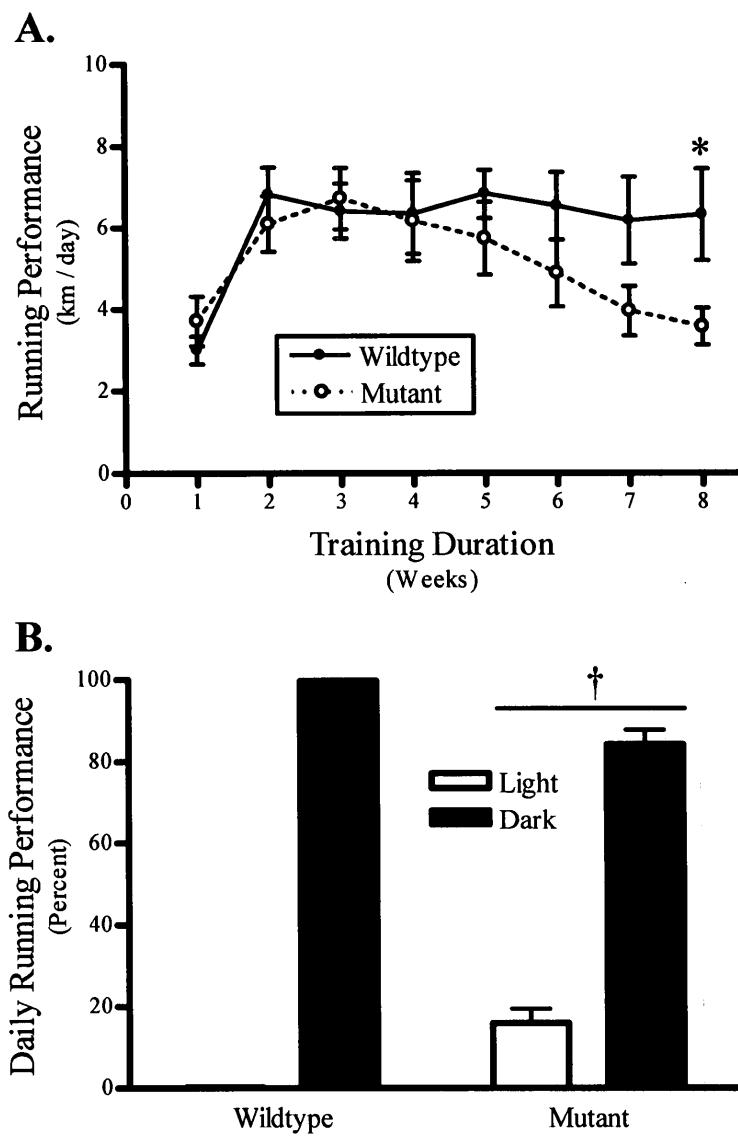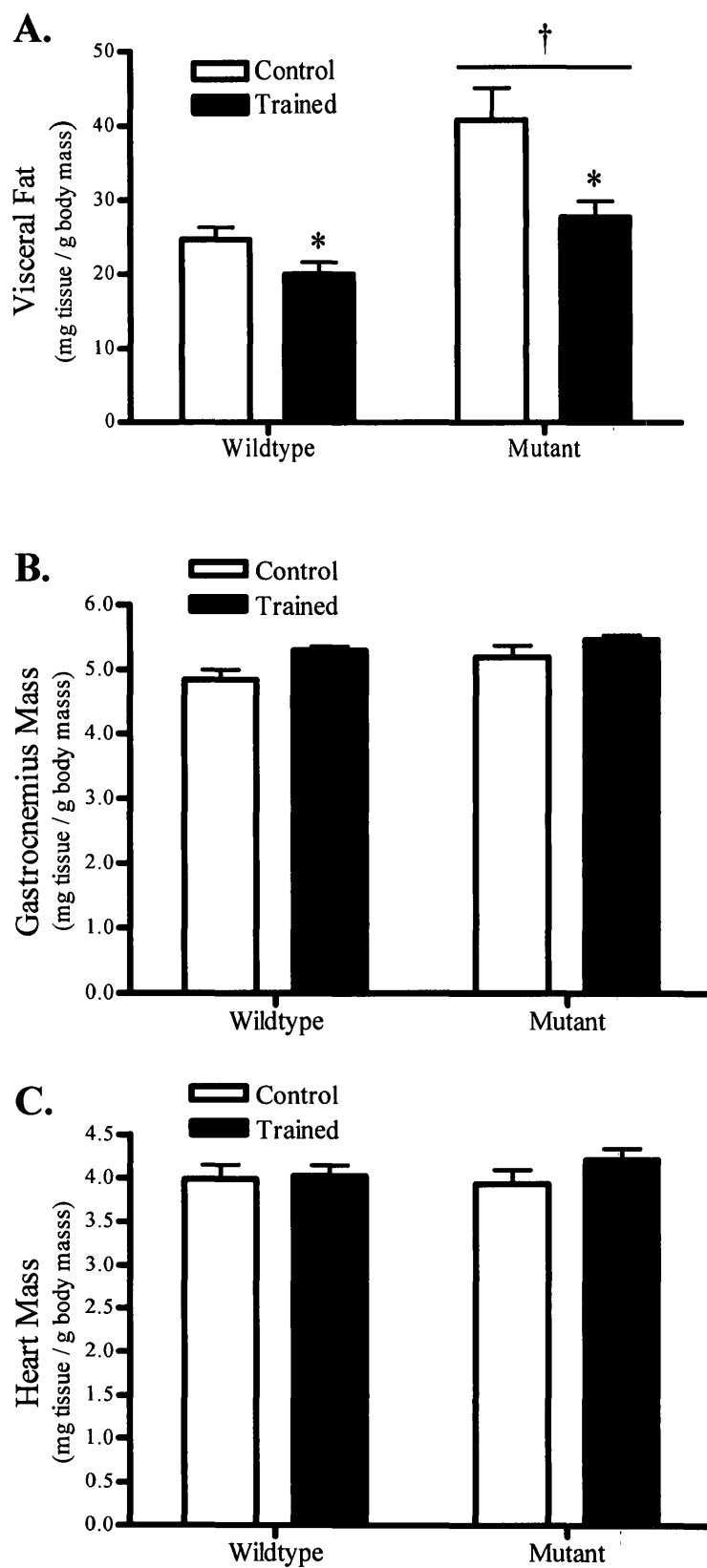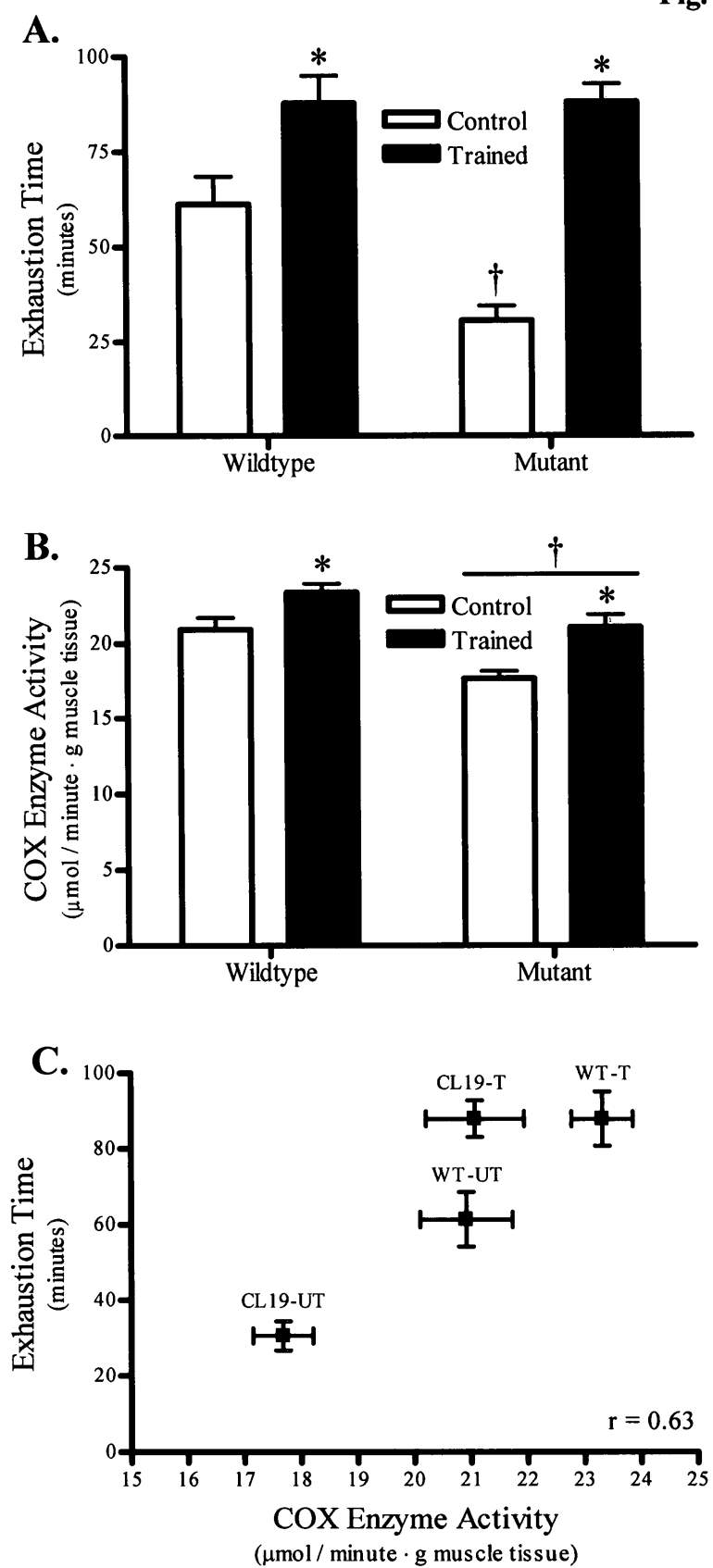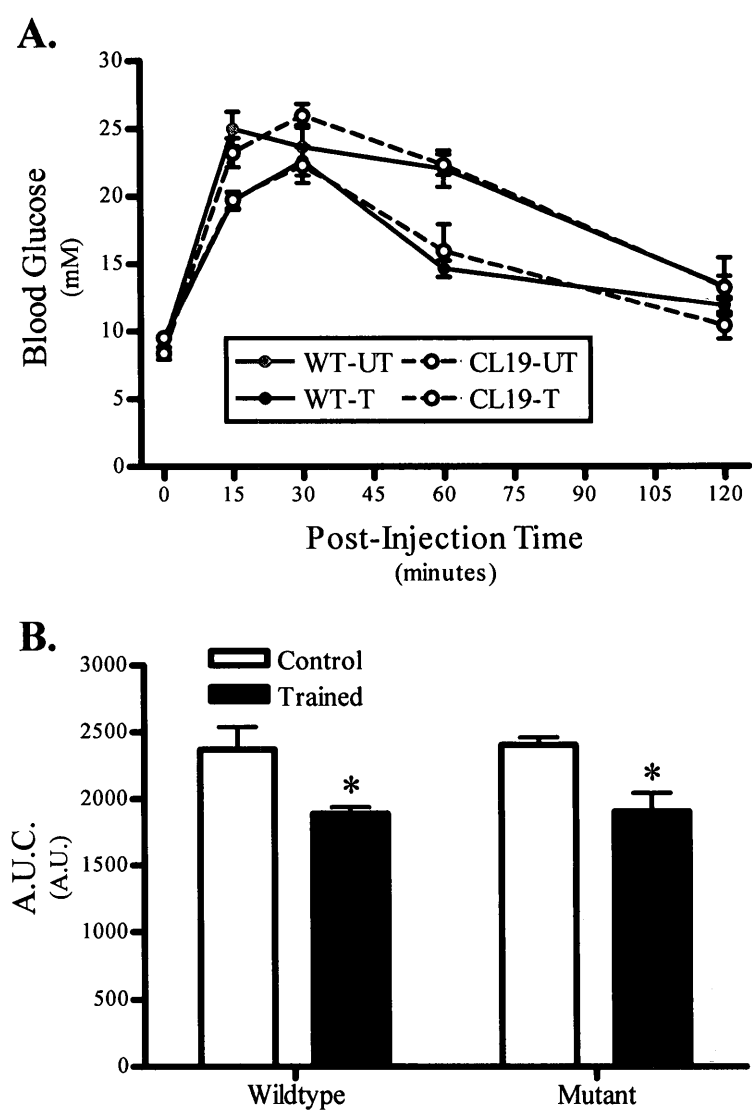
Fig. 6
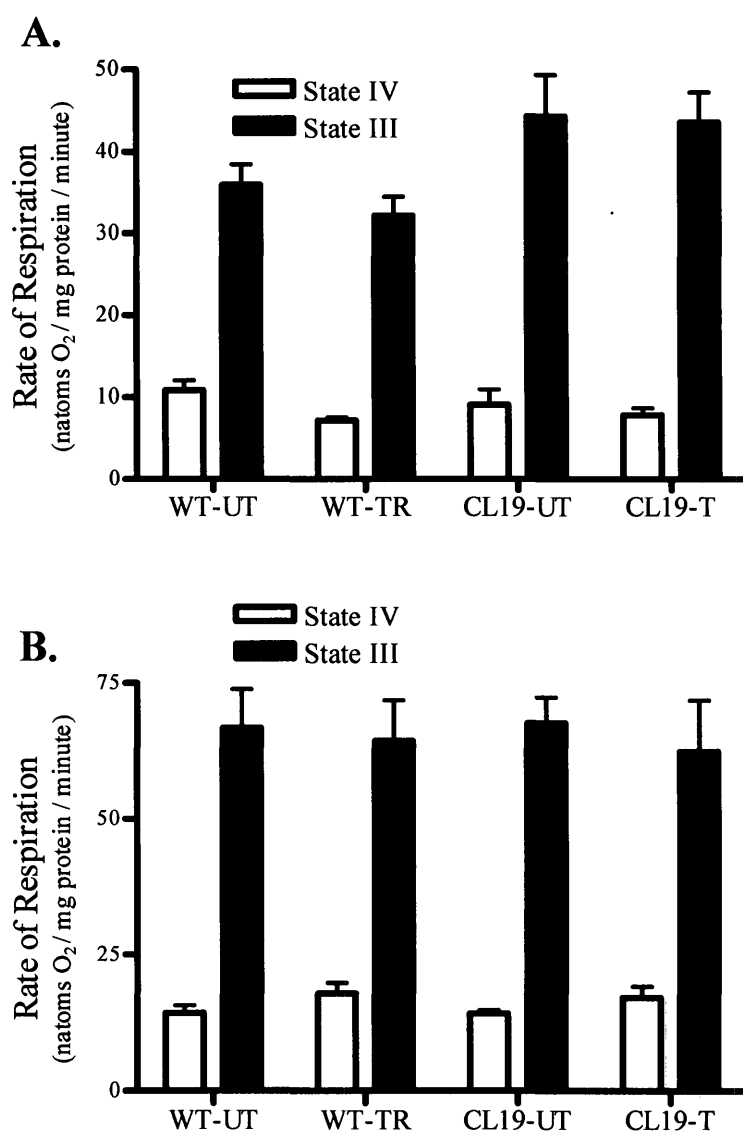
Fig. 7
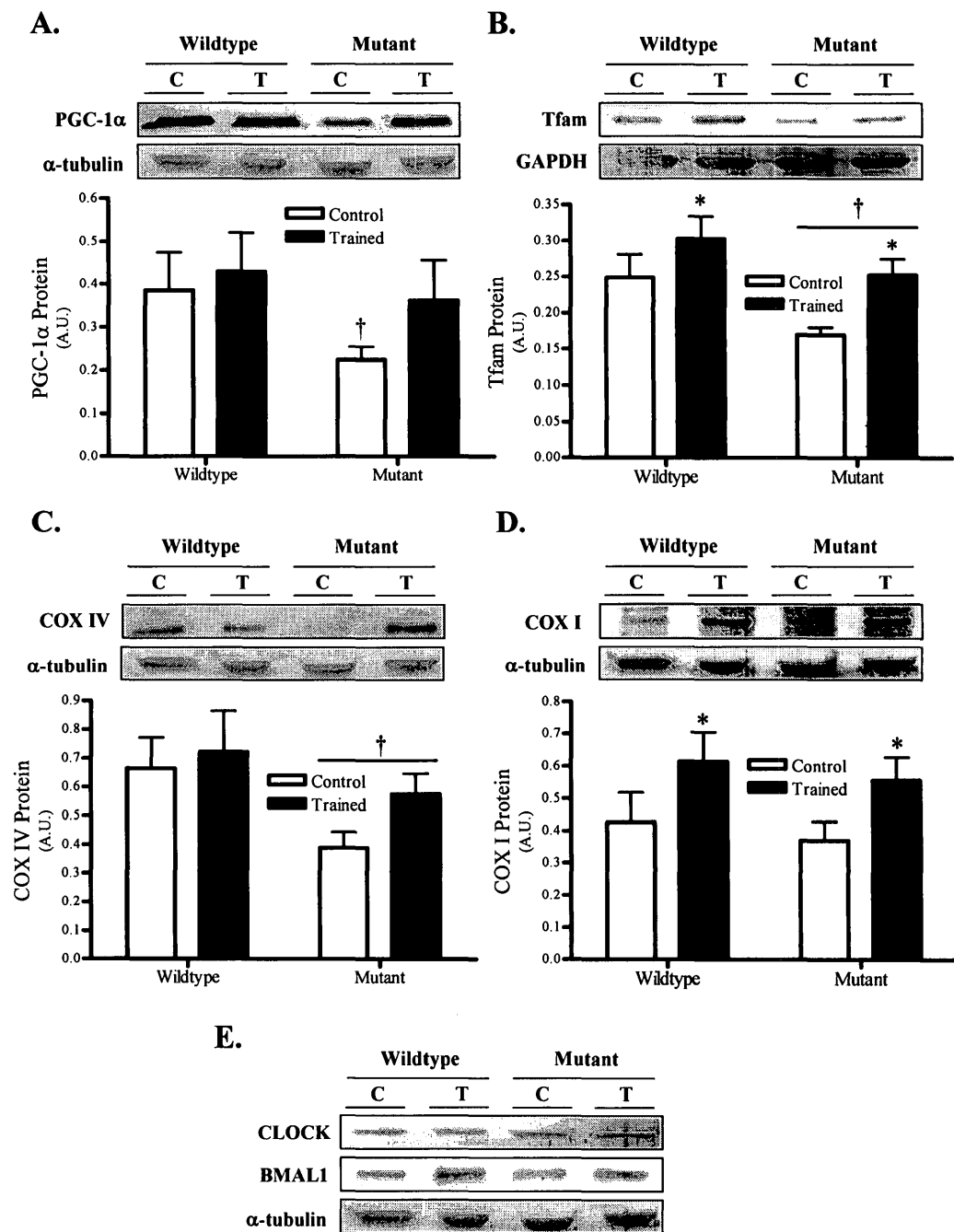
SUMMARY AND FUTURE WORK

The results obtained from this thesis are important for the understanding of the interaction between biological rhythms and skeletal muscle physiology, a novel avenue of research that has not been extensively explored. This study utilized circadian locomotor output cycles kaput (CLOCK) mutant mice, which possess a truncated and dysfunctional $CLOCK^{\Delta 19}$ protein, resulting in numerous deleterious phenotypes. Previous studies concerning these *Clock* mutant animals have revealed several phenotypic abnormalities, including altered sleep homeostasis, disrupted gene expression, obesity and metabolic syndrome, impaired glucose tolerance, and attenuated skeletal muscle contractility and myofilament organization. However, no research has been devoted to discerning the extent whereby these maladaptive phenotypes can potentially be restored through endurance training.

Therefore, this thesis sought to investigate two distinct objectives: 1) to assess the effects of the *Clock* mutation on specific indices of mitochondrial and systemic physiology, and 2) to evaluate the results of a chronic voluntary endurance training protocol on eliciting adaptations that restore functionality to these mutant animals. Our results indicate that skeletal muscle mitochondrial content is reduced in *Clock* mutant mice, although no mitochondrial dysfunction is observed. Furthermore, endurance training elicits numerous improvements in these mutant animals that culminate in a dramatic improvement in exercise tolerance. Our results provide evidence that the coordination of biological timing is intimately involved in the regulation of physiological properties within peripheral tissues.

Given the present findings, future studies should focus on the following avenues:

1. Further exploring the ramifications of the *Clock* mutation on mitochondrial physiology within skeletal muscle. Specifically, indices such as mitochondrial protein import and pore kinetics should be assessed in both subsarcolemmal (SS) and intermyofibrillar (IMF) isolated mitochondrial subfractions, as well as mitochondrial membrane potential as determined through flow cytometry.

2. Manipulating the expression of a metabolic sensor to investigate the biological clock within skeletal muscle. The activity of CLOCK and the histone deacetylase sirtuin 1 (SirT1) exert opposite effects on circadian gene transcription within the central autoregulatory feedback loop. A hybrid mutant-knockout (CLOCK$^{\Delta 19}$; SirT1$^{-/-}$) animal model sacrificed at different time points would provide insight regarding peripheral gene expression.

3. Extensively profiling diurnal changes in mitochondrial content by assessing the interaction between mitochondrial biogenesis and degradation throughout the light-dark cycle in both wildtype and *Clock* mutant mice.

    i. Harvest the gastrocnemius muscle and isolate nuclear and cytoplasmic cell fractions. Harvest and freeze the contralateral gastrocnemius muscle.

    ii. Measure protein expression of components involved in transcriptional coactivation during mitochondrial biogenesis in the nuclear cell fraction, including peroxisome proliferator-activated

receptor-γ coactivator 1-α (PGC-1α) and nuclear respiratory factors (NRF)-1 and -2.

iii. Measure protein expression of components involved in autophagy and mitochondrial degradation in the cytoplasmic cell fractions, including microtubule-associated proteins 1A-1B light chain 3A (LC3), autophagy-related protein 7 (ATG7) and phosphatase and tensin homolog-induced putative kinase 1 (PINK1).

APPENDIX A

DATA TABLES AND STATISTICAL ANALYSES

Table 1A: Body Mass Progression (Week 0)

N	Week 0			
	WT-UT	WT-T	$CL^{\Delta19}$-UT	$CL^{\Delta19}$-T
1	28.6	27.8	31.5	29.4
2	29.3	28.5	32.3	28.5
3	29	29.3	30.3	30.5
4	26.9	27.1	30.5	29.6
5	29.4	27.1	30.2	31.5
6	27.9	27.7	30.4	30.8
7	29		30.4	31.9
8	27.6		33.3	30.4
9	28		31.6	
Average	28.41	27.92	31.17	30.33
S.D.	0.86	0.85	1.09	1.12
S.E.	0.30	0.38	0.38	0.42

Two-way ANOVA			
Source of Variation	P-Value	P-Value Summary	Significant?
Interaction	0.6306	NS	No
Training	0.1719	NS	No
Genotype	P < 0.0001	***	Yes

Bonferroni post-hoc test -- Untrained vs. Trained				
Treatment	Difference	t	P-Value	P-Value Summary
Wildtype	-0.4944	0.9416	P > 0.05	NS
Mutant	-0.8417	1.739	P > 0.05	NS

Table 1A: Body Mass Progression (Week 1 – Week 4)

N	Week 1				Week 2			
	WT-UT	WT-T	CL$^{\Delta 19}$-UT	CL$^{\Delta 19}$-T	WT-UT	WT-T	CL$^{\Delta 19}$-UT	CL$^{\Delta 19}$-T
1	32	28.2	33.4	28.8	32.2	28.3	35.3	28.5
2	31.6	28.6	35.6	28.6	31.8	28.6	38.3	29.1
3	29.4	28.6	32.2	30.9	29.6	28.6	34.9	31
4	28.1	27.5	32.3	29.4	28.1	27.7	35.2	30.4
5	30.3	27.8	32.8	29.4	30.8	28.2	34.8	30.3
6	30.7	27.8	33.9	29.1	31.2	28.7	35.3	29.7
7	30.1		32.9	29.3	31.4		34.5	30.2
8	28.3		35.9	30.1	28.9		37.3	30.3
9	28.6		34.5		28.8		36.8	
Average	29.90	28.08	33.72	29.45	30.31	28.35	35.82	29.94
S.D.	1.41	0.46	1.36	0.74	1.49	0.37	1.32	0.80
S.E.	0.50	0.20	0.48	0.28	0.53	0.17	0.47	0.30

N	Week 3				Week 4			
	WT-UT	WT-T	CL$^{\Delta 19}$-UT	CL$^{\Delta 19}$-T	WT-UT	WT-T	CL$^{\Delta 19}$-UT	CL$^{\Delta 19}$-T
1	32.5	29.5	35.3	29.1	34.0	29.4	35.4	29.8
2	31.9	29.2	38.3	30.1	32.9	28.7	39.2	30.7
3	29.6	30	34.9	32.6	30.0	29.5	32.6	33.6
4	28.2	28.4	35.2	31.8	28.4	28.6	37.3	32.7
5	31.3	29.3	34.8	29.5	31.9	29.1	34.2	30.7
6	31.6	29.9	35.3	30.3	32.0	29.3	35.8	30.7
7	32.7		34.5	31.9	34.9		35.6	32.9
8	29.5		37.3	30.9	31.6		38.6	31.8
9	29		36.8		31.1		36	
Average	30.70	29.38	35.82	30.78	31.87	29.10	36.08	31.61
S.D.	1.64	0.58	1.32	1.24	1.97	0.37	2.06	1.34
S.E.	0.58	0.26	0.47	0.47	0.70	0.17	0.73	0.51

Table 1A: Body Mass Progression (Week 5 – Week 8)

N	Week 5				Week 6			
	WT-UT	WT-T	CL$^{\Delta 19}$-UT	CL$^{\Delta 19}$-T	WT-UT	WT-T	CL$^{\Delta 19}$-UT	CL$^{\Delta 19}$-T
1	32.5	29.6	41.4	30.3	33.6	30	41.5	31.1
2	34.3	28.7	36.7	31.8	33	29.8	38	32.8
3	31.2	29.8	33.7	33.8	31.5	29.9	34.6	33.3
4	31	28.2	35.8	32.8	32.2	28.4	36.6	35
5	28.3	29.3	37.4	31.2	29.9	30.5	38.6	31.7
6	31.9	30.0	36.6	31.4	32.4	29.8	37.4	32.1
7	32.2		37	33	32.9		37.2	33.1
8	31.8		40.6	32	32.5		40.5	32.6
9	36		37.6		36		36.5	
Average	32.13	29.27	37.42	32.04	32.67	29.73	37.88	32.71
S.D.	2.14	0.69	2.34	1.12	1.64	0.70	2.11	1.18
S.E.	0.76	0.31	0.83	0.42	0.58	0.31	0.74	0.45

N	Week 7				Week 8			
	WT-UT	WT-T	CL$^{\Delta 19}$-UT	CL$^{\Delta 19}$-T	WT-UT	WT-T	CL$^{\Delta 19}$-UT	CL$^{\Delta 19}$-T
1	36.5	30	42.8	31.8	37.3	31.1	42.8	33.9
2	31.8	29.2	37.8	34	31.9	29.5	37.3	34.8
3	33.9	29.5	34.6	33.6	33.5	30.7	35	34.9
4	33	28.3	35.9	35.6	33.9	28.5	36.3	37.4
5	31.9	30.7	35.5	32.2	32.5	32.2	38.7	32.9
6	36	31.3	37.3	32.9	36.3	31.8	37.4	33.7
7	35.1		37	33.7	31.4		38	34.1
8	33.2		40.5	33.6	33.5		41.5	34.1
9	30.5		36.3				35.6	
Average	33.54	29.83	37.52	33.43	33.79	30.63	38.07	34.48
S.D.	2.02	1.08	2.60	1.17	2.06	1.41	2.60	1.34
S.E.	0.72	0.48	0.92	0.44	0.73	0.63	0.92	0.51

Table 1A: Body Mass Progression (Week 9)

N	Week 9			
	WT-UT	WT-T	CL19-UT	CL19-T
1	37.7	31.4	43.6	34.1
2	33.7	30.1	38.3	34.5
3	35.4	30.7	35.9	36.3
4	37.9	28.9	36.2	37.1
5	33.2	32.4	39.5	33.8
6	34.8	33.4	38.3	34.1
7	32.3		39.2	34.9
8	35		42.4	34.8
9			37.4	
Average	35.00	31.15	38.98	34.95
S.D.	2.00	1.62	2.60	1.16
S.E.	0.71	0.72	0.92	0.44

Two-way ANOVA			
Source of Variation	P-Value	P-Value Summary	Significant?
Interaction	0.9020	NS	No
Training	$P < 0.0001$	***	Yes
Genotype	$P < 0.0001$	***	Yes

Bonferroni post-hoc test -- Untrained vs. Trained			
Treatment	Difference	t	P-Value	P-Value Summary
Wildtype	-3.850	3.622	$P < 0.01$	**
Mutant	-4.028	4.211	$P < 0.001$	***

Table 1B: Daily Food Intake

N	WT-UT	WT-T	$CL^{\Delta 19}$-UT	$CL^{\Delta 19}$-T
1	1.8	3.7	3.55	5
2	2.6	3.9	5.075	4.7
3	2.3	4.6	3.15	5.4
4		2.4	3.15	5.2
5		4.7	3.7	
6		4.2		
Average	2.23	3.92	3.73	5.08
S.D.	0.40	0.84	0.79	0.30
S.E.	0.29	0.37	0.40	0.17

Two-way ANOVA			
Source of Variation	P-Value	P-Value Summary	Significant?
Interaction	0.5895	NS	No
Training	0.0013	**	Yes
Genotype	0.0005	***	Yes

Bonferroni post-hoc test – Untrained vs. Trained			
Treatment	Difference	t	P-Value	P-Value Summary
Wildtype	1.527	3.055	P < 0.05	*
Mutant	1.158	2.623	P < 0.05	*

Table 1C: Circadian Cycle Food Intake

N	WT-UT		WT-T		CL$^{\Delta 19}$-UT		CL$^{\Delta 19}$-T	
	Light	Dark	Light	Dark	Light	Dark	Light	Dark
1	0.1	1.7	1	2.7	0.5	3.1	1.9	3.1
2	0.4	2.2	1.3	2.6	1.65	3.4	1.6	3.1
3	0.5	1.8	0.6	4	2.3	0.9	2.5	2.9
4			0.4	2	1.2	2.0	2	3.2
5			0.7	4	1.425	2.3		
6			1.1	3.1				
Average	0.33	1.90	0.85	3.07	1.42	2.31	2.00	3.08
S.D.	0.21	0.26	0.34	0.80	0.66	1.01	0.37	0.13
S.E.	0.15	0.19	0.15	0.36	0.33	0.50	0.22	0.07

Two-way ANOVA -- WT-UT vs. WT-T			
Source of Variation	P-Value	P-Value Summary	Significant?
Interaction	0.246	NS	No
Circadian Cycle	P < 0.0001	***	Yes
Training	0.0073	**	Yes

Bonferroni post-hoc test -- Light Cycle vs. Dark Cycle			
Treatment	Difference	t	P-Value	P-Value Summary
WT-UT	1.567	3.574	P < 0.01	**
WT-T	2.217	7.152	P < 0.001	***

Two-way ANOVA -- WT-UT vs. CL$^{\Delta 19}$-UT			
Source of Variation	P-Value	P-Value Summary	Significant?
Interaction	0.4666	NS	No
Circadian Cycle	0.0032	**	Yes
Genotype	0.0420	*	Yes

Bonferroni post-hoc test -- Light Cycle vs. Dark Cycle			
Treatment	Difference	t	P-Value	P-Value Summary
WT-UT	1.567	2.709	P < 0.05	*
CL$^{\Delta 19}$-UT	1.027	2.394	P > 0.05	NS

Two-way ANOVA -- WT-UT vs. CL$^{\Delta 19}$-T			
Source of Variation	P-Value	P-Value Summary	Significant?
Interaction	0.0876	NS	No
Circadian Cycle	P < 0.0001	***	Yes
Tr. + Genotype	P < 0.0001	***	Yes

Bonferroni post-hoc test -- Light Cycle vs. Dark Cycle			
Treatment	Difference	t	P-Value	P-Value Summary
WT-UT	1.567	5.982	P < 0.001	***
CL$^{\Delta 19}$-T	0.9458	4.568	P < 0.01	**

Table 2A: Daily Running Performance (Week 1 – Week 4)

N	Week 1		Week 2		Week 3		Week 4	
	Wildtype	Mutant	Wildtype	Mutant	Wildtype	Mutant	Wildtype	Mutant
1	1.59	5.97	7.12	9.88	6.46	11.04	5.68	11.93
2	3.08	4.28	8.94	6.73	8.55	6.55	10.87	6.82
3	4.15	3.73	8.47	6.29	7.47	5.69	6.85	4.59
4	2.85	6.21	5.12	7.41	4.24	6.94	3.84	6.90
5	3.06	1.61	6.07	4.84	7.04	7.82	4.90	6.41
6	3.27	3.25	5.16	4.14	4.67	4.11	5.95	2.92
7		1.81		4.34		4.67		3.41
8		2.86		5.12		6.89		6.37
Average	3.00	3.72	6.81	6.09	6.40	6.71	6.35	6.17
S.D.	0.83	1.72	1.64	1.92	1.66	2.14	2.44	2.80
S.E.	0.37	0.65	0.73	0.73	0.74	0.81	1.09	1.06

Student's Unpaired *t*-test -- Wildtype vs. Mutant (Week 1)	
P-value	0.3682
P-value Summary	NS
Are means significantly different? (P < 0.05)	No

Student's Unpaired *t*-test -- Wildtype vs. Mutant (Week 2)	
P-value	0.4765
P-value Summary	NS
Are means significantly different? (P < 0.05)	No

Student's Unpaired *t*-test -- Wildtype vs. Mutant (Week 3)	
P-value	0.7750
P-value Summary	NS
Are means significantly different? (P < 0.05)	No

Student's Unpaired *t*-test -- Wildtype vs. Mutant (Week 4)	
P-value	0.9024
P-value Summary	NS
Are means significantly different? (P < 0.05)	No

Table 2A: Daily Running Performance (Week 5 – Week 8)

N	Week 5		Week 6		Week 7		Week 8	
	Wildtype	Mutant	Wildtype	Mutant	Wildtype	Mutant	Wildtype	Mutant
1	7.09	10.97	6.07	10.02	6.48	7.60	5.63	5.35
2	9.02	6.59	9.85	5.69	11.01	3.32	11.41	3.20
3	7.47	4.16	7.08	3.53	6.18	1.69	5.96	1.87
4	4.95	5.82	4.87	4.54	4.50	3.32	6.79	3.11
5	6.98	6.01	7.23	4.69	5.43	4.74	4.89	5.37
6	5.45	2.74	4.07	2.36	3.44	3.22	3.23	2.32
7		3.55		3.29		3.68		3.53
8		5.98		4.89		4.06		3.81
Average	6.83	5.73	6.53	4.87	6.17	3.95	6.32	3.57
S.D.	1.47	2.52	2.04	2.33	2.62	1.71	2.77	1.27
S.E.	0.66	0.95	0.91	0.88	1.17	0.65	1.24	0.48

Student's Unpaired *t*-test -- Wildtype vs. Mutant (Week 5)	
P-value	0.3615
P-value Summary	NS
Are means significantly different? (P < 0.05)	No

Student's Unpaired *t*-test -- Wildtype vs. Mutant (Week 6)	
P-value	0.1920
P-value Summary	NS
Are means significantly different? (P < 0.05)	No

Student's Unpaired *t*-test -- Wildtype vs. Mutant (Week 7)	
P-value	0.0784
P-value Summary	NS
Are means significantly different? (P < 0.05)	No

Student's Unpaired *t*-test -- Wildtype vs. Mutant (Week 8)	
P-value	0.0278
P-value Summary	*
Are means significantly different? (P < 0.05)	Yes

Table 2B: Circadian Cycle Locomotor Activity

N	Wildtype		Mutant	
	Light	Dark	Light	Dark
1	0.19	99.81	7.52	92.48
2	0.46	99.54	38.30	61.70
3	0.09	99.91	10.75	89.25
4	0.73	99.27	13.15	86.85
5	0.11	99.89	17.33	82.67
6	0.06	99.94	11.35	88.65
7			8.75	91.25
8			19.76	80.24
Average	0.27	99.73	15.86	84.14
S.D.	0.27	0.27	9.96	9.96
S.E.	0.12	0.12	3.77	3.77

Two-way ANOVA			
Source of Variation	P-Value	P-Value Summary	Significant?
Interaction	P < 0.0001	***	Yes
Circadian Cycle	P < 0.0001	***	Yes
Genotype	1.0000	NS	No

Bonferroni post-hoc test -- Light Cycle vs. Dark Cycle				
Treatment	Difference	t	P-Value	P-Value Summary
Wildtype	99.46	22.63	P < 0.001	***
Mutant	68.28	17.94	P < 0.001	***

Table 3A: Visceral Fat Mass (Normalized to Body Mass)

N	WT-UT	WT-T	CL$^{\Delta 19}$-UT	CL$^{\Delta 19}$-T
1	21.15	15.18	29.35	22.39
2	27.49	16.03	59.78	21.81
3	25.14	21.97	56.42	32.89
4	22.39	20.16	41.15	25.73
5	27.49	21.02	41.87	35.09
6	26.21	25.78	38.77	35.55
7	31.45		33.69	28.06
8	16.34		26.28	20.78
Average	24.98	20.02	44.56	28.91
S.D.	4.65	3.93	11.96	6.07
S.E.	1.76	1.76	4.52	2.29

Two-way ANOVA			
Source of Variation	P-Value	P-Value Summary	Significant?
Interaction	0.1416	NS	No
Genotype	0.0036	**	Yes
Training	0.0002	***	Yes

Bonferroni post-hoc test – Untrained vs. Trained				
Treatment	Difference	t	P-Value	P-Value Summary
Wildtype	-4.684	1.146	P > 0.05	NS
Mutant	-13.13	3.469	P < 0.01	**

Table 3B: Gastrocnemius Muscle Mass (Normalized to Body Mass)

N	WT-UT	WT-T	$CL^{\Delta 19}$-UT	$CL^{\Delta 19}$-T
1	5.03	5.08	5.21	5.16
2	4.47	5.48	4.70	5.71
3	5.13	5.42	5.11	5.31
4	4.64	5.27	4.70	5.36
5	4.05	5.28	4.79	5.53
6	5.16	5.26	5.42	5.54
7	4.96		5.58	5.62
8	5.34		6.08	5.53
Average	4.75	5.30	4.99	5.44
S.D.	0.43	0.14	0.48	0.18
S.E.	0.16	0.06	0.18	0.07

Two-way ANOVA			
Source of Variation	P-Value	P-Value Summary	Significant?
Interaction	0.4965	NS	No
Genotype	0.2101	NS	No
Training	0.1551	NS	No

Table 3C: Heart Mass (Normalized to Body Mass)

N	WT-UT	WT-T	CL$^{\Delta 19}$-UT	CL$^{\Delta 19}$-T
1	4.21	3.56	3.82	4.48
2	3.88	4.02	4.31	4.79
3	3.97	3.87	3.69	4.28
4	4.21	4.30	3.63	3.78
5	3.34	3.98	3.66	3.72
6	3.80	4.40	3.87	4.32
7	3.62		3.54	4.32
8	4.86		4.92	4.01
Average	3.90	4.02	3.83	4.23
S.D.	0.46	0.30	0.46	0.36
S.E.	0.17	0.14	0.18	0.14

Two-way ANOVA			
Source of Variation	P-Value	P-Value Summary	Significant?
Interaction	0.4185	NS	No
Genotype	0.2999	NS	No
Training	0.6580	NS	No

Table 4B: Exercise Tolerance

N	WT-UT	WT-T	CL$^{\Delta 19}$-UT	CL$^{\Delta 19}$-T
1	80	73	28	60
2	74	101	29	81
3	44	100	19	99
4	78	68	41	94
5	48	97	52	103
6	44		23	93
7			24	92
8			29	81
Average	61.33	87.80	30.63	87.88
S.D.	17.69	15.96	10.78	13.65
S.E.	7.91	7.98	4.08	5.16

Two-way ANOVA			
Source of Variation	P-Value	P-Value Summary	Significant?
Interaction	0.0112	*	Yes
Genotype	P < 0.0001	***	Yes
Training	0.0122	*	Yes

Bonferroni post-hoc test -- Untrained vs. Trained				
Treatment	Difference	t	P-Value	P-Value Summary
Wildtype	26.47	3.061	P < 0.05	*
Mutant	57.38	8.036	P < 0.001	***

Table 4C: COX Enzyme Activity

N	WT-UT	WT-T	$CL^{\Delta19}$-UT	$CL^{\Delta19}$-T
1	24.47	24.12	17.89	17.80
2	20.70	23.47	17.10	18.53
3	18.69	23.33	18.46	20.02
4	23.34	24.38	19.02	23.10
5	22.80	21.30	19.57	20.09
6	16.53		17.68	22.04
7	21.81		17.52	23.85
8	21.49		14.27	23.20
9	18.40		17.65	
10	20.99			
Average	21.09	23.32	17.69	21.08
S.D.	2.58	1.21	1.61	2.29
S.E.	1.15	0.61	0.61	0.86

Two-way ANOVA			
Source of Variation	P-Value	P-Value Summary	Significant?
Interaction	0.5305	NS	No
Genotype	0.0005	***	Yes
Training	0.0009	***	Yes

Bonferroni post-hoc test -- Untrained vs. Trained			
Treatment	Difference	t	P-Value	P-Value Summary
Wildtype	2.450	2.209	$P > 0.05$	NS
Mutant	3.392	3.447	$P < 0.01$	**

Table 4D: Exercise Tolerance + COX Enzyme Activity Correlation

N	WT-UT		WT-T		CL$^{\Delta19}$-UT		CL$^{\Delta19}$-T	
	E.T.	C.A.	E.T.	C.A.	E.T.	C.A.	E.T.	C.A.
1	80	24.47	73	24.12	28	17.89	60	17.80
2	74	20.70	101	23.47	29	17.10	81	18.53
3	44	18.69	100	23.33	19	18.46	99	20.02
4	78	23.34	68	24.38	41	19.02	94	23.10
5	48	22.80	97	21.30	52	19.57	103	20.09
6	44	16.53			23	17.68	93	22.04
7					24	17.52	92	23.85
8					29	14.27	81	23.20
9								
10								
Average	61.33	21.09	87.80	23.32	30.63	17.69	87.88	21.08
S.D.	17.69	2.58	15.96	1.21	10.78	1.61	13.65	2.29
S.E.	7.91	1.15	7.98	0.61	4.08	0.61	5.16	0.86

Correlation	
Slope	5.470 ± 1.372
Y-intercept	-48.05 ± 28.68
r	0.6288
P-Value	0.0005
Is slope significantly non-zero?	Yes

Table 5A: Glucose Tolerance

N	Baseline			
	WT-UT	WT-T	CL$^{\Delta 19}$-UT	CL$^{\Delta 19}$-T
1	9.1	9.4	6.9	9.3
2	8.1	9.6	9.6	11.7
3	8.1	8.8	8.2	9.1
4	9.4	9.2	8.8	9.1
5	9.9	10.1	8.4	9.2
6	9.3	9.4	10	8.8
7			8.8	8.7
8			6.2	10.2
Average	8.98	9.42	8.36	9.51
S.D.	0.73	0.43	1.28	0.99
S.E.	0.33	0.19	0.48	0.38

N	15-min.				30-min.			
	WT-UT	WT-T	CL$^{\Delta 19}$-UT	CL$^{\Delta 19}$-T	WT-UT	WT-T	CL$^{\Delta 19}$-UT	CL$^{\Delta 19}$-T
1	23.9	17.8	15.2	21.3	22.9	18.9	16.8	28.6
2	27.7	20.8	22.7	21	25.6	24.5	23.4	23.5
3	28.5	20.9	16.8	20.6	30.6	20.2	22.3	21.6
4	26.3	19.3	18.6	21	22.3	24.5	20.8	22.3
5	20.1	21.2	23.9	18.8	19.7	22.2	27.4	22.8
6	23.6	18	16.6	20.5	21	25.6	24.6	16.2
7			22.2	18.2			27.8	25.3
8			30.2	16.5			29.8	18.4
Average	25.02	19.67	20.78	19.74	23.68	22.65	24.11	22.34
S.D.	3.11	1.52	4.98	1.72	3.93	2.68	4.23	3.84
S.E.	1.39	0.68	1.88	0.65	1.76	1.20	1.60	1.45

N	60-min.				120-min.			
	WT-UT	WT-T	CL$^{\Delta 19}$-UT	CL$^{\Delta 19}$-T	WT-UT	WT-T	CL$^{\Delta 19}$-UT	CL$^{\Delta 19}$-T
1	21.1	15.4	23.9	20.3	11	10.6	7.4	12.6
2	21.9	15.3	24.4	18.8	9.7	12.3	11	12.8
3	28.8	15.1	21.5	13.5	23.9	10.3	11.8	12.3
4	21.1	11.9	22.8	17.9	10.4	10.9	8.7	12.2
5	19.6	15.2	24.9	12.6	12.3	14.2	18	9.5
6	19.8	15.2	19.4	10.4	12.4	13	13.3	5.3
7			22.9	25.2			14.9	11.1
8			19.1	8.9			10.5	7.2
Average	22.05	14.68	22.36	15.95	13.28	11.88	11.95	10.38
S.D.	3.42	1.37	2.19	5.53	5.31	1.54	3.41	2.80
S.E.	1.53	0.61	0.83	2.09	2.37	0.69	1.29	1.06

Table 5B: Blood-Glucose A.U.C.

N	WT-UT	WT-T	CL$^{\Delta19}$-UT	CL$^{\Delta19}$-T
1	2221	1774	2405	2324
2	2328	1993	2397	2162
3	3189	1833	2212	1840
4	2228	1759	2438	2057
5	2070	2003	2699	1716
6	2198	1991	2225	1430
7			2502	2375
8			2351	1355
Average	2372.33	1892.17	2403.63	1907.38
S.D.	408.52	116.12	155.63	387.97
S.E.	182.70	51.93	58.82	146.64

Two-way ANOVA			
Source of Variation	P-Value	P-Value Summary	Significant?
Interaction	0.9442	NS	No
Training	0.0002	***	Yes
Genotype	0.8396	NS	No

Bonferroni post-hoc test -- Untrained vs. Trained			
Treatment	Difference	t	P-Value	P-Value Summary
Wildtype	-480.2	2.795	P < 0.05	*
Mutant	-496.3	3.335	P < 0.01	**

Table 6A: SS Mitochondrial Respiration

N	WT-UT		WT-T		$CL^{\Delta19}$-UT		$CL^{\Delta19}$-T	
	State IV	State III	State IV	State III	State IV	State III	State IV	State III
1	9.13	31.49	5.94	39.53	3.99	42.90	10.58	31.98
2	8.47	31.82	7.04	30.23	12.09	51.01	10.1	32.62
3	12.69	38.80	8.00	25.78	6.79	21.69	7.19	50.52
4	13.13	41.61	7.28	31.97	6.01	55.40	5.25	50.92
5			7.55	33.50	9.42	42.81	7.9	48.35
6					16.28	52.19	6.11	47.34
Average	10.85	35.93	7.16	32.20	9.10	44.33	7.86	43.62
S.D.	2.39	5.07	0.77	5.01	4.51	12.21	2.13	8.87
S.E.	1.38	2.93	0.38	2.51	2.02	5.46	0.95	3.97

Two-way ANOVA -- SS Mitochondrial Subfractions (State IV)			
Source of Variation	P-Value	P-Value Summary	Significant?
Interaction	0.3545	NS	No
Training	0.1723	NS	No
Genotype	0.6843	NS	No

Two-way ANOVA -- SS Mitochondrial Subfractions (State III)			
Source of Variation	P-Value	P-Value Summary	Significant?
Interaction	0.7034	NS	No
Training	0.5762	NS	No
Genotype	0.2209	NS	No

Table 6B: IMF Mitochondrial Respiration

N	WT-UT		WT-T		CL$^{\Delta19}$-UT		CL$^{\Delta19}$-T	
	State IV	State III	State IV	State III	State IV	State III	State IV	State III
1	12.36	54.73	14.25	54.05	13.80	55.99	14.34	43.41
2	13.38	59.73	16.31	75.68	15.18	73.17	14.33	45.96
3	14.01	54.59	16.80	51.16	15.49	91.89	17.6	92.29
4	12.04	72.91	27.21	96.33	11.42	59.58	12.35	45.72
5	19.73	91.82	16.01	52.20	15.28	75.05	26.21	90.15
6			17.38	57.02	13.53	51.59	18.57	57.25
7					12.67	60.64		
8					16.59	73.44		
Average	14.30	66.76	17.99	64.41	14.12	67.88	17.23	62.46
S.D.	3.13	15.88	4.64	18.07	1.55	15.04	4.96	22.80
S.E.	1.81	9.17	2.32	9.03	0.70	6.73	2.22	10.20

Two-way ANOVA -- IMF Mitochondrial Subfractions (State IV)

Source of Variation	P-Value	P-Value Summary	Significant?
Interaction	0.8185	NS	No
Training	0.2380	NS	No
Genotype	0.7886	NS	No

Two-way ANOVA -- IMF Mitochondrial Subfractions (State III)

Source of Variation	P-Value	P-Value Summary	Significant?
Interaction	0.8428	NS	No
Training	0.6009	NS	No
Genotype	0.9429	NS	No

Table 7A: PGC-1α Protein Expression

N	WT-UT	WT-T	CL^{Δ19}-UT	CL^{Δ19}-T
1	0.2155	0.2883	0.2343	0.3462
2	0.2763	0.2797	0.1256	0.0641
3	0.2145	0.2554	0.1361	0.3721
4	0.3620	0.3085	0.2779	0.1557
5	0.7016	0.7419	0.2894	0.5977
6	0.5851	0.6972	0.2786	0.6338
Average	0.39	0.43	0.22	0.36
S.D.	0.20	0.23	0.07	0.23
S.E.	0.09	0.10	0.03	0.09

Two-way ANOVA			
Source of Variation	P-Value	P-Value Summary	Significant?
Interaction	0.5638	NS	No
Training	0.2715	NS	No
Genotype	0.1709	NS	No

Student's Unpaired t-test -- vs. WT-UT	WT-T	CL^{Δ19}-UT	CL^{Δ19}-T
P-value	0.7787	0.0491	0.8102
P-value Summary	NS	*	NS
Are means significantly different? (P < 0.05)	No	Yes	No

Table 7B: Tfam Protein Expression

N	WT-UT	WT-T	$CL^{\Delta 19}$-UT	$CL^{\Delta 19}$-T
1	0.279	0.444	0.134	0.309
2	0.202	0.241	0.176	0.273
3	0.232	0.336	0.183	0.191
4	0.171	0.263	0.201	0.184
5	0.389	0.273	0.144	0.301
6	0.221	0.261	0.179	0.256
Average	0.25	0.30	0.17	0.25
S.D.	0.08	0.08	0.03	0.05
S.E.	0.03	0.03	0.01	0.02

Two-way ANOVA			
Source of Variation	P-Value	P-Value Summary	Significant?
Interaction	0.5747	NS	No
Training	0.0135	*	Yes
Genotype	0.0180	*	Yes

Bonferroni post-hoc test -- Untrained vs. Trained				
Treatment	Difference	t	P-Value	P-Value Summary
Wildtype	0.05400	1.511	P > 0.05	NS
Mutant	0.08283	2.318	P > 0.05	NS

Table 7C: COX IV Protein Expression

N	WT-UT	WT-T	CL$^{\Delta 19}$-UT	CL$^{\Delta 19}$-T
1	0.4633	0.6357	0.3866	0.6138
2	0.7009	0.6831	0.5652	0.3030
3	0.3237	0.2578	0.1898	0.5619
4	0.5798	0.5266	0.2769	0.5848
5	0.9291	1.2495	0.4590	0.5340
6	0.9885	0.9808	0.4561	0.8498
Average	0.66	0.72	0.39	0.57
S.D.	0.26	0.35	0.14	0.17
S.E.	0.12	0.16	0.05	0.07

Two-way ANOVA			
Source of Variation	P-Value	P-Value Summary	Significant?
Interaction	0.5298	NS	No
Training	0.2361	NS	No
Genotype	0.0467	*	Yes

Bonferroni post-hoc test – Untrained vs. Trained				
Treatment	Difference	t	P-Value	P-Value Summary
Wildtype	0.05805	0.4116	P > 0.05	NS
Mutant	0.1856	1.316	P > 0.05	NS

Table 7D: COX I Protein Expression

N	WT-UT	WT-T	CL$^{\Delta19}$-UT	CL$^{\Delta19}$-T
1	0.2603	0.6316	0.2808	0.5050
2	0.4870	0.7368	0.5652	0.3030
3	0.2253	0.4414	0.1898	0.5619
4	0.3148	0.2996	0.2769	0.5848
5	0.4411	0.6596	0.4590	0.5340
6	0.8333	0.9226	0.4561	0.8498
Average	0.43	0.62	0.37	0.56
S.D.	0.22	0.22	0.14	0.18
S.E.	0.10	0.10	0.05	0.07

Two-way ANOVA			
Source of Variation	P-Value	P-Value Summary	Significant?
Interaction	0.5237	NS	No
Training	0.0277	*	Yes
Genotype	0.9597	NS	No

Bonferroni post-hoc test -- Untrained vs. Trained				
Treatment	Difference	t	P-Value	P-Value Summary
Wildtype	0.1883	1.219	P > 0.05	NS
Mutant	0.3300	2.137	P > 0.05	NS

APPENDIX B

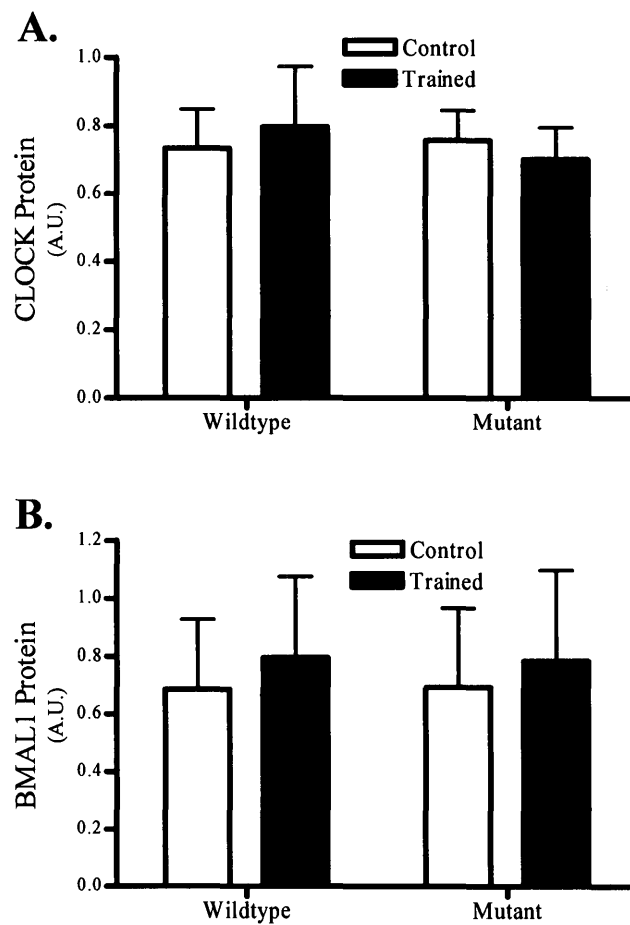## SUPPLEMENTAL FIGURES AND STATISTICAL ANALYSES (MANUSCRIPT DATA)

Fig. S1

Figure S1. *Circadian rhythm protein expression in muscle.* Representative western blot quantifications of **A)** CLOCK and **B)** BMAL1. Values are displayed as mean ± SE (n = 6).
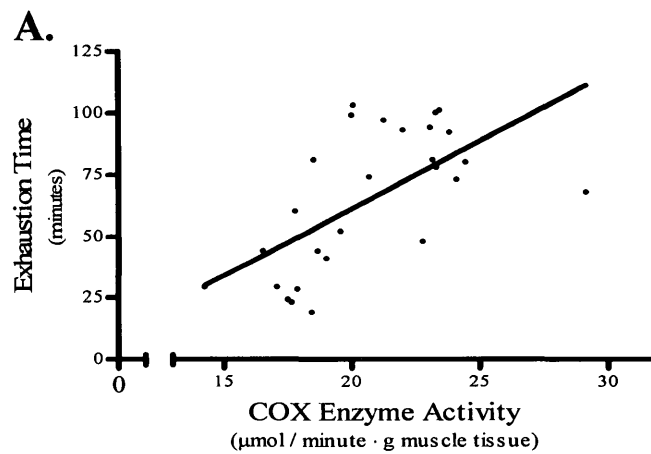
Fig. S4

A.

Figure S4. *Exercise tolerance and mitochondrial content.* Individual animal values displaying the correlation ($r = 0.63$; $p < 0.05$) between exercise tolerance and skeletal muscle COX enzyme activity. Values are displayed as individual data points ($n = 27$).

Table S1A: CLOCK Protein Expression

N	WT-UT	WT-T	$CL^{\Delta 19}$-UT	$CL^{\Delta 19}$-T
1	0.5734	0.5821	0.9463	0.5799
2	0.5985	0.5904	0.5582	0.6589
3	0.7487	0.4223	0.9936	0.5393
4	0.3980	0.5429	0.4276	0.5430
5	1.2132	1.1314	0.8538	0.7464
6	0.8679	1.5180	0.7535	1.1420
Average	0.73	0.80	0.76	0.70
S.D.	0.28	0.43	0.22	0.23
S.E.	0.13	0.19	0.08	0.09

Two-way ANOVA			
Source of Variation	P-Value	P-Value Summary	Significant?
Interaction	0.6379	NS	No
Training	0.9661	NS	No
Genotype	0.7683	NS	No

Table S1B: BMAL1 Protein Expression

N	WT-UT	WT-T	$CL^{\Delta 19}$-UT	$CL^{\Delta 19}$-T
1	1.5411	1.2473	1.8844	1.8622
2	1.2774	1.8478	0.9922	1.6063
3	0.1390	0.0773	0.1370	0.1273
4	0.1333	0.1036	0.0563	0.0617
5	0.4153	0.8880	0.5746	0.5891
6	0.5999	0.6108	0.5061	0.4624
Average	0.68	0.80	0.69	0.78
S.D.	0.59	0.69	0.67	0.77
S.E.	0.27	0.31	0.25	0.29

Two-way ANOVA			
Source of Variation	P-Value	P-Value Summary	Significant?
Interaction	0.9740	NS	No
Training	0.7175	NS	No
Genotype	0.9950	NS	No

Table S4: Exercise Tolerance + COX Enzyme Activity Correlation

N	E.T.	C.A.	Treatment
1	19	18.458	$CL^{\Delta19}$-UT
2	23	17.678	$CL^{\Delta19}$-UT
3	24	17.516	$CL^{\Delta19}$-UT
4	28	17.893	$CL^{\Delta19}$-UT
5	29	17.099	$CL^{\Delta19}$-UT
6	29	14.267	$CL^{\Delta19}$-UT
7	41	19.023	$CL^{\Delta19}$-UT
8	44	18.687	WT-UT
9	44	16.534	WT-UT
10	48	22.804	WT-UT
11	52	19.575	$CL^{\Delta19}$-UT
12	60	17.799	$CL^{\Delta19}$-T
13	68	24.380	WT-T
14	73	24.122	WT-T
15	74	20.705	WT-UT
16	78	23.337	WT-UT
17	80	24.472	WT-UT
18	81	18.525	$CL^{\Delta19}$-T
19	81	23.199	$CL^{\Delta19}$-T
20	92	23.853	$CL^{\Delta19}$-T
21	93	22.037	$CL^{\Delta19}$-T
22	94	23.100	$CL^{\Delta19}$-T
23	97	21.297	WT-T
24	99	20.019	$CL^{\Delta19}$-T
25	100	23.327	WT-T
26	101	23.467	WT-T
27	103	20.086	$CL^{\Delta19}$-T

Correlation	
Slope	5.470 ± 1.372
Y-intercept	-48.05 ± 28.68
r	0.6288
P-Value	0.0005
Is slope significantly non-zero?	Yes

APPENDIX C

**SUPPLEMENTAL DATA, RESULTS, DISCUSSION AND STATISTICAL ANALYSES
(ADDITIONAL DATA)**

Rationale

Recent literature has revealed that PGC-1α, a transcriptional coactivator that induces mitochondrial biogenesis, exhibits diurnal oscillations at the mRNA level within skeletal muscle. This pilot study sought to ascertain if the expression pattern of PGC-1α was evident at the protein level within rodent skeletal muscle, and if there were any apparent downstream differences in mitochondrial content throughout the day.

Experimental Design

Following 10 – 14 days of entrainment, male Sprague-Dawley rats were sacrificed at four distinct time points throughout the circadian cycle (CT 0, CT 6, CT 12, CT 18). The soleus muscle was harvested, and nuclear cell fractions were isolated from these tissues. The contralateral soleus muscle was removed, frozen and pulverized into powder. COX enzyme activity was then performed on these frozen tissues.
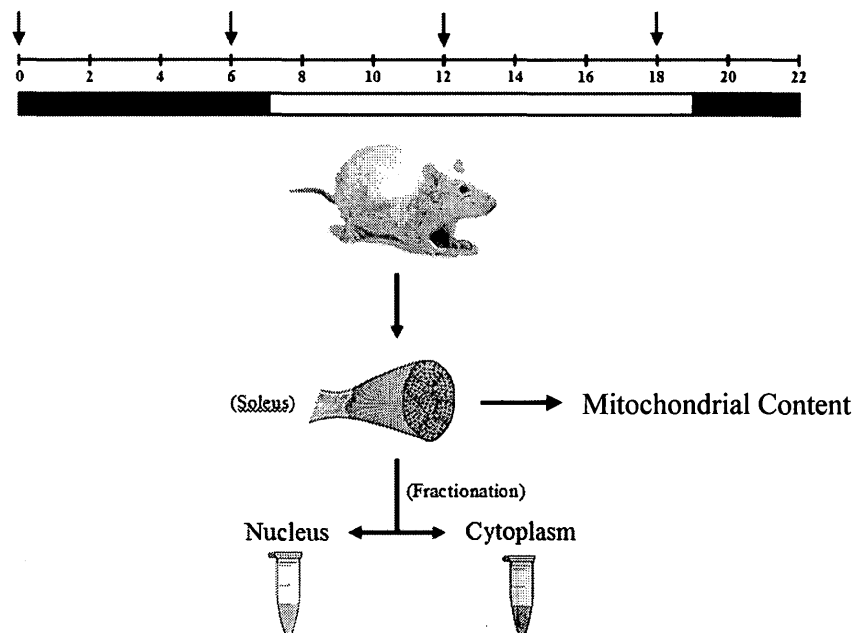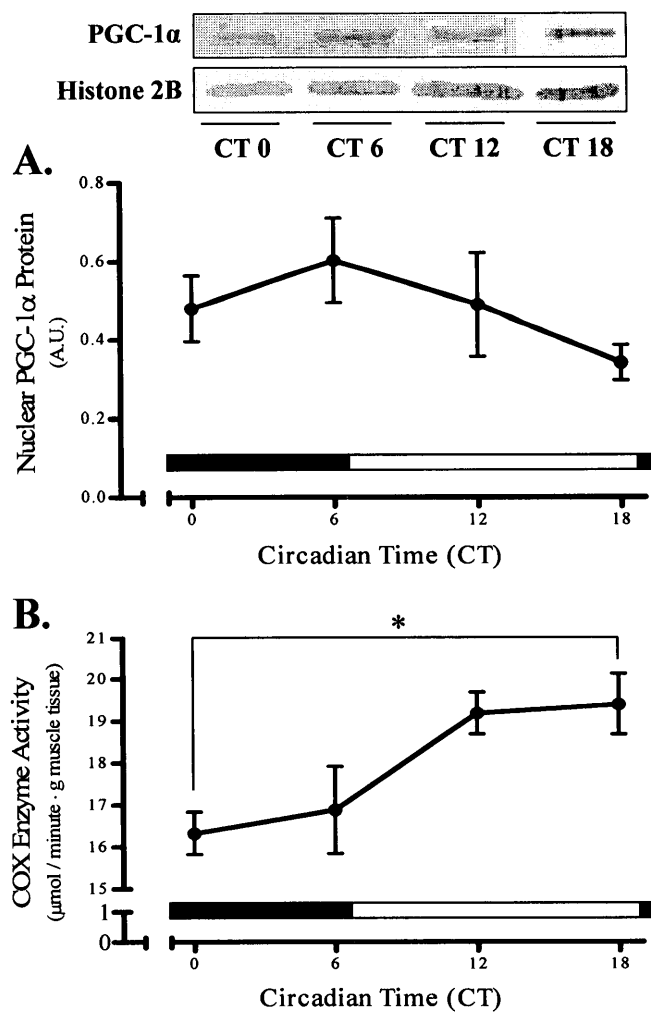
Fig. S2

Figure S2. *Diurnal initiation of mitochondrial biogenesis.* **A)** Representative western blot images and quantifications of PGC-1α in nuclear cell extracts (n = 6); **B)** COX enzyme activity (n = 5 – 6). Values are displayed as mean ± SE. *p < 0.05, CT 0 vs. CT 18.
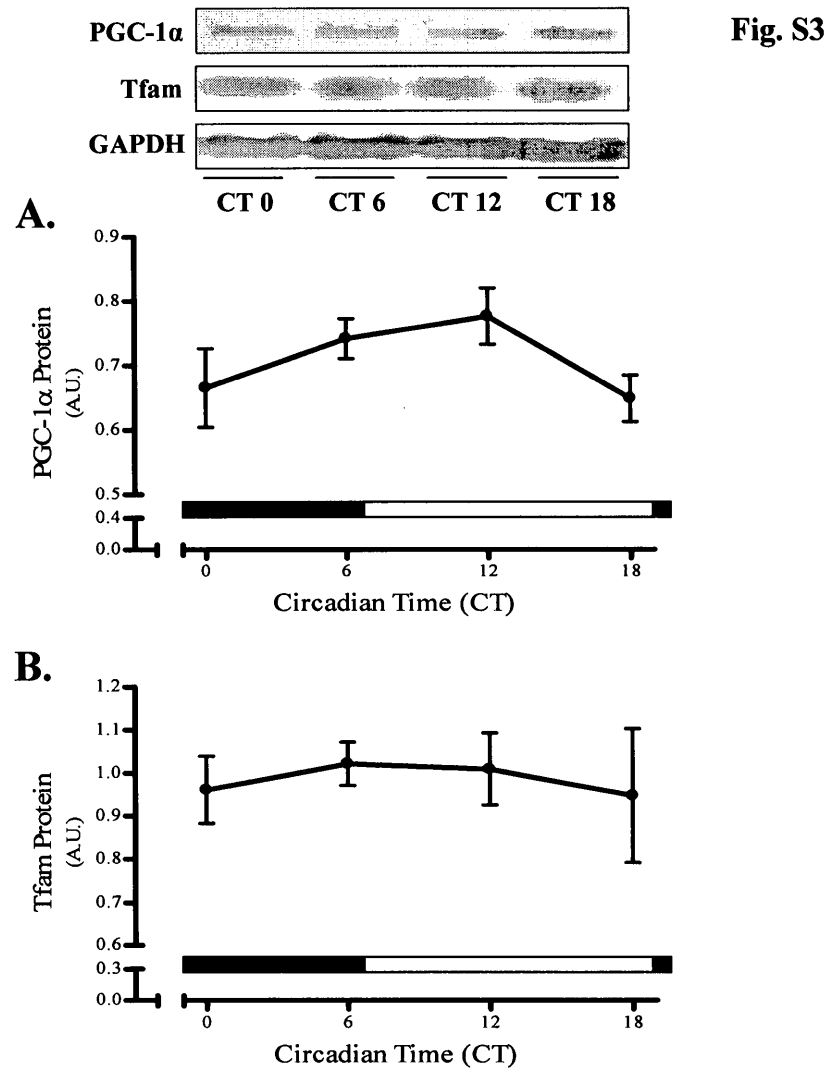
Figure S3. *Diurnal expression of transcriptional coactivators for mitochondrial biogenesis.* Representative western blot images and quantifications of **A)** PGC-1α and **B)** Tfam (n = 3).

Results

No differences in temporal protein expression of the transcriptional coactivator PGC-1α was evident in isolated nuclear cell fractions from the soleus muscle (Fig. S2A). Despite this result, soleus mitochondrial content as inferred from COX enzyme activity appeared to differ between CT 0 and CT 18 by 19% (Fig. S2B; $p < 0.05$). Whole-muscle protein expression of both PGC-1α and Tfam did not exhibit any temporal alterations (Fig. S3).

Discussion

It was initially hypothesized that PGC-1α would exhibit robust temporal changes in protein expression within the isolated nuclear cell fractions, however possibly due to insufficient sample size, as well as inter-sample variation, this was not evident. PGC-1α has been shown to be a CCG, as well as a potent inducer of mitochondrial biogenesis, and therefore it was expected to see diurnal rhythms of COX enzyme activity. It is possible that temporal protein changes are not robust enough to be detected at the whole-muscle level, therefore explaining the results observed in both PGC-1α and Tfam.

Table S2A: Circadian Nuclear PGC-1α Protein Expression

N	CT 0	CT 6	CT 12	CT 18
1	0.882	0.351	0.224	0.15
2	0.34	0.344	0.895	0.439
3	0.363	0.681	0.485	0.334
4	0.482	1.054	0.194	0.372
5	0.435	0.661	0.256	0.451
6	0.3720	0.522	0.882	0.301
Average	0.48	0.60	0.49	0.34
S.D.	0.20	0.26	0.33	0.11
S.E.	0.09	0.12	0.15	0.05

One-way ANOVA	
P-value	0.3382
P-value Summary	NS
Are means significantly different? (P < 0.05)	No

Table S2B: Circadian COX Enzyme Activity

N	CT 0	CT 6	CT 12	CT 18
1	15.79	17.85	21.07	21.43
2	15.76	14.19	18.79	19.94
3	18.15	18.05	19.55	18.7
4	15.94	13.29	19.57	21.23
5	15.79	19.82	17.33	17.23
6		18.08	18.79	18.07
Average	16.29	16.88	19.18	19.43
S.D.	1.04	2.55	1.23	1.72
S.E.	0.52	1.14	0.55	0.77

One-way ANOVA	
P-value	0.0140
P-value Summary	*
Are means significantly different? (P < 0.05)	Yes

Bonferroni's Multiple Comparison post-hoc test				
Treatment	Difference	t	P-Value	P-Value Summary
CT 0 vs. CT 6	-0.594	0.5558	P > 0.05	NS
CT 0 vs. CT 12	-2.897	2.711	P > 0.05	NS
CT 0 vs. CT 18	-3.147	2.945	P < 0.05	*
CT 6 vs. CT 12	-2.303	2.26	P > 0.05	NS
CT 6 vs. CT 18	-2.553	2.506	P > 0.05	NS
CT 12 vs. CT 18	-0.250	0.2453	P > 0.05	NS

Table S3A: Circadian Whole-Muscle PGC-1α Protein Expression

N	CT 0	CT 6	CT 12	CT 18
1	0.5937	0.7559	0.8534	0.5902
2	0.7873	0.6822	0.7021	0.7156
3	0.6148	0.7871	0.7739	0.6398
Average	0.67	0.74	0.78	0.65
S.D.	0.11	0.05	0.08	0.06
S.E.	0.08	0.04	0.05	0.04

One-way ANOVA	
P-value	0.2126
P-value Summary	NS
Are means significantly different? (P < 0.05)	No

Table S3B: Circadian Whole-Muscle Tfam Protein Expression

N	CT 0	CT 6	CT 12	CT 18
1	0.8116	1.0752	1.136	1.0795
2	0.9978	1.0687	0.8506	1.1247
3	1.0739	0.9211	1.0401	0.6362
Average	0.96	1.02	1.01	0.95
S.D.	0.13	0.09	0.15	0.27
S.E.	0.10	0.06	0.10	0.19

One-way ANOVA	
P-value	0.9384
P-value Summary	NS
Are means significantly different? (P < 0.05)	No

133

APPENDIX D

EXPERIMENTAL PROTOCOLS

Mitochondrial Isolation (Muscle Tissue)

Reagents

All buffers are set to pH 7.4 and stored at 4 °C

- Buffer 1
    100 mM KCl
    5 mM MgSO4
    5 mM EDTA
    50 mM Tris base

- Buffer 1 + ATP
    Add 1 mM ATP to Buffer 1

- Buffer 2
    100 mM KCl
    5 mM MgSO4
    5 mM EGTA
    50 mM Tris base
    1 mM ATP

- Resuspension medium
    100 mM KCl
    10 mM MOPS
    0.2% BSA

- Nagarse protease (Sigma, P-4789)
    10 mg/ml in Buffer 2
    Make fresh for each isolation, keep on ice

Procedure

1. Remove muscle tissue from the animal, and put it in a beaker containing 5 ml Buffer 1, on ice immediately.
2. Place muscle tissue on a watch glass that is also on ice and trim away fat and connective tissue. Proceed to thoroughly mince the muscle sample with forceps and scissors, until no large pieces are remaining.
3. Place the minced tissue in a plastic centrifuge tube and record the exact weight of tissue.
4. Add a 10-fold dilution of Buffer 1 + ATP to the tube.
5. Homogenize the samples using the Ultra-Turrax polytron with 40% power output and 10 s exposure time. Rinse the shaft with 0.5 ml of Buffer 1 + ATP to help minimize sample loss.
6. Using a Beckman JA 25.50 rotor, spin the homogenate at a centrifuge setting of 800 g for 10 min. This step divides the IMF and SS mitochondrial subfractions. The supernate will contain the SS mitochondria and the pellet will contain the IMF mitochondria.

SS Mitochondrial Isolation

7. Filter the supernate through a single layer of cheesecloth into a second set of 50 ml plastic centrifuge tubes.
8. Spin tubes at 9000 g for 10 min. Upon completion of the spin discard the supernate and gently resuspend the pellet in 3.5 ml of Buffer 1 + ATP. Since the mitochondria are easily damaged, it is important that the resuspension of the pellet is done carefully.
9. Repeat the centifugation of the previous step (9000 g for 10 min) and discard the supernate.
10. Resuspend the pellet in 200 µl of Resuspension medium, being gentle so as to prevent damage to the SS mitochondria. Some extra time is needed during this final resuspension to ensure the SS pellet is completely resuspended.
11. Keep the SS samples on ice while proceeding to islolate the IMF subfraction.

IMF Mitochondrial Isolation

7. Gently resuspend the pellet (from step 6) in a 10-fold dilution of Buffer 1 + ATP using a teflon pestle.
8. Using the Ultra-Turrax polytron set at 40% power output, polytron the resuspended pellet for 10 s. Rinse the shaft with 0.5 ml of Buffer 1 + ATP.
9. Spin at 800 g for 10 min and discard the resulting supernate.
10. Resuspend the pellet in a 10-fold dilution of Buffer 2 using a teflon pestle.
11. Add the appropriate amount of nagarse. The calculation for the appropriate volume is 0.025 ml/g of tissue. Mix gently and let stand exactly 5 min.
12. Dilute the nagarse by adding 20 ml of Buffer 2.
13. Spin the diluted samples at 5000 g for 5 min and discard the resulting supernate.
14. Resuspend the pellet in a 10-fold dilution of Buffer 2. Gentle resuspension is with a teflon pestle.
15. Spin the samples at 800 g for 10 min. Upon the completion of the spin, the supernate is poured into another set of 50 ml plastic tubes (on ice), and the pellet is discarded.
16. Spin the supernate at 9000 g for 10 min. The supernate is discarded and the pellet is resuspended in 3.5 ml of Buffer 2.
17. Spin samples at 9000 g for 10 min and discard the supernate.
18. Gently resuspend the pellet in 300 µl of Resuspension medium.

Bradford Total Protein Assay

Reagents

- Extraction buffer
    100 mM Na/K PO4
    2 mM EDTA
    pH to 7.2

- 5X Bradford dye
    250 ml 85% Phosphoric acid
    250 ml 100% Ethanol
    500 ml ddH$_2$O
    0.235 g Coomassie Brilliant Blue G250

- Bovine Serum Albumin (BSA)
    2 mg/ml in ddH$_2$O

Procedure

1. Prepare the test tubes allowing for duplicates of each sample.
2. Add 95 µl of extraction buffer to each tube.
3. Add 5 µl of sample to each tube containing the extraction buffer.
4. To generate the standard curve, add the following volumes (in µl) of extraction buffer: BSA, each in separate tubes – 100:0, 95:5, 90:10, 85:15, 80:20, 75:25.
5. Pipette 5 ml of 1 X Bradford reagent into each tube and mix by gentle vortexing.
6. In duplicate, add 0.2 ml of each test tube to 96 well plate wells.
7. Measure absorbance of wells at 595 nm with a microplate reader.
8. Calculate the protein concentration of each sample using the standard curve.

SDS Polyacrylamide Gel Electrophoresis (SDS-PAGE)

Reagents

- Polyacrylamide solution
    30% (w/v) Acrylamide
    0.8% (w/v) Bisacrylamide
    Filter and store at 4 °C

- Under Tris buffer
    1 M Tris•HCl
    pH to 8.8, store at 4 °C

- Ammonium Persulfate (APS)
    10% (w/v) in ddH$_2$O
    Store at 4 °C

- Sodium Dodecyl Sulfate (SDS)
    10% (w/v) in ddH$_2$O

- Over Tris buffer
    1 M Tris•HCl
    Spatula tip of Bromophenol Blue
    pH to 6.8, store at 4 °C

- TEMED (Sigma, T-9281)
    Store at 4 °C

- 15% Acrylamide separating gel
    5 ml 30% acrylamide
    1.8 ml ddH$_2$O
    3 ml Under Tris
    0.1 ml SDS
    0.1 ml APS
    0.01 ml TEMED

- Electrophoresis buffer
    25 mM Tris
    192 mM Glycine
    0.1% (w/v) SDS
    pH to 8.3

- 3% Acrylamide stacking gel
    0.5 ml 30% Acrylamide
    3.75 ml ddH$_2$O
    0.625 ml Over Tris
    0.05 ml SDS
    0.05 ml APS
    7.5 µl TEMED

- Lysis buffer
    10% (w/v) glycerol
    2.3% (w/v) SDS
    62.5 mM Tris•HCl
    pH to 6.8
    add 5% β-mercaptoethanol

- Sample dye
    40% (w/v) sucrose in electrophoresis buffer
    spatula tip of Bromophenol Blue
    store at -20 °C

Procedure

1. Prepare the separating gel solution and pour it between the glass plates of a gel apparatus assembly.
2. Add 100 µl of Tert-amyl alcohol overlay and allow 30 min for gel polymerization.

3. Prepare the stacking gel.

4. Once the separating gel has polymerized, pour off the Tert-amyl alcohol, insert the lane comb, and pipette the stacking gel around the comb. Allow 30 min for the stacking gel to polymerize.

5. Turn on the block heater to 95 °C.

6. Mix each sample with a 1:1 volume of lysis buffer.

7. Add 7 µl of sample dye to each sample and mix by tapping.

8. Denature the samples at 95 °C for 5 min, followed by a quick cool on ice and a brief spin.

9. Remove the comb and place the gel in the electrophoresis chamber. Fill the chamber with electrophoresis buffer.

10. Add 10 µl of protein molecular weight marker to the first lane.

11. Load the samples into the remaining lanes by slowly ejecting the entire sample volume at the bottom of the lane.

12. Run the gel for 2 hr at 120 V.

13. Once the Bromophenol Blue band has reached the bottom of the gel, turn off the power supply and remove the gel. The gel slab is ready for electroblotting (see Western Blot).

Western Blot

Reagents

- Transfer buffer
  - 0.025 M Tris•HCl
  - 0.15 M Glycine
  - 20% Methanol
  - pH to 8.3
- Ponceau stain (Sigma)
  - Dilute with 150 ml ddH$_2$O

- Wash buffer
  - 10 mM Tris•HCl
  - 100 mM NaCl
  - 0.1% TWEEN
  - pH to 7.5
- Blocking buffer
  - % skim milk powder in wash buffer

- Enhanced chemiluminescence (ECL) fluid (Santa Cruz)
  - Store at 4 °C

Procedure

1. Remove the gel from the electrophoresis chamber, and separate the glass plates from the gel slab, keeping the gel moist at all times with transfer buffer.
2. Place three sheets of Whatman paper soaked in transfer buffer onto the plastic sandwich, with a scrubbie. These sheets must be cut to the exact dimensions of the gel slab.
3. Carefully place the gel on top of the Whatman paper.
4. Cut a piece of nitrocellulose membrane to the exact specifications of the gel, soak it in ddH$_2$O, and place it on top of the gel slab.
5. Stack three more sheets of transfer buffer-soaked Whatman paper (same dimensions as gel) on top of membrane. Roll out any air bubbles with a glass rod.
6. Secure the top of the sandwich with a scrubbie soaked in transfer buffer.
7. Transfer the proteins from the gel to the membrane for 1.5 hours at 120V.
8. Once the transfer is complete, place the membrane in Ponceau stain and gently agitate. Pour off the stain and rinse with ddH$_2$O until the protein bands on the blot are revealed.
9. Wrap the membrane in plastic wrap and scan.
10. Remove the membrane from the wrap and rinse off the stain with wash buffer.
11. Pour off the wash buffer and block the membrane in blocking solution on a shaker for 1 hour at room temperature.
12. Incubate the membrane with primary antibody diluted in blocking buffer overnight at 4°C. This is done by placing the membrane face-down on a pool of the antibody solution.
13. The following morning, wash the membrane with rotation 3 X 5 min in wash buffer.

14. Incubate the membrane with the appropriate secondary antibody for 1 hr at room temperature. This is done by laying the membrane face-up and pipetting the secondary antibody solution on top of it.
15. Wash the membrane with rotation 3 X 5 min in wash buffer.
16. In the dark room, apply ECL fluids (1:1) to the membrane for 2 min.
17. Remove the membrane from the ECL fluid, wrap the membrane in plastic wrap, turn off the lights, and expose the blot to film.
18. Develop until bands are visualized and place the film into fixer fluid for 2 min.

Cytochrome *c* Oxidase (COX) Enzyme Activity Assay

Reagents

- 100 mM KPO$_4$ buffer
      0.1 M KH$_2$PO$_4$
      0.1 M K$_2$HPO$_4$•3H$_2$O
      Mix equal portions of above, pH to 7.0

- 10 mM KPO$_4$ buffer
      Dilute the 100 mM KPO$_4$ buffer 1:10 with ddH$_2$O.

- Test solution (prepare in tinted jar)
      20 mg horse heart cytochrome c (Sigma, C-2506)
      1 ml 10 mM KPO$_4$ buffer
      40 μl sodium dithionite
      8 ml ddH$_2$O
      1 ml 100 mM KPO$_4$ buffer

- Muscle extraction buffer
      100 mM Na/K PO$_4$
      2 mM EDTA
      pH to 7.2

Procedure

1. Add ~5-10 μg of frozen, powdered muscle tissue to 10-200 μl (to obtain a 80-fold dilution) of extraction buffer in an Eppendorf tube.
2. Add a micro stir bar to the tube and stir the tissue extract for 15 min on ice. Make the Test solution during this time and wrap the tinted jar in foil.
3. Sonicate each sample 3 X 3 s.
4. Pipette 250 μl of the Test solution into a 96 well plate and incubate them at 30 °C for 10 min.
5. In a second 96 well plate, pipette 30 μl of sample into 4-8 empty plates. Using the multipipette, quickly draw up the test solution and pipette into the wells with the sample extracts.
6. Place well plate into microplate reader and start recording the change in absorbance at 550 nm for 1 min.
7. Calculate cytochrome c oxidase enzyme activity (μmol/min/g or U/g) using the following formula:

$$\frac{\Delta \text{ Abs/min x total volume (ml) x 80 (dilution)}}{18.5 \text{ Abs/μmol x sample volume (ml)}}$$

Mitochondrial Respiration

Reagents

- VO$_2$ buffer
    250 mM sucrose
    50 mM KCl
    25 mM Tris base
    10 mM K$_2$HPO$_4$
    pH to 7.4, store at 4 °C

- 10 mM Glutamate (Sigma, G-1501)

- 0.44 mM ADP (Sigma, A-2754)

- 30 mM NADH (Sigma, N-9534)

Procedure

1. Set water circulation temperature through respiration chambers to 30 °C. Place a stir bar in a chamber.
2. Add 250 µl of respiration buffer to the chamber, and begin stirring. Allow the buffer to equilibrate to the chamber temperature for 5-10 min.
3. Cease spinning and pipette 50 µl of the mitochondrial suspension into the chamber.
4. Carefully close the chamber, ensuring no air bubbles remain. Resume spinning.
5. Set the Strathkelvin 782 oxygen consumption software to begin recording data.
6. Once a steady state VO$_2$ is reached, add glutamate through the electrode port to initiate state 4 respiration.
7. After a satisfactory gradient has been achieved (~3 min later), add ADP to begin state 3 respiration.
8. To assess the integrity of the inner membrane, add NADH during state 3 respiration.
9. Calculate state 4 and state 3 respiration rate (natoms O$_2$/min/mg) as follows:

$$\text{Respiration rate (\%/mg/min)} = \frac{\text{respiration rate (\%/min)}}{([\text{protein}] \ (\mu g/\mu l) \times \text{sample vol.} \ (\mu l)) / 1000}$$

followed by:

$$\text{Respiration rate (natomsO}_2\text{/min/mg)} = \frac{\text{respiration rate (\%/mg/min)} \times 112.5 \ (\text{natoms O}_2)}{100\%}$$

Nuclear and Cytosolic Fractionation (Muscle Tissue)

Reagents

1. NE-PER® Nuclear and Cytoplasmic Extraction Kit (Fisher Scientific PI78833)
   a. Contains three buffers CER I, CER II and NER
2. PBS (Sigma D-8537)
3. Protease Inhibtors
   a. Leupeptin (10mg/ml stock)
   b. Aprotinin (10mg/ml stock)
   c. Pepstatin (10mg/ml stock)
   d. PMSF (500mM stock)
   e. DTT (1M stock)
4. Phosphatase Inhibitors
   a. Sodium Orthovanadate (250mM stock)
   b. PhosSTOP tablets (10X concentrated stock)

Procedure

Tissue Preparation

1. Cut 20-100mg of tissue into small pieces and place in a microcentrifuge tube.
2. Wash tissue with PBS. Centrifuge tissue at $500 \times g$ for 5 minutes.
3. Using a pipette, carefully remove and discard the supernatant, leaving cell pellet as dry as possible.
4. Homogenize tissue using a Dounce homogenizer or a tissue grinder in the appropriate volume of CER I (Table 1). Proceed Cytoplasmic and Nuclear Protein Extraction, using the reagent volumes indicated in Table 1.

Table 1. Reagent volumes for different tissue masses.

Tissue Mass (mg)	CER I (µl)	CER II (µl)	NER (µl)
20	200	11	100
40	400	22	200
80	800	44	400
100	1000	55	500

*Different tissue types may require more or less NE-PER Reagents per weight to optimally extract cytoplasmic and nuclear proteins.

Cytoplasmic and Nuclear Protein Extraction

Note: Scale this protocol depending on the tissue mass (Table 1). Maintain the volume ratio of CER I: CER II: NER reagents at 200:11:100 µl, respectively.

1. Vortex the tube vigorously on the highest setting for 15 seconds to fully suspend the cell pellet. Incubate the tube on ice for 10 minutes.
2. Add ice-cold CER II to the tube.
3. Vortex the tube for 5 seconds on the highest setting. Incubate tube on ice for 1 minute.
4. Vortex the tube for 5 seconds on the highest setting. Centrifuge the tube for 5 minutes at maximum speed in a microcentrifuge ($\sim$16,000 $\times$ g).
5. Immediately transfer the supernatant (cytoplasmic extract) to a clean pre-chilled tube. Place this tube on ice until use or storage (see Step 10).
6. Suspend the insoluble (pellet) fraction produced in Step 4, which contains nuclei, in ice-cold NER.
7. Vortex on the highest setting for 15 seconds. Place the sample on ice and continue vortexing for 15 seconds every 10 minutes, for a total of 40 minutes.
8. Centrifuge the tube at maximum speed ($\sim$16,000 $\times$ g) in a microcentrifuge for 10 minutes.
9. Immediately transfer the supernatant (nuclear extract) fraction to a clean pre-chilled tube. Place on ice.
10. Store extracts at -80°C until use.

Sakamoto Muscle Extract Preparation

Reagents

- Sakamoto muscle extraction buffer
    20 mM Hepes (ph 7.4)
    2 mM EGTA
    1% Trition-X100
    50% Glycerol
    50 mM β-Glycerophosphate
    pH to 7.4, store at 4 °C

Table 1. Protease inhibitor volumes for Sakamoto muscle extraction buffer.

Reagent	Volume (for 10 mL)	Volume (for 5 mL)
Muscle Extraction Buffer	9.8 mL	4.9 mL
1mM DTT	10 µl	5 µl
1mM PMSF	100 µl	50 µl
1mM Sodium Orthovan.	50 µl	25 µl
2µl/ml Leupeptin	20 µl	10 µl
1µl/ml Pepstatin A	10 µl	5 µl
1µl/ml Aprotinin	10 µl	5 µl

Procedure

1. Label two sets of eppendorf tubes accordingly.
2. Add 100 µl of above solution (Table 1) to the first set of eppendorf tubes.
3. Weigh out 15-20 mg of tissue into the first set of eppendorf tubes and record the exact weight of each sample in a table.
4. Add the appropriate volume of solution to each eppendorf to produce 20x volume.
5. Rotate homogenates end over end for 1 hour at 4°C.
6. Sonicate 3 x 3seconds at 30%.
7. Centrifuge at 14000 rcf for 10 minutes at 4°C.
8. Completely withdraw the supernatant and pipette the solution into the new pre-labeled eppendorf tubes.
9. Store at -20°C .

Exercise Tolerance Test

Acclimatization

1. One week before the exercise tolerance test (at the same approximate time), acclimatize the animals to the treadmill (10° incline) over a period of three days.

> Day 1: Place all animals on the treadmill belt, and allow them to remain on the stationary belt for five minutes.
>
> Day 2: Allow all animals to remain on the stationary belt for five minutes, followed by walking on the treadmill at 5 m/min. for five minutes.
>
> Day 3: Allow all animals to walk on the treadmill at 5 m/min. for five minutes, followed by 10 m/min. for 10 minutes.

Exercise Tolerance Test

1. Place each of the four animals onto their respective treadmill belts, and label the condition and genotype that corresponds to each animal.
2. Allow animals to perform the acclimatization protocol prior to the exercise test.
3. Gradually increase the speed of the treadmill for each exercise increment (see Figure 1), while continuously encouraging the animals to run.
4. As animals complete each exercise increment, record this in the observations table (see Table 1).
5. As animals begin to fatigue, administer electric shocks from the rear force plate.
6. Complete fatigue is achieved when the animals remain on the rear force plate and endure continuous electric shock for five consecutive seconds.
7. When animals have reached the level of complete fatigue, remove them from the treadmill and gently place them back in their cage, and note the time.

Table 1. Sample data table for exercise tolerance test.

Animal	5 m/min (5 min)	10 m/min (5 min)	20 m/min (30 min)	24 m/min (15 min)	28 m/min (30 min)	32 m/min (15 min)	Total T (min)
A1RF	X	X	X	X	X	3:35	88:35
A2LB	X	X	X	X	X	7:07	92:07

Figure 1. Exercise tolerance test protocol.
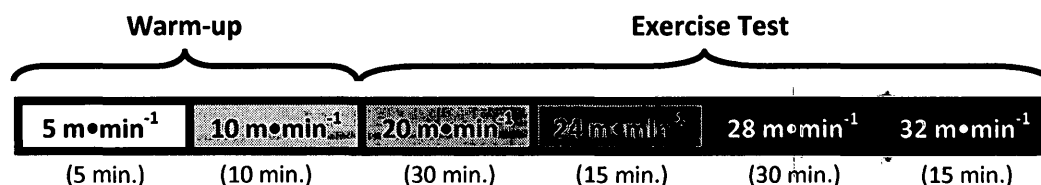
Intraperitoneal (I.P.) Glucose Tolerance Assay

Reagents

- D-Glucose solution (0.2 g/ml)
  - 2 g D-glucose
  - 0.09 g NaCl
  - 10 ml water

Procedure

8. 6 hours prior to I.P. injection, transfer animals to a clean cage and do not provide any food pellets (water is still provided *ad libitum*).
9. Weigh animals and record exact weights.
10. Restrain animals in an inverted beaker and allow the tail to protrude from the spout of the beaker.
11. Make a small incision in the tail with a razor blade and collect a sample of blood (5 μl) on the test strip, and then place the test strip in the blood glucose meter.
12. Administer I.P. injections of the D-glucose solution (dosage: 2 g/kg; see below) to animals (staggered in 60 – 90 second intervals). Record this as "time 0" (see Table 1).
13. Collect blood samples (using the same incision) at 15-, 30-, 45- (optional), 60-, 90- (optional) and 120-minutes post-injection.
14. Following the last blood collection, place animals back in their original cage and replenish their food source.

Table 1. Sample data table for glucose tolerance assay.

Animal ID	Weight (g)	0 min.	Injection Time	15 min.	30 min.	60 min.	120 min.
A1RF	32.7	6.7	2:30	23.6	25.4	14.3	8.1
A2LB	31.8	5.8	2:32	21.0	27.9	14.2	5.3
A3LF	30.3	6.2	2:34	19.8	25.9	13.7	5.8

Example calculation (for a 30 g animal):

2 g/kg glucose required x 0.03 kg = 0.06 g glucose (for a 30 g animal)

$$\frac{0.2 \text{ g/ml glucose solution}}{0.06 \text{ g glucose required}} = 0.3 \text{ ml } (300 \mu l)$$

Clock Mutant Genotyping

Reagents

- Lysis buffer
      10 mM Tris HCl
      150 mM NaCl
      20 mM EDTA
      pH to 8.0, store at 25°C

- Supermix
      Sigma Jumpstart REDtaq Ready Mix PCR Reaction Mix (P0982)
      20 mM Tris-HCl (pH to 8.3)
      100 mM KCl
      4 mM MgCl2
      0.002% gelatin
      0.4 mM (dATP, dCTP, dGTP, TTP)
      0.06 unit/μl Taq DNA polymerase
      JumpStart Taq antibody

- Primers
      Forward and reverse primers for wildtype and mutant strains (stock: 500 pmol/μl)

- Proteinase K (1 mg/ml)

- Agarose
      50X TAE
      1X TAE (dilute 50X TAE with stH$_2$O)
      10 mg/ml EtBr
      Sterile water

- 50X TAE (1 L)
      242 g Tris
      500 ml dH$_2$O
      100 ml 0.5M EDTA (pH 8.0)
      57.1 ml Glacial Acetic Acid

Procedure

DNA Extraction

1. Make (fresh) 10:1 mixture of lysis buffer to Proteinase K (1 mg/ml; fresh).
2. Add 20 μl of this mixture to a 1.5 ml sterile eppendorf tube.

3. Obtain ear clipping from animal, add to tube and vortex (ensure ear clipping is immersed in solution).
4. Incubate solutions in a 55 °C water bath for 30min.
5. Add 180 µl of sterile distilled water.
6. Place in boiling water for 5 minutes (use hot plate), and then vortex.
7. Store at -20°C, or use immediately for PCR.

PCR

1. Prepare three individual mastermix solutions (one for each potential genotype), each containing a different combination of primers (see Table 1).

A) Wildtype	B) Mutant
25 µl Supermix	25 µl Supermix
1 µl WT Forward Primer	1 µl Mutant Reverse Primer
1 µl Common Primer	1 µl Mutant Forward Primer
23 µl Sterile Water	23 µl Sterile Water
50 µl Total	50 µl Total

2. For each ear clipping, use 40 µl of mastermix and 10 µl of template DNA (extracted previously). Repeat this for each potential genotype (2 PCR reaction tubes per animal).
3. Add 1 drop of mineral oil to each PCR tube to prevent evaporation of sample during cycling.
4. Include negative controls using ddH$_2$O (instead of DNA template) with mastermix for each potential genotype (optional).
5. Cycling times: Initial Denaturation   94°C   2 min

     35 cycles: Denaturation   94°C   30 sec
             Annealing   60°C   30 sec
             Extension   72°C   45 sec

   Final Extension   72°C   5 min

     Hold   4°C

Agarose Gel Electrophoresis

1. Prepare a large 1.5% agarose gel.
     4.5 g Agarose
     6 ml 50X TAE
     294 ml Sterile Water
2. Mix solution, cover the beaker with saran wrap and boil in the microwave.

3. Upon complete dissolving of agarose (ensuring a homogenous and relatively clear agarose solution), add 30 μl of EtBr (10 mg/ml), slightly cool solution at room and then pour into caster.
4. Load PCR products (30 μl) onto gel and run for 120 minutes.
5. Visualize PCR products using UV lightbox in the molecular core facility.

Table 1. *Clock* mutant and wildtype genotyping primers.

Mutant Forward	5'-AGC ACC TTC CTT TGC AGT TCG-3'
Mutant Reverse	5'-TGT GCT CAG ACA GAA TAA GTA-3'
Common	5'-TGG GGT AAA AAG ACC TCT TGC C-3'
Wildtype Forward	5'-GGT CAA GGG CTA CAG GTA-3'

Figure 1. Sample agarose gel displaying PCR products.
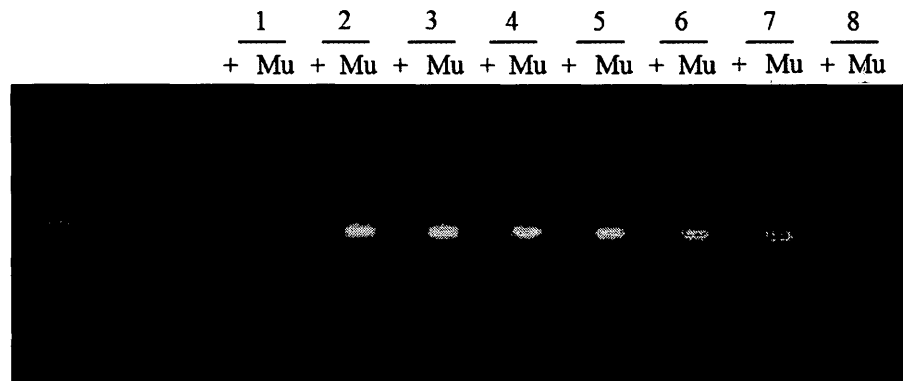
Genotype Analysis

Wildtype *Clock* gene: 150 kbp
Mutant *Clock* gene: 475 kbp

1 – Wildtype homozygote	5 – Heterozygote
2 – Mutant homozygote	6 – Heterozygote
3 – Heterozygote	7 – Heterozygote
4 – Heterozygote	8 – Mutant homozygote

APPENDIX E

AUTHOR CONTRIBUTIONS TO LITERATURE

Published Abstracts

1. M.F.N. O'Leary, A. Vainshtein, S. Iqbal, K.J. Menzies, O. Ostojic, **S.F. Pastore** and D.A. Hood. (2012). The effects of chronic contractile activity on autophagy protein expression in young and aged skeletal muscle. [in preparation]

2. L. Tryon, **S.F. Pastore** and D.A. Hood. Regulation of Tfam expression at the onset of muscle disuse. (2012). *Experimental Biology (EB) Conference.* April 20 – 24, 2013. Boston, MA.

3. H.N. Carter, M.F.N. O'Leary, S. Iqbal*, A. Vainshtein*, O. Ostojic*, **S.F. Pastore** and D.A. Hood. Profiling mitochondrial turnover in aged skeletal muscle: mitophagy arrested? (2012). *Muscle Health Awareness Day.* May 25, 2012. York University, ON.

Oral Presentations

1. **S.F. Pastore** and D.A. Hood. Clock gene regulation of mitochondrial biogenesis in skeletal muscle. (2012). *Graduate Student (Faculty of Health) Seminar Series.* January 20, 2012. York University, ON.

2. **S.F. Pastore** and D.A. Hood. Clock gene regulation of mitochondrial biogenesis in skeletal muscle. (2012). *Ontario Exercise Physiology (OEP) Conference.* January 13 – 15, 2012. Barrie, ON.

3. **S.F. Pastore**, A. Vainshtein and D.A. Hood. The effects of exercise on circadian rhythm protein expression in skeletal muscle. (2011). *Canadian Society for Exercise Physiology (CSEP) Conference.* October 19 – 22, 2011. Quebec City, QC.

Published Abstracts

1. M.F.N. O'Leary, A. Vainshtein, S. Iqbal, K.J. Menzies, O. Ostojic, **S.F. Pastore** and D.A. Hood. (2012). The effects of chronic contractile activity on autophagy protein expression in young and aged skeletal muscle. [in preparation]

2. L. Tryon, **S.F. Pastore** and D.A. Hood. Regulation of Tfam expression at the onset of muscle disuse. (2012). *Experimental Biology (EB) Conference.* April 20 – 24, 2013. Boston, MA.

3. H.N. Carter, M.F.N. O'Leary, S. Iqbal*, A. Vainshtein*, O. Ostojic*, **S.F. Pastore** and D.A. Hood. Profiling mitochondrial turnover in aged skeletal muscle: mitophagy arrested? (2012). *Muscle Health Awareness Day.* May 25, 2012. York University, ON.

Oral Presentations

1. **S.F. Pastore** and D.A. Hood. Clock gene regulation of mitochondrial biogenesis in skeletal muscle. (2012). *Graduate Student (Faculty of Health) Seminar Series.* January 20, 2012. York University, ON.

2. **S.F. Pastore** and D.A. Hood. Clock gene regulation of mitochondrial biogenesis in skeletal muscle. (2012). *Ontario Exercise Physiology (OEP) Conference.* January 13 – 15, 2012. Barrie, ON.

3. **S.F. Pastore**, A. Vainshtein and D.A. Hood. The effects of exercise on circadian rhythm protein expression in skeletal muscle. (2011). *Canadian Society for Exercise Physiology (CSEP) Conference.* October 19 – 22, 2011. Quebec City, QC.